CENTRO DE CIENCIAS BÁSICAS

DEPARTAMENTO DE MATEMÁTICAS Y FÍSICA

TESIS

DESIGN AND ANALYSIS OF COMPUTATIONAL ALGORITHMS FOR COMPLEX COMPARTMENTAL MODELS IN EPIDEMIOLOGY

PRESENTA

Jorge Eduardo Herrera Serrano

PARA OPTAR POR EL GRADO DE DOCTOR EN CIENCIAS APLICADAS Y TECNOLOGÍA

CO-TUTORES

Dr. José Antonio Guerrero Díaz de León

Dr. Jorge Eduardo Macíaz Díaz

COMITÉ TUTORAL

Dr. Ángel Eduardo Muñoz Zavala

Aguascalientes, Ags., 07 de noviembre de 2025

CARTA DE VOTO APROBATORIO

M.C. JORGE MARTÍN ALFÉREZ CHÁVEZ
DECANO DEL CENTRO **DE CIENCIAS BÁSICAS**

P R E S E N T E

Por medio del presente como ***CODIRECTOR*** designado del estudiante ***HERRERA SERRANO JORGE EDUARDO*** con ID *138041* quien realizó *la tesis* titulada: ***DESIGN AND ANALYSIS OF COMPUTATIONAL ALGORITHMS FOR COMPLEX COMPARTMENTAL MODELS IN EPIDEMIOLOGY***, un trabajo propio, innovador, relevante e inédito y con fundamento en la facción IX del Artículo 43 del Reglamento General de Posgrados, doy mi consentimiento de que la versión final del documento ha sido revisada y las correcciones se han incorporado apropiadamente, por lo que me permito emitir el **VOTO APROBATORIO**, para que *el* pueda continuar con el procedimiento administrativo para la obtención del grado.

Pongo lo anterior a su digna consideración y sin otro particular por el momento, me permito enviarle un cordial saludo.

A T E N T A M E N T E
"Se Lumen Proferre"
Aguascalientes, Ags., a *24 de octubre* de *2025*.

Dr. José Antonio Guerrero Díaz de León
Codirector de tesis

c.c.p.- Interesado
c.c.p.- Coordinación del Programa de Posgrado

CARTA DE VOTO APROBATORIO

M.C. JORGE MARTÍN ALFÉREZ CHÁVEZ
DECANO DEL CENTRO **DE CIENCIAS BÁSICAS**

P R E S E N T E

Por medio del presente como ***CODIRECTOR*** designado del estudiante ***HERRERA SERRANO JORGE EDUARDO*** con ID *138041* quien realizó *la tesis* titulada: ***DESIGN AND ANALYSIS OF COMPUTATIONAL ALGORITHMS FOR COMPLEX COMPARTMENTAL MODELS IN EPIDEMIOLOGY***, un trabajo propio, innovador, relevante e inédito y con fundamento en la facción IX del Artículo 43 del Reglamento General de Posgrados, doy mi consentimiento de que la versión final del documento ha sido revisada y las correcciones se han incorporado apropiadamente, por lo que me permito emitir el **VOTO APROBATORIO**, para que *el* pueda continuar con el procedimiento administrativo para la obtención del grado.

Pongo lo anterior a su digna consideración y sin otro particular por el momento, me permito enviarle un cordial saludo.

A T E N T A M E N T E
"Se Lumen Proferre"
Aguascalientes, Ags., a 24 de *octubre* de 2025.

Dr. Jorge Eduardo Macías Díaz
Codirector de tesis

c.c.p.- Interesado
c.c.p.- Coordinación del Programa de Posgrado

CARTA DE VOTO APROBATORIO

M.C. JORGE MARTÍN ALFÉREZ CHÁVEZ
DECANO DEL CENTRO **DE CIENCIAS BÁSICAS**

_____
P R E S E N T E

Por medio del presente como ***ASESOR*** designado del estudiante ***HERRERA SERRANO JORGE EDUARDO*** con ID *138041* quien realizó *la tesis* titulada: ***DESIGN AND ANALYSIS OF COMPUTATIONAL ALGORITHMS FOR COMPLEX COMPARTMENTAL MODELS IN EPIDEMIOLOGY***, un trabajo propio, innovador, relevante e inédito y con fundamento en la facción IX del Artículo 43 del Reglamento General de Posgrados, doy mi consentimiento de que la versión final del documento ha sido revisada y las correcciones se han incorporado apropiadamente, por lo que me permito emitir el **VOTO APROBATORIO**, para que *el* pueda continuar con el procedimiento administrativo para la obtención del grado.

Pongo lo anterior a su digna consideración y sin otro particular por el momento, me permito enviarle un cordial saludo.

A T E N T A M E N T E
"Se Lumen Proferre"
Aguascalientes, Ags., a *24* de *octubre* de *2025*.

Dr. Ángel Eduardo Muñoz Zavala
Asesor de *tesis*

c.c.p.- Interesado
c.c.p.- Coordinación del Programa de Posgrado

UNIVERSIDAD AUTÓNOMA DE AGUASCALIENTES

DICTAMEN DE LIBERACIÓN ACADÉMICA PARA INICIAR LOS TRÁMITES DEL EXAMEN DE GRADO

POSGRADOS UAA

Fecha de dictaminación (dd/mm/aaaa): 24/10/2025

NOMBRE: JORGE EDUARDO HERRERA SERRANO **ID** 138041

PROGRAMA: DOCTORADO EN CIENCIAS APLICADAS Y TECNOLOGIA **LGAC (del posgrado):** INTELIGENCIA ARTIFICIAL Y MODELACIÓN ESTADÍSTICA

MODALIDAD DEL PROYECTO DE GRADO: Tesis Tradicional ( ) *Tesis por artículos científicos (X) **Tesis por Patente ( ) Trabajo Práctico ( )

TITULO: DESIGN AND ANALYSIS OF COMPUTATIONAL ALGORITHMS FOR COMPLEX COMPARTMENTAL MODELS IN EPIDEMIOLOGY

IMPACTO SOCIAL (señalar el impacto logrado): Articulos publicados. Participación en talleres y conferencia. Transferencia de conocimiento

INDICAR SEGÚN CORRESPONDA: **SI, NO, NA** (No Aplica)

	Elementos para la revisión académica del trabajo de tesis o trabajo práctico:
SI	El trabajo es congruente con las LGAC del programa de posgrado
SI	La problemática fue abordada desde un enfoque multidisciplinario
SI	Existe coherencia, continuidad y orden lógico del tema central con cada apartado
SI	Los resultados del trabajo dan respuesta a las preguntas de investigación o a la problemática que aborda
SI	Los resultados presentados en el trabajo son de gran relevancia científica, tecnologíca o profesional según el área
SI	El trabajo demuestra más de una aportación original al conocimiento de su área
SI	Las aportaciones responden a los problemas prioritarios del país
SI	Generó transferencia del conocimiento o tecnológica
SI	Cumple con la ética para la investigación (reporte de la herramienta antiplagio)
	El egresado cumple con lo siguiente:
SI	Cumple con lo señalado por el Reglamento General de Posgrados
SI	Cumple con los requisitos señalados en el plan de estudios (créditos curriculares, optativos, actividades complementarias, estancia, predoctoral, etc.)
SI	Cuenta con los votos aprobatorios del comité tutorial
NA	Cuenta con la carta de satisfacción del Usuario (En caso de que corresponda)
SI	Coincide con el título y objetivo registrado
SI	Tiene congruencia con cuerpos académicos
SI	Tiene el CVU de la SECIHTI actualizado
SI	Tiene el o los artículos aceptados o publicados y cumple con los requisitos institucionales (en caso de que proceda)
	****En caso de Tesis por artículos científicos publicados*** *(completar solo si la tesis fue por artículos)*
SI	Aceptación o Publicación de los artículos en revistas indexadas de alto impacto según el nivel del programa
SI	El (la) estudiante es el primer autor(a)
SI	El (la) autor(a) de correspondencia es el Director (a) del Núcleo Académico
SI	En los artículos se ven reflejados los objetivos de la tesis, ya que son producto de este trabajo de investigación.
SI	Los artículos integran los capítulos de la tesis y se presentan en el idioma en que fueron publicados
	*****En caso de Tesis por Patente***
NA	Cuenta con la evidencia de solicitud de patente en el Departamento de Investigación (anexarla al presente formato)

Con base en estos criterios, se autoriza continuar con los trámites de titulación y programación del examen de grado: **Sí** X **No**

FIRMAS

Elaboró:

*NOMBRE Y FIRMA DEL(LA) CONSEJERO(A) SEGÚN LA LGAC DE ADSCRIPCION: Dr. Francisco Javier Álvarez Rodríguez

** En caso de conflicto de intereses, firmará un revisor miembro del NA de la LGAC correspondiente distinto al director o miembro del comité tutorial, asignado por el Decano.*

NOMBRE Y FIRMA DEL COORDINADOR DE POSGRADO: P.D. Dr. José Antonio Guerrero Díaz de León.

Revisó:

NOMBRE Y FIRMA DEL SECRETARIO DE INVESTIGACIÓN Y POSGRADO: Dr. Alejandro Padilla Díaz

Autorizó:

NOMBRE Y FIRMA DEL DECANO: Mtro. en C. Jorge Martín Alférez Chávez

Nota: procede el trámite para el Depto. de Apoyo al Posgrado

En cumplimiento con el Art. 24 fracción V del Reglamento General de Posgrado, que a la letra señala entre las funciones del Consejo Académico: Proponer criterios y mecanismos de selección, permanencia, egreso y titulación de estudiantes para asegurar la eficiencia terminal y la titulación y el Art. 28 fracción IX, atender, asesorar y dar el seguimiento del estudiantado desde su ingreso hasta su titulación.

Computer Methods and Programs in Biomedicine 221 (2022) 106920

Contents lists available at ScienceDirect

Computer Methods and Programs in Biomedicine

journal homepage: www.elsevier.com/locate/cmpb

An efficient nonstandard computer method to solve a compartmental epidemiological model for COVID-19 with vaccination and population migration

Jorge E. Herrera-Serrano [a,b], Jorge E. Macías-Díaz [c,d,*], Iliana E. Medina-Ramírez [e], J.A. Guerrero [f]

[a] Centro de Ciencias Básicas, Universidad Autónoma de Aguascalientes, Aguascalientes, Mexico
[b] Dirección Académica de Tecnologías de la Información y Mecatrónica, Universidad Tecnológica del Norte de Aguascalientes, Mexico
[c] Department of Mathematics and Didactics of Mathematics, School of Digital Technologies, Tallinn University, Estonia
[d] Departamento de Matemáticas y Física, Universidad Autónoma de Aguascalientes, Aguascalientes, Mexico
[e] Departamento de Química, Universidad Autónoma de Aguascalientes, Aguascalientes, Mexico
[f] Departamento de Estadística, Universidad Autónoma de Aguascalientes, Aguascalientes, Mexico

ARTICLE INFO

Article history:
Received 11 April 2022
Revised 25 May 2022
Accepted 26 May 2022

MSC:
65M06
39A14
35L53
92D25

Keywords:
Compartmental epidemiological model
Vaccination regime and migration
Steady-state solutions
Local stability analysis
Non-standard finite-difference scheme
Positivity preservation
Stability and convergence analysis

ABSTRACT

Background and objective: In this manuscript, we consider a compartmental model to describe the dynamics of propagation of an infectious disease in a human population. The population considers the presence of susceptible, exposed, asymptomatic and symptomatic infected, quarantined, recovered and vaccinated individuals. In turn, the mathematical model considers various mechanisms of interaction between the sub-populations in addition to population migration. *Methods:* The steady-state solutions for the disease-free and endemic scenarios are calculated, and the local stability of the equilibium solutions is determined using linear analysis, Descartes' rule of signs and the Routh–Hurwitz criterion. We demonstrate rigorously the existence and uniqueness of non-negative solutions for the mathematical model, and we prove that the system has no periodic solutions using Dulac's criterion. To solve this system, a nonstandard finite-difference method is proposed. *Results:* As the main results, we show that the computer method presented in this work is uniquely solvable, and that it preserves the non-negativity of initial approximations. Moreover, the steady-state solutions of the continuous model are also constant solutions of the numerical scheme, and the stability properties of those solutions are likewise preserved in the discrete scenario. Furthermore, we establish the consistency of the scheme and, using a discrete form of Gronwall's inequality, we prove theoretically the stability and the convergence properties of the scheme. For convenience, a Matlab program of our method is provided in the appendix. *Conclusions:* The computer method presented in this work is a nonstandard scheme with multiple dynamical and numerical properties. Most of those properties are thoroughly confirmed using computer simulations. Its easy implementation make this numerical approach a useful tool in the investigation on the propagation of infectious diseases. From the theoretical point of view, the present work is one of the few papers in which a nonstandard scheme is fully and rigorously analyzed not only for the dynamical properties, but also for consistently, stability and convergence.

1. Introduction

Epidemiology is considered a scientific discipline that studies the distribution, frequency, determinants, relationships, predictions, and control of factors related to health and disease in human populations [1]. Nowadays, epidemiology has a relevant place in many scientific areas, including the biomedical sciences, social sciences and even in the exact sciences [2]. In fact, it is worth pointing out that the study of diseases is an area which is as old as the birth of human writing. Indeed, the origins of the word "epidemiology" date back to ancient Greece, to some classical texts by Hippocrates of Kos, Aristotle and Galen [3]. Some of these scientists and philosophers were the first to use the terms "endemic" and "epidemic" in their works [4], though these concepts could

* Corresponding author.
E-mail addresses: jorge.herrera@edu.uaa.mx (J.E. Herrera-Serrano), jemacias@correo.uaa.mx (J.E. Macías-Díaz), iemedina@correo.uaa.mx (I.E. Medina-Ramírez), jaguerrero@correo.uaa.mx (J.A. Guerrero).

https://doi.org/10.1016/j.cmpb.2022.106920
0169-2607/

Computer Methods and Programs in Biomedicine 236 (2023) 107526

Contents lists available at ScienceDirect

Computer Methods and Programs in Biomedicine

journal homepage: www.elsevier.com/locate/cmpb

A multiconsistent computational methodology to resolve a diffusive epidemiological system with effects of migration, vaccination and quarantine

Jorge E. Herrera-Serrano [a,b], José A. Guerrero-Díaz-de-León [c], Iliana E. Medina-Ramírez [d], Jorge E. Macías-Díaz [e,f,*]

[a] Basic Sciences Faculty, Aguascalientes Autonomous University, Ave. Universidad 940, Ciudad Universitaria, Aguascalientes, Ags. 201000, Mexico
[b] Academic Direction of Information Technologies and Mechatronics, Technological University of the North of Aguascalientes, Ave. Universidad 1001, La Estación Rincón, Rincón de Romos, Ags. 20400, Mexico
[c] Department of Statistics, Aguascalientes Autonomous University, Ave. Universidad 940, Ciudad Universitaria, Aguascalientes, Ags. 20100, Mexico
[d] Department of Chemistry, Aguascalientes Autonomous University, Ave. Universidad 940, Ciudad Universitaria, Aguascalientes, Ags. 20100, Mexico
[e] Department of Mathematics and Didactics of Mathematics, School of Digital Technologies, Tallinn University, Narva Rd. 25, 10120 Tallinn, Estonia
[f] Department of Mathematics and Physics, Aguascalientes Autonomous University, Ave. Universidad 940, Ciudad Universitaria, Aguascalientes, Ags. 20100, Mexico

ARTICLE INFO

Article history:
Received 31 January 2023
Revised 21 March 2023
Accepted 2 April 2023

2020 MSC:
39A14
35L53
65M06
92D30

Keywords:
nonlinear parabolic systems of partial differential equations
compartmental epidemiological model
nonstandard computer method
non-singular inverse-positive matrices
nonlinear analysis of convergence and stability
computational simulations

ABSTRACT

Background: We provide a compartmental model for the transmission of some contagious illnesses in a population. The model is based on partial differential equations, and takes into account seven subpopulations which are, concretely, susceptible, exposed, infected (asymptomatic or symptomatic), quarantined, recovered and vaccinated individuals along with migration. The goal is to propose and analyze an efficient computer method which resembles the dynamical properties of the epidemiological model.

Materials and methods: A non-local approach is utilized for finding approximate solutions for the mathematical model. To that end, a non-standard finite-difference technique is introduced. The finite-difference scheme is a linearly implicit model which may be rewritten using a suitable matrix. Under suitable circumstances, the matrices representing the methodology are M-matrices.

Results: Analytically, the local asymptotic stability of the constant solutions is investigated and the next generation matrix technique is employed to calculate the reproduction number. Computationally, the dynamical consistency of the method and the numerical efficiency are investigated rigorously. The method is thoroughly examined for its convergence, stability, and consistency.

Conclusions: The theoretical analysis of the method shows that it is able to maintain the positivity of its solutions and identify equilibria. The method's local asymptotic stability properties are similar to those of the continuous system. The analysis concludes that the numerical model is convergent, stable and consistent, with linear order of convergence in the temporal domain and quadratic order of convergence in the spatial variables. A computer implementation is used to confirm the mathematical properties, and it confirms the ability in our scheme to preserve positivity, and identify equilibrium solutions and their local asymptotic stability.

1. Introduction

During the final months in 2019, humanity began a struggle against a new virus called SARS-CoV-2, which is a pathogen that has caused almost 6.7 million human casualties around the world until January 2023 [1]. This disease is known also as COVID-19, and it will be in the history annals along with others pandemics such as the black plague, the smallpox and the Spanish flu among many others [2]. It is worth mentioning that COVID-19 has not been as

* Corresponding author at Department of Mathematics and Physics, Aguascalientes Autonomous University, 940 University Ave, Aguascalientes 20100, Mexico.
E-mail addresses: jorge.herrera@edu.uaa.mx (J.E. Herrera-Serrano), jaguerrero@correo.uaa.mx (J.A. Guerrero-Díaz-de-León), iemedina@correo.uaa.mx (I.E. Medina-Ramírez), jorge.macias_diaz@tlu.ee, jemacias@correo.uaa.mx (J.E. Macías-Díaz).

https://doi.org/10.1016/j.cmpb.2023.107526
0169-2607/

ARTICLE TYPE

Analytical and numerical study of a diffusive epidemiological model with migration, Crowley–Martin infection and treatment

Jorge E. Herrera-Serrano[1,2] | Jorge E. Macíaz-Díaz[3,4] | J. Antonio Guerrero[5] | Ángel E. Muñoz-Zavala[5]

[1]Centro de Ciencias Básicas, Universidad Autónoma de Aguascalientes, Aguascalientes, México
[2]Dirección Académica de Tecnologías de la Información y Mecatrónica, Universidad Tecnológica del Norte de Aguascalientes, Aguascalientes, México
[3]Department of Mathematics and Didactics of Mathematics, School of Digital Technologies | Tallin University, Tallinn, Estonia
[4]Department of Mathematics and Physics, Autonomous University of Aguascalientes, Aguascalientes,, Mexico
[5]Department of Statistics, Autonomous University of Aguascalientes, Aguascalientes, Mexico

Correspondence
*Department of Mathematics and Physics, Autonomous University of Aguascalientes, Avenida Universidad 940, Ciudad Universitaria, 20131, Aguascalientes, México. Email: jemacias@correo.uaa.mx

Summary

KEYWORDS:
Compartmental epidemiological model, Martin-Crowler incidence rate, generation matrix, treatment

1 | INTRODUCTION

Recall that epidemiology is the study of the patterns, causes, and effects of diseases in populations. From the mathematical point of view, this discipline uses mathematical models to understand and analyze the spread of infectious illnesses within communities[1,2]. Among those mathematical model used in epidemiology, some of them are based on the use of compartments. It is worth recalling that compartmental models divide the population into different compartments or disjoint groups based on their disease status[1]. The compartments typically include categories such as susceptible (individuals who are susceptible to the disease), infected (individuals who are currently infected), and recovered (individuals who have recovered from the disease and gained immunity). Depending on the specific disease and model, additional compartments may be included to represent factors such as exposed individuals or those requiring medical treatment[3,4]. In that sense, some compartmental models consider subpopulations of quarantined, vaccinated and exposed individuals, not to mention effects of migration between populations[5]. Meanwhile, other epidemiological models consider even the effect of spatial diffusion of diseases[6].

The movement of individuals between compartments is described by a set of differential equations, which govern the rates of transition from one compartment to another. These equations can take various forms, including ordinary differential

Acknowledgments

I am very grateful to **Dr. Ángel Eduardo Muñoz Zavala** and **Dr. José Antonio Guerrero Díaz de León** for their steady support during these four years. Your guidance, time for discussion, and clear feedback helped me at every step. Thank you for your trust and for your professional example.

My deepest thanks go to **Dr. Jorge Eduardo Macías Díaz**. Your dedication, patience, and wisdom guided me through the hardest moments. You read my work with care, challenged my ideas, and encouraged me when the path felt long. Without your constant mentorship and hard work, I could not have finished this thesis.

To my parents: your love and sacrifice made this possible. You taught me to work hard, to keep going, and to start again after setbacks. During the late nights and early mornings, your example kept me moving forward. This achievement is yours too. Thank you for lifting me when I felt I could not continue, and for reminding me why finishing matters.

To my **brothers and sisters**, thank you for your constant encouragement, your timely messages, and your patient listening. Your humor and advice made difficult days easier.

To my **daughter**, my greatest motivation: you are the reason I kept going and tried to give my best. Your curiosity and joy gave meaning to long hours of work. I hope this shows you that persistence and hope can take us far.

I thank the **Universidad Autónoma de Aguascalientes (UAA)** and the **Universidad Tecnológica El Retoño (UTR)** for giving me an academic home and the support to complete this work. The learning environment, colleagues, and students in both institutions inspired me.

A heartfelt thank you to **Karen**, who helped me when I needed it most and kept me from leaving the doctoral program. Your kindness and practical support made a real difference.

Contents

List of Figures

List of Tables

Resumen

Esta tesis integra dos estudios sobre modelación epidemiológica con ecuaciones en derivadas parciales y esquemas numéricos que preservan estructura. En ambos trabajos se considera una población segmentada en clases susceptibles, expuestas, infectadas sintomáticas y asintomáticas, en cuarentena, recuperadas y vacunadas, incorporando migración y difusión espacial.

El primer artículo propone un esquema de diferencias finitas no estándar, linealmente implícito y escribible en forma matricial. El método está diseñado para reproducir propiedades cualitativas del sistema continuo: positividad, invariancia del conjunto admisible, preservación de equilibrios y estabilidad local. Se prueban consistencia (orden lineal en tiempo y cuadrático en espacio), estabilidad bajo restricciones de paso temporal y convergencia. La demostración se apoya en teoría de matrices M y en desigualdades discretas tipo Gronwall–Young. Las simulaciones en MATLAB corroboran el análisis y muestran aproximaciones robustas en todo el dominio.

El segundo artículo se centra en la dinámica del modelo. Se obtienen los equilibrios libre de enfermedad y endémico, se calcula el número reproductivo básico mediante la matriz de próxima generación y se analiza la estabilidad local de ambos estados. Además, se presenta un análisis de sensibilidad de $\mathscr{R}_0$ respecto a parámetros clave (contacto, cuarentena, vacunación y migración). Los experimentos numéricos validan la preservación de positividad del método y muestran transiciones claras entre regímenes con $\mathscr{R}_0 < 1$ y $\mathscr{R}_0 > 1$, así como convergencia hacia estados estacionarios. En conjunto, la tesis ofrece un marco continuo–discreto coherente para modelos compartimentales con difusión, que equilibra fidelidad cualitativa y garantías numéricas.

Abstract

This thesis comprises two studies on PDE-based epidemic modeling and structure-preserving discretization. In both, the host population is split into S, E, I_S, I_A, Q, R, and V classes, with spatial mobility represented by diffusion and inter-compartment migration.

The first article develops a linearly implicit nonstandard finite-difference scheme that can be written in matrix form. The method is built to mirror key qualitative features of the continuous model: positivity, invariance of the admissible set, preservation of equilibria, and local stability. We prove consistency (first order in time, second order in space), step-size–dependent stability, and convergence. The analysis relies on M-matrix theory and discrete Gronwall–Young inequalities. MATLAB simulations confirm the theory and deliver robust approximations across the computational domain.

The second article focuses on system-level behavior. We derive the disease-free and endemic equilibria, compute the basic reproduction number via the next-generation matrix, and study local stability for both steady states. A sensitivity analysis of $\mathscr{R}_0$ with respect to transmission, quarantine, vaccination, and migration parameters is presented. Numerical experiments validate positivity preservation and display sharp transitions between regimes with $\mathscr{R}_0 < 1$ and $\mathscr{R}_0 > 1$, together with convergence to steady states. Overall, the thesis offers a coherent continuous–discrete framework for diffusive compartmental models that balances qualitative fidelity with rigorous numerical guarantees.

Introduction

Aims and scope

The aims and scope of this thesis are to develop, analyze, and compute reliable frameworks for modeling the spread of infectious diseases in heterogeneous populations. First, I formulate mechanistic epidemiological models that incorporate spatial diffusion, migration, vaccination, quarantine, and multiple infectious states. Second, I carry out a rigorous mathematical study of these models, including the identification of equilibria, the derivation of the basic reproduction number through the next-generation approach, and local asymptotic stability results around the disease-free and endemic states. Third, I design nonstandard finite-difference schemes that preserve the key dynamical features of the continuous problem—positivity, boundedness, and the location and stability of equilibria—and I prove their consistency, stability, and convergence with respect to the temporal and spatial discretizations. Fourth, I implement the proposed schemes efficiently and validate them through numerical experiments. Fifth, I estimate model parameters from data or literature ranges and conduct sensitivity analyses to quantify the influence of epidemiological and control parameters. Finally, I use the calibrated models to assess and propose realistic intervention strategies (such as vaccination, quarantine, or mobility policies), with the goal of supporting evidence-based decision making.

Summary

Chapter 1. A linearly implicit non-standard finite-difference (NSFD) scheme is proposed for a spatial compartmental epidemic model with vaccination, quarantine, and migration. The method admits a compact matrix formulation and, under natural assumptions, the discrete operators are M-matrices, which implies nonsingularity and inverse positivity. We prove nonnegativity preservation, consistency (first-order in time (t) and also second-order in space (x)), stability for mild time-step restrictions, and convergence. MATLAB simulations corroborate the theoretical properties.

Chapter 2. We examine the dynamics in depth: the disease-free and endemic equilibria are characterized, the basic reproduction number $\mathscr{R}_0$ is derived via the next-generation matrix, and local stability of both states is proved. A parameter sensitivity study for $\mathscr{R}_0$ is included. The NSFD scheme inherits its key qualitative properties of the continuous model (nonnegativity, equilibrium preservation, and stability) and is validated computationally. Numerical experiments display threshold behavior across $\mathscr{R}_0 < 1$ and $\mathscr{R}_0 > 1$ and show temporal convergence toward steady states.

1. An efficient nonstandard computer method to solve a compartmental epidemiological model for COVID-19 with vaccination and population migration

1.1 Introduction

This chapter develops a compartmental model to describe the spread of an infectious disease in a single population with vaccination, quarantine, recovery, natural deaths, and migration. The population is divided into seven groups: susceptible, vaccinated, exposed, asymptomatic infected, symptomatic infected, quarantined, and recovered. The model is stated as a system of ordinary differential equations that connects these groups through biologically meaningful flows. This structure makes it possible to study key questions such as when an outbreak fades out, when it becomes endemic, and how policy levers (like vaccination or quarantine) affect those outcomes.

The analytical study identifies the disease-free and endemic equilibria and computes the basic reproduction number using the next-generation approach. A main result is that the disease-free equilibrium is locally asymptotically stable whenever the reproduction number is below one. These results give a clear threshold condition that separates control from persistence of the disease.

On the computational side, the chapter proposes a nonstandard finite-difference time integrator designed to mimic the qualitative behavior of the continuous model. The scheme preserves nonnegativity and boundedness, shares the same equilibria as the ODE system, and maintains their local stability. The analysis also establishes consistency, conditional stability, and convergence of the discrete model, and numerical experiments confirm these properties.

1.2 Article 1

Computer Methods and Programs in Biomedicine 221 (2022) 106920

Contents lists available at ScienceDirect

Computer Methods and Programs in Biomedicine

journal homepage: www.elsevier.com/locate/cmpb

An efficient nonstandard computer method to solve a compartmental epidemiological model for COVID-19 with vaccination and population migration

Jorge E. Herrera-Serrano[a,b], Jorge E. Macías-Díaz[c,d,*], Iliana E. Medina-Ramírez[e], J.A. Guerrero[f]

[a] Centro de Ciencias Básicas, Universidad Autónoma de Aguascalientes, Aguascalientes, Mexico
[b] Dirección Académica de Tecnologías de la Información y Mecatrónica, Universidad Tecnológica del Norte de Aguascalientes, Mexico
[c] Department of Mathematics and Didactics of Mathematics, School of Digital Technologies, Tallinn University, Estonia
[d] Departamento de Matemáticas y Física, Universidad Autónoma de Aguascalientes, Aguascalientes, Mexico
[e] Departamento de Química, Universidad Autónoma de Aguascalientes, Aguascalientes, Mexico
[f] Departamento de Estadística, Universidad Autónoma de Aguascalientes, Aguascalientes, Mexico

ARTICLE INFO

Article history:
Received 11 April 2022
Revised 25 May 2022
Accepted 26 May 2022

MSC:
65M06
39A14
35L53
92D25

Keywords:
Compartmental epidemiological model
Vaccination regime and migration
Steady-state solutions
Local stability analysis
Non-standard finite-difference scheme
Positivity preservation
Stability and convergence analysis

ABSTRACT

Background and objective: In this manuscript, we consider a compartmental model to describe the dynamics of propagation of an infectious disease in a human population. The population considers the presence of susceptible, exposed, asymptomatic and symptomatic infected, quarantined, recovered and vaccinated individuals. In turn, the mathematical model considers various mechanisms of interaction between the sub-populations in addition to population migration. *Methods:* The steady-state solutions for the disease-free and endemic scenarios are calculated, and the local stability of the equilibium solutions is determined using linear analysis, Descartes' rule of signs and the Routh–Hurwitz criterion. We demonstrate rigorously the existence and uniqueness of non-negative solutions for the mathematical model, and we prove that the system has no periodic solutions using Dulac's criterion. To solve this system, a nonstandard finite-difference method is proposed. *Results:* As the main results, we show that the computer method presented in this work is uniquely solvable, and that it preserves the non-negativity of initial approximations. Moreover, the steady-state solutions of the continuous model are also constant solutions of the numerical scheme, and the stability properties of those solutions are likewise preserved in the discrete scenario. Furthermore, we establish the consistency of the scheme and, using a discrete form of Gronwall's inequality, we prove theoretically the stability and the convergence properties of the scheme. For convenience, a Matlab program of our method is provided in the appendix. *Conclusions:* The computer method presented in this work is a nonstandard scheme with multiple dynamical and numerical properties. Most of those properties are thoroughly confirmed using computer simulations. Its easy implementation make this numerical approach a useful tool in the investigation on the propagation of infectious diseases. From the theoretical point of view, the present work is one of the few papers in which a nonstandard scheme is fully and rigorously analyzed not only for the dynamical properties, but also for consistently, stability and convergence.

1. Introduction

Epidemiology is considered a scientific discipline that studies the distribution, frequency, determinants, relationships, predictions, and control of factors related to health and disease in human populations [1]. Nowadays, epidemiology has a relevant place in many scientific areas, including the biomedical sciences, social sciences and even in the exact sciences [2]. In fact, it is worth pointing out that the study of diseases is an area which is as old as the birth of human writing. Indeed, the origins of the word "epidemiology" date back to ancient Greece, to some classical texts by Hippocrates of Kos, Aristotle and Galen [3]. Some of these scientists and philosophers were the first to use the terms "endemic" and "epidemic" in their works [4], though these concepts could

* Corresponding author.
E-mail addresses: jorge.herrera@edu.uaa.mx (J.E. Herrera-Serrano), jemacias@correo.uaa.mx (J.E. Macías-Díaz), iemedina@correo.uaa.mx (I.E. Medina-Ramírez), jaguerrero@correo.uaa.mx (J.A. Guerrero).

https://doi.org/10.1016/j.cmpb.2022.106920
0169-2607/

have been used even before. However, epidemiology has witness a tremendous development since those times, being nowadays a useful discipline which encompasses various branches of human knowledge, even mathematical modeling and mathematical analysis [5]. These areas play an increasingly important role in the prediction and control of new pandemics like the coronavirus disease 2019 (SARS-CoV-2) or other diseases throughout human history [6].

It is important to recall that infectious diseases progress within populations due to both the behavior of the infectious agents and the population itself. Mathematical models which describe how an epidemic progresses are based on a set of assumptions and statistics that are used to establish suitable model parameters. In turn, these parameters completely determine the mechanics of propagation of the disease to a certain degree of reliability [7]. The mathematical models obtained in the way can be used then to predict which interventions to implement or avoid in order to control a disease, as well as patterns of growth and expansion that may result [8]. As expected, there is a vast amount of mathematical models which try to predict the evolution of a disease, and these models vary in complexity from simple deterministic models [9] to complex stochastic systems [10]. The former are usually based on differential or difference equations, while the latter employ usually stochastic equations. The approach chosen by epidemiologists depends on several variables including how much is known about the epidemiology of the disease, the purpose of the study, and the quantity and quality of data available [11].

Among the mathematical models used in mathematical epidemiology, compartment-based systems are a widely used technique for the quantitative and qualitative descriptions of the propagation of a disease [12]. This technique hinges mainly on describing the possible phases of interaction that a disease can have in a population [13]. It is worth pointing out that this type of models has been used to describe various diseases, and those systems are frequently based on the use of coupled ordinary differential equations [14]. Using this approach, several studies have been carried out to simulate the spreading of some diseases that have caused havoc in recent decades. For example, there are works which model and simulate the spread of Chikungunya disease [15], the control of measles in a human population [16], the epidemiology of diabetes mellitus with lifestyle and genetic factors [17], the epidemiology of sexually transmitted diseases [18], the modeling of tuberculosis disease in the Philippines [19], and the modeling of the coronavirus disease 2019 (COVID-19) pandemic [20], among other examples.

In the particular case of COVID-19, countries are currently working hard to fight this disease. To this day, this disease accounts for 5,732,354 deaths worldwide just 2 years after its first case [21]. Since then, many studies have been reported on the mathematical model of COVID-19, including some works using compartmental models to predict the effect of social distancing and vaccination as control measures [22], compartmental models for the COVID-19 pandemic with immunity loss [23], mathematical models for the calculation of COVID-19 lockdown efficiency [24] or the assessment of sensitivity and optimal economic evaluation with control intervention [25], a simple model without vaccination and migration [26], and even some compartmental models which employ various types of fractional-order operators in both space and time [27] among many examples available in the recent literature. In summary, various models have been proposed to describe the propagation of COVID-19 under various mathematical assumptions. It is worth mentioning that some of those works provide comparisons between various models and propose improvements in order to obtain more reliable paradigms. As an example, the authors of [28] carry out some detailed comparisons between various mathematical models and, after a careful analysis, they suggest that susceptible-exposed-infected-recovered-quarantined models are fundamental in order to capture the essential characteristics in the modeling of COVID-19.

The purpose of this work is to propose a general model that allows describing the spread of various diseases (including COVID-19) under general epidemiological assumptions. To that end, we will propose a compartmental system for an arbitrary human population. In particular, we will suppose that the population is separated into subpopulations of susceptible, exposed, symptomatic and asymptomatic infected, quarantined, recovered and vaccinated individuals. Various possible interactions between them will be taken into account, including the fact that recovered individuals may become susceptible. It is important to mention that the use of suitable model parameters will allow for the application of our mathematical model to particular diseases and epidemics. Our mathematical model will be based on the use of ordinary differential equations. We will determine the equilibrium points of this system along with their local and global stability properties, as well as the basic reproductive number. We will provide several simulations in this work, all of them obtained with a computer implementation of a nonstandard finite-difference method which is capable of preserving the most relevant analytical features of the solutions of the mathematical model. We must mention beforehand that the computational results will confirm the validity of our analytical properties. Finally, we will close this manuscript with a brief summary of the conclusions obtained in our study.

2. Methods

In this section, we deduce the mathematical model used to describe the propagation of a disease under suitable epidemiological assumptions. The epidemiological model will be analyzed to determine the equilibrium solutions and their stability properties. Among other analytical results presented in this section, we will derive the expression of the basic reproductive number using the next generation matrix approach [29].

To start with, we will consider a population of human individuals which are exposed to some contagious infection. Throughout, $P(t)$ will represent the population size at the time $t \geq 0$, and we will suppose that the population is partitioned into the following seven compartments or subpopulations:

- Susceptible individuals (S).
- Exposed individuals (E).
- Asymptomatic infected individuals (I_A).
- Symptomatic infected individuals (I_S).
- Quarantined individuals (Q).
- Recovered/remove individuals (R).
- Vaccinated individuals (V).

Obviously, the sizes of these subpopulations at time $t \geq 0$ will be represented by $S(t)$, $E(t)$, $I_A(t)$, $I_S(t)$, $Q(t)$, $R(t)$ and $V(t)$, respectively. Under these assumptions, we have that

$$P(t) = S(t) + E(t) + Q(t) + I_A(t) + I_S(t) + R(t) + V(t). \tag{2.1}$$

Moreover, to provide a more realistic epidemiological model, we consider in this work a constant migration into the population. More precisely, we will assume that a rate of people equal to m_S, m_E, m_{I_A} and m_{I_S} will migrate into the sub-populations of susceptible, exposed, asymptomatic and symptomatic.

Throughout this manuscript, all the parameters and variables in our mathematical model will take on non-negative real values. We will suppose that the population has natural birth and mortality rates which will be denoted by Λ and μ, respectively. Susceptible individuals may become exposed if they have enough contact with exposed individuals at a rate of α. On the other hand, susceptible individuals will be vaccinated a rate denoted by ω. Here, we will

Table 1
Notations used in this work and their meaning.

Notations used in this manuscript and their meaning	
Parameter	Description
Λ	Recruitment rate.
τ	Rate of transfer from vaccinated individuals to susceptible.
ω	Rate of transfer from susceptible individuals to vaccinated.
α	Contact rate between susceptible individuals and exposed individuals.
ζ	Rate of transfer of exposed individuals to quarantine.
ϵ	Rate of transfer of exposed individuals to symptomatic infected individuals.
δ	Rate of transfer of exposed individuals to asymptomatic infected individuals.
ι	Recovery rate of quarantine individuals.
υ	Mortality rate due to coronavirus in quarantine individuals.
κ	Rate of transfer of symptomatic infected individuals to quarantine.
ρ	Mortality rate due to coronavirus in symptomatic infected individuals.
θ	Recovery rate of transfer of symptomatic infected individuals.
σ	Rate of transfer of recovered individuals to susceptible.
μ	Natural mortality rate.
m_S	Rate of immigration of susceptible individuals.
m_E	Rate of immigration of exposed individuals.
m_{I_A}	Rate of immigration of asymptomatic infected individuals.
m_{I_S}	Rate of immigration of symptomatic infected individuals.

suppose that the vaccine is complete effective for all individuals, so it is appropriate to consider that vaccinated people will become susceptible at a rate equal to τ.

On the other hand, exposed individuals change compartment according to three possible options. The first one is to become quarantined, and we will assume that this will take place at a rate equal to ζ. Alternatively, some exposed persons will become asymptomatic or symptomatic infected at rate equal to δ and ϵ, respectively. In turn, asymptomatic individuals may move to the recovered state at a rate given by η. Individuals in the symptomatic compartment will become quarantined at a rate of κ. This may occur when the individuals present obvious symptoms of the disease. However, individuals can just move to the recovered state at a rate of ι or θ depending on whether then were quarantined or symptomatic. It is important to notice here that some quarantined and symptomatic individuals may die from the infectious disease, and we will employ υ and ρ, respectively, to denote the rates at which these events occur. Finally, recovered individuals may become susceptible class with a rate equal to σ, under the assumption that the human body does not entirely create immunity to the disease. For convenience, Table 1 provides a summary of all the epidemiological parameters employed in this manuscript.

Figure 1 provides a flow chart which illustrates the epidemiological assumptions described above. Under these circumstances, the mathematical model describing the dynamics of propagation of the infectious disease is given by the following system of coupled nonlinear ordinary differential equations:

$$\begin{aligned}
\frac{dS}{dt} &= \Lambda + m_S + \sigma R - \alpha SE + \tau V - (\omega + \mu)S,\\
\frac{dV}{dt} &= \omega S - (\tau + \mu)V,\\
\frac{dE}{dt} &= m_E + \alpha SE - (\zeta + \epsilon + \delta + \mu)E,\\
\frac{dI_A}{dt} &= m_{I_A} + \delta E - (\eta + \mu)I_A,\\
\frac{dQ}{dt} &= \zeta E + \kappa I_S - (\iota + \upsilon + \mu)Q,\\
\frac{dI_S}{dt} &= m_{I_S} + \epsilon E - (\kappa + \rho + \theta + \mu)I_S,\\
\frac{dR}{dt} &= \iota Q + \theta I_S + \eta I_A - (\sigma + \mu)R.
\end{aligned} \tag{2.2}$$

The model will be complemented with initial conditions at the time $t = 0$. More precisely, we will assume that the initial compartment sizes will be provided by the non-negative numbers S^0, V^0, E^0, Q^0, I_A^0, I_S^0 and R^0. Obviously, they will represent respectively the initial populations of susceptible, vaccinated, exposed, quarantined, asymptomatic infected, symptomatic infected and recovered.

It is important to notice that the mathematical model (2.2) has one disease-free equilibrium solution. To check this fact, let us assume a constant solution for the mathematical model in which $E = Q = I_A = I_S = R = 0$. After some algebra, we readily check that the disease-free equilibrium P_{DFE} is the point whose coordinates are given by

$$\begin{aligned}
P_{DFE} &= (S_0, V_0, 0, 0, 0, 0, 0)\\
&= \left(\frac{(\Lambda + m_S)(\mu + \tau)}{\mu(\mu + \omega + \tau)}, \frac{\omega(\Lambda + m_S)}{\mu(\mu + \omega + \tau)}, 0, 0, 0, 0, 0\right).
\end{aligned} \tag{2.3}$$

In order to calculate the basic reproductive number $\mathcal{R}_0$, we will employ the next generation matrix technique. Beforehand, recall that $\mathcal{R}_0$ is the expected value of infection rate per time unit. Let us consider only those compartments of the mathematical model (2.2) which contribute to the dynamics of the infection, that is, let us consider the system

$$\begin{aligned}
\frac{dE}{dt} &= m_E + \alpha SE - (\zeta + \epsilon + \delta + \mu)E,\\
\frac{dI_A}{dt} &= m_{I_A} + \delta E - (\eta + \mu)I_A,\\
\frac{dQ}{dt} &= \zeta E + \kappa I_S - (\iota + \upsilon + \mu)Q,\\
\frac{dI_S}{dt} &= m_{I_S} + \epsilon E - (\kappa + \rho + \theta + \mu)I_S,
\end{aligned} \tag{2.4}$$

Following the approach in [29], we define the vectors

$$\mathcal{F} = \begin{pmatrix} \alpha S(t)E(t) \\ 0 \\ 0 \\ 0 \end{pmatrix} \tag{2.5}$$

and

$$\mathcal{V} = \begin{pmatrix} -m_E + (\zeta + \epsilon + \delta + \mu)E \\ -m_{I_A} - \delta E + (\eta + \mu)I_A \\ -\zeta E - \kappa I_S + (\iota + \upsilon + \mu)Q, \\ -m_{I_S} - \epsilon E + (\kappa + \rho + \theta + \mu)I_S \end{pmatrix}. \tag{2.6}$$

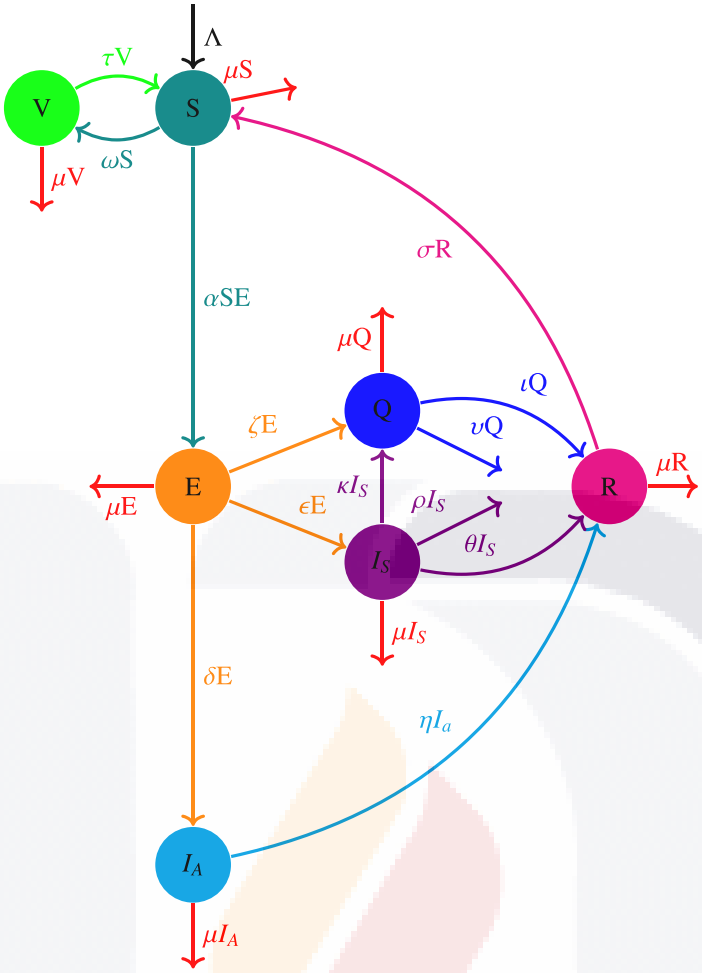

Fig. 1. Flow chart describing graphically the dynamics of the compartmental epidemiological model proposed in this work.

Their Jacobian matrices are, respectively,

$$F = \begin{pmatrix} \frac{\alpha(\Lambda+m_S)}{\omega+\mu} & 0 & 0 & 0 \\ 0 & 0 & 0 & 0 \\ 0 & 0 & 0 & 0 \\ 0 & 0 & 0 & 0 \end{pmatrix} \tag{2.7}$$

and

$$V = \begin{pmatrix} \zeta+\epsilon+\delta+\mu & 0 & 0 & 0 \\ -\delta & \eta+\mu & 0 & 0 \\ -\zeta & 0 & \iota+\upsilon+\mu & -\kappa \\ -\epsilon & 0 & 0 & \kappa+\rho+\theta\mu \end{pmatrix}. \tag{2.8}$$

A straightforward calculation shows that

$$G = FV^{-1} = \begin{pmatrix} \frac{\alpha(\Lambda+m_S)}{X(\omega+\mu)} & g_{12} & g_{13} & g_{14} \\ 0 & 0 & 0 & 0 \\ 0 & 0 & 0 & 0 \\ 0 & 0 & 0 & 0 \end{pmatrix}, \tag{2.9}$$

where g_{12}, g_{13} and g_{14} are real numbers, and

$$X = \delta+\epsilon+\mu+\zeta. \tag{2.10}$$

As a consequence, we obtain that the basic reproductive number is provided by the expression

$$\mathcal{R}_0 = \frac{\alpha(\Lambda+m_S)}{(\delta+\epsilon+\mu+\zeta)(\omega+\mu)}. \tag{2.11}$$

Our next result summarizes the local stability analysis of the disease-free equilibrium.

Theorem 1. *The disease-free equilibrium of system (2.2) is locally asymptotically stable if* $\mathcal{R}_0 < 1$.

Proof. Let J represent the Jacobian matrix of associated to the system (2.2), and use J^* to represent the matrix J evaluated at the disease-free equilibrium solution. It is easy to check then that the Jacobian matrix is given by

$$J = \begin{pmatrix} J_{11} & \tau & -\alpha S & 0 & 0 & 0 & \sigma \\ \omega & J_{22} & 0 & 0 & 0 & 0 & 0 \\ \alpha E & 0 & J_{33} & 0 & 0 & 0 & 0 \\ 0 & 0 & \delta & J_{44} & 0 & 0 & 0 \\ 0 & 0 & \zeta & 0 & J_{55} & \kappa & 0 \\ 0 & 0 & \epsilon & 0 & 0 & J_{66} & 0 \\ 0 & 0 & 0 & \eta & \iota & \theta & J_{77} \end{pmatrix} \tag{2.12}$$

where

$$J_{11} = -\alpha E - (\omega+\mu), \tag{2.13}$$

$$J_{22} = -(\tau+\mu), \tag{2.14}$$

$$J_{33} = \alpha S - (\zeta+\epsilon+\delta+\mu), \tag{2.15}$$

$$J_{44} = -(\eta+\mu), \tag{2.16}$$

$$J_{55} = -(\iota + \upsilon + \mu), \tag{2.17}$$

$$J_{66} = -(\kappa + \rho + \theta + \mu), \tag{2.18}$$

$$J_{77} = -(\sigma + \mu). \tag{2.19}$$

Let λ be any complex number, and let I be the identity matrix of order 7. If we let $M = J^* - \lambda I$, then it is easy to check that

$$M = \begin{pmatrix} M_{11} & \tau & M_{13} & 0 & 0 & 0 & \sigma \\ \omega & M_{22} & 0 & 0 & 0 & 0 & 0 \\ 0 & 0 & M_{33} & 0 & 0 & 0 & 0 \\ 0 & 0 & \delta & M_{44} & 0 & 0 & 0 \\ 0 & 0 & \zeta & 0 & M_{55} & \kappa & 0 \\ 0 & 0 & \epsilon & 0 & 0 & M_{66} & 0 \\ 0 & 0 & 0 & \eta & \iota & \theta & M_{77} \end{pmatrix}. \tag{2.20}$$

In this expression for the matrix M, we observe the following definitions for the components:

$$M_{11} = -(\omega + \mu) - \lambda, \tag{2.21}$$

$$M_{13} = \frac{\alpha(\Lambda + m_S)(\mu + \tau)}{\mu(\mu + \omega + \tau)}, \tag{2.22}$$

$$M_{22} = -(\tau + \mu) - \lambda, \tag{2.23}$$

$$M_{33} = \frac{\alpha(\Lambda + m_S)(\mu + \tau)}{\mu(\mu + \omega + \tau)} - (\zeta + \epsilon + \delta + \mu) - \lambda, \tag{2.24}$$

$$M_{44} = -(\eta + \mu) - \lambda, \tag{2.25}$$

$$M_{55} = -(\iota + \upsilon + \mu) - \lambda, \tag{2.26}$$

$$M_{66} = -(\kappa + \rho + \theta + \mu) - \lambda, \tag{2.27}$$

$$M_{77} = -(\sigma + \mu) - \lambda. \tag{2.28}$$

Using properties of determinants, it is possible to check that

$$\det M = (M_{11}M_{22} - \omega\tau)M_{33}M_{44}M_{55}M_{66}M_{77}. \tag{2.29}$$

Setting the determinant equal to zero, solving for the unknown λ and rearranging terms algebraically, it follows that five of the eigenvalues of J^* are

$$\lambda_1 = (\zeta + \epsilon + \delta + \mu)(\mathcal{R}_0 - 1), \tag{2.30}$$

$$\lambda_2 = -(\eta + \mu) < 0, \tag{2.31}$$

$$\lambda_3 = -(\iota + \upsilon + \mu) < 0, \tag{2.32}$$

$$\lambda_4 = -(\kappa + \rho + \theta + \mu) < 0, \tag{2.33}$$

$$\lambda_5 = -(\sigma + \mu) < 0, \tag{2.34}$$

The remaining eigenvalues satisfy the quadratic equation

$$\lambda^2 + (\omega + \tau + 2\mu)\lambda + (\omega + \tau + \mu)\mu = 0. \tag{2.35}$$

Descartes' rule of signs imply that the number of negative roots for this polynomial is 0 or 2. However, the quadratic formula shows that the roots are

$$\lambda_{6,7} = \frac{-(\omega + \tau + 2\mu) \pm \sqrt{\omega^2 + \tau^2 + \omega\tau}}{2}. \tag{2.36}$$

It follows that λ_6 and λ_7 are negative. Summarizing, notice that all the eigenvalues are negative if $\mathcal{R}_0 < 1$, in which case the disease-free equilibrium solution is locally asymptotically stable, as desired. □

Next, we proceed to calculate the endemic equilibrium solution. To that end, we assume a constant solution for the system (2.2), of the form $S(t) = S^*$, $E(t) = E^*$, $V(t) = V^*$, $I_A(t) = I_A^*$, $Q(t) = Q^*$, $I_S(t) = I_S^*$ and $R(t) = R^*$, valid for all $t \geq 0$. Here, S^*, E^*, V^*, I_A^*, Q^*, I_S^* and R^* are non-negative constants. For the sake of convenience, we define

$$P_{EE} = (S^*, V^*, E^*, I_A^*, Q^*, I_S^*, R^*). \tag{2.37}$$

Under these hypotheses, the mathematical model (2.2) reduces to the following system of algebraic equations:

$$\begin{aligned} &\Lambda + m_S + \sigma R^* - \alpha S^* E^* + \tau V^* - (\omega + \mu)S^* = 0, \\ &\omega S^* - (\tau + \mu)V^* = 0, \\ &m_E + \alpha S^* E^* - (\zeta + \epsilon + \delta + \mu)E^* = 0, \\ &m_{I_A} + \delta E^* - (\eta + \mu)I_A^* = 0, \\ &\zeta E^* + \kappa I_S^* - (\iota + \upsilon + \mu)Q^* = 0, \\ &m_{I_S} + \epsilon E^* - (\kappa + \rho + \theta + \mu)I_S^* = 0, \\ &\iota Q^* + \theta I_S^* + \eta I_A^* - (\sigma + \mu)R^* = 0. \end{aligned} \tag{2.38}$$

Proceeding algebraically, we may reach the identities:

$$S^* = \frac{\Lambda + m_s + \sigma R^* + \tau V^*}{\mu + \omega + \alpha E^*}, \tag{2.39}$$

$$V^* = \frac{S^*\omega}{\mu + \tau}, \tag{2.40}$$

$$E^* = \frac{m_e}{\delta + \epsilon + \mu + \zeta - \alpha S^*}, \tag{2.41}$$

$$I_A^* = \frac{m_{I_A} + \delta E^*}{\eta + \mu}, \tag{2.42}$$

$$Q^* = \frac{\kappa^* I_S + \zeta E^*}{\iota + \mu + \upsilon}, \tag{2.43}$$

$$I_S^* = \frac{m_{I_S} + \epsilon E^*}{\kappa + \mu + \rho + \theta}, \tag{2.44}$$

$$R^* = \frac{\eta I_A^* + \iota Q^* + \theta I_S^*}{\mu + \sigma}. \tag{2.45}$$

Moreover, after more tedious algebraic manipulations (or, equivalently, using symbolic software), it is possible to find out that

$$S^* = \frac{\delta + \epsilon + \mu + \zeta}{\alpha}, \tag{2.46}$$

$$V^* = \frac{\omega(\delta + \epsilon + \mu + \zeta)}{\alpha(\mu + \tau)}. \tag{2.47}$$

We provide here the exact expressions for S^* and V^* only in view that they are relatively short. The expressions for the remaining coordinates of the endemic equilibrium point are actually too long to be written in this column. However, we must mention that all the coordinates are non-negative real numbers.

Theorem 2. *The endemic equilibrium point of system (2.2) is locally asymptotically stable if* $\mathcal{R}_0 < 1$.

Proof. Notice that the Jacobian matrix evaluated at the endemic equilibrium point is given now by

$$J^* = \begin{pmatrix} J_{11}^* & \tau & -\alpha S^* & 0 & 0 & 0 & \sigma \\ \omega & J_{22}^* & 0 & 0 & 0 & 0 & 0 \\ \alpha E^* & 0 & J_{33}^* & 0 & 0 & 0 & 0 \\ 0 & 0 & \delta & J_{44}^* & 0 & 0 & 0 \\ 0 & 0 & \zeta & 0 & J_{55}^* & \kappa & 0 \\ 0 & 0 & \epsilon & 0 & 0 & J_{66}^* & 0 \\ 0 & 0 & 0 & \eta & \iota & \theta & J_{77}^* \end{pmatrix}, \tag{2.48}$$

where

$$J_{11}^* = -\alpha E^* - (\omega + \mu), \tag{2.49}$$

$$J_{22}^* = -(\tau + \mu), \tag{2.50}$$

$$J_{33}^* = \alpha S^* - (\zeta + \epsilon + \delta + \mu), \tag{2.51}$$

$$J_{44}^* = -(\eta + \mu), \tag{2.52}$$

$$J_{55}^* = -(\iota + \upsilon + \mu), \tag{2.53}$$

$$J_{66}^* = -(\kappa + \rho + \theta + \mu), \tag{2.54}$$

$$J_{77}^* = -(\sigma + \mu). \tag{2.55}$$

However, the value of S^* in the endemic case guarantees that $J_{33}^* = 0$. Using this fact and the properties of determinants, it is easy to check that the determinant of $M = J^* - \lambda I$ is given by

$$\det M = \lambda^7 + Q_1\lambda^6 + \ldots + Q_6\lambda + Q_7, \tag{2.56}$$

where the expressions of the coefficients Q_i can be algebraically obtained, and are given in terms of the model parameters and the endemic equilibrium point. The exact expressions of these coefficients are long, and they were computed using symbolic algebra. We omit their expressions in view of the space available. The system is stable if the eigenvalues of the Jacobian matrix at the endemic point all have negative real parts. Using the Routh–Hurwitz criterion [30] and symbolic algebra, we obtain that the endemic equilibrium is stable if $\mathcal{R}_0 < 1$. □

In the next result, we will employ the gradient operator

$$\nabla = \left(\frac{\partial}{\partial S}, \frac{\partial}{\partial V}, \frac{\partial}{\partial E}, \frac{\partial}{\partial I_A}, \frac{\partial}{\partial Q}, \frac{\partial}{\partial I_S}, \frac{\partial}{\partial R} \right). \tag{2.57}$$

Theorem 3. *The system (2.2) has no periodic solutions.*

Proof. To establish this proposition, we will use the well known Dulac's criterion. Let $F : \mathbb{R} \to \mathbb{R}^7$ be the function defined component-wise for each $t \in \mathbb{R}$ by the expression

$$F(t) = (S(t), V(t), E(t), I_A(t), Q(t), I_S(t), R(t)). \tag{2.58}$$

Moreover, let

$$G(t) = \frac{1}{S(t)E(t)}, \quad \forall t \geq 0. \tag{2.59}$$

Using differentiation, it is easy to check that

$$\frac{\partial}{\partial S}\left(G\frac{dS}{dt}\right) = -\frac{\Lambda + m_S + \sigma R + \tau V}{S^2 E}, \tag{2.60}$$

$$\frac{\partial}{\partial V}\left(G\frac{dV}{dt}\right) = -\frac{\tau + \mu}{SE}, \tag{2.61}$$

$$\frac{\partial}{\partial E}\left(G\frac{dE}{dt}\right) = -\frac{m_E}{SE^2}, \tag{2.62}$$

$$\frac{\partial}{\partial I_A}\left(G\frac{dI_A}{dt}\right) = -\frac{\eta + \mu}{SE}, \tag{2.63}$$

$$\frac{\partial}{\partial Q}\left(G\frac{dQ}{dt}\right) = -\frac{\iota + \upsilon + \mu}{SE}, \tag{2.64}$$

$$\frac{\partial}{\partial I_S}\left(G\frac{dI_S}{dt}\right) = -\frac{\kappa + \rho + \theta + \mu}{SE}, \tag{2.65}$$

$$\frac{\partial}{\partial R}\left(G\frac{dR}{dt}\right) = -\frac{\sigma + \mu}{SE}. \tag{2.66}$$

We can check now that

$$\nabla \cdot \left(G\frac{dF}{dt}\right) < 0. \tag{2.67}$$

The conclusion follows now from Dulac's criterion. □

Finally, we turn our attention to the problem on the existence and uniqueness of non-negative solutions of the mathematical model (2.2). To start with, it is obvious that solutions of (2.2) exist and are unique, for any set of initial conditions. This is a straightforward consequence of the fact that the model can be equivalently rewritten in the form

$$\frac{d\mathbf{x}}{dt} = \mathbf{F}(\mathbf{x}), \tag{2.68}$$

where the function $\mathbf{x} : [0, \infty) \to \mathbb{R}^7$ is given by

$$\mathbf{x}(t) = (S(t), E(t), Q(t), I_A(t), I_S(t), R(t), V(t)), \tag{2.69}$$

for each $t \geq 0$. Moreover, the function $\mathbf{F} : \mathbb{R}^7 \to \mathbb{R}^7$ is given component-wise by $\mathbf{F} = (F_1, \ldots, F_7)$, where each of the functions F_i depends on $\mathbf{x}$, and is given by the right-hand side of the ith differential equation in (2.2). The fact that $\mathbf{F}$ is continuously differentiable assures the existence and uniqueness of continuous solutions for the mathematical model (2.2), for any set of initial conditions.

Theorem 4. *If the initial conditions* S^0, V^0, E^0, Q^0, I_A^0, I_S^0 *and* R^0 *are non-negative numbers, then the corresponding solution functions of the model (2.2) are likewise non-negative.*

Proof. We proceed by contradiction. Suppose that some of the solutions take on negative values, and let $t_0 \geq 0$ be the greatest lower bound for which any of the solution functions is negative. Let U represent the function for which this greatest lower bound occurs, and notice that $U(t_0) = 0$. There are several cases whose proofs are entirely similar. We will only consider here the case in which $U = S$. Observe then that $S(t_0) = 0$ and all the other functions at that time take on non-negative values. In particular, this implies that $R(t_0) \geq 0$ and $V(t_0) \geq 0$. Using now that first equation of (2.2), it follows that

$$\begin{aligned} \frac{dS(t_0)}{dt} &= \Lambda + m_S + \sigma R(t_0) + \tau V(t_0) \\ &\geq \Lambda + m_S > 0. \end{aligned} \tag{2.70}$$

Thus, there exists $\delta > 0$ with the property that $S(t) > 0$, for each $t \in (t_0, t_0 + \delta)$. This contradicts the definition of t_0, and we conclude that all the solution functions of the mathematical model (2.2) are non-negative for all times $t \geq 0$. □

Next, we would like to establish a bound for the growth of the population described by the epidemiological model (2.2). To that

end, we add all the ordinary differential equations in (2.2) and simplify terms algebraically. It is easy to check that

$$\frac{dN}{dt} = \Lambda + m_S + m_E + m_{I_A} + m_{I_S} - \mu N - \nu Q - \rho I_S. \tag{2.71}$$

Assuming that the initial population sizes of the compartments are non-negative, then the solution functions are likewise non-negative. As a consequence, the rate of change of increase of the total population is bounded from above by the non-negative constant $\Lambda + m_S + m_E + m_{I_A} + m_{I_S}$. A straightforward integration yields then that, for each $t \geq 0$,

$$P(t) \leq P^0 + (\Lambda + m_S + m_E + m_{I_A} + m_{I_S})t, \tag{2.72}$$

where $P^0 = S^0 + V^0 + E^0 + Q^0 + I_A^0 + I_S^0 + R^0$. In view of this inequality, the following result is trivial.

Theorem 5. *Suppose that the initial conditions S^0, V^0, E^0, Q^0, I_A^0, I_S^0 and R^0 are non-negative numbers, and let T be a positive time period. Then the non-negative constant*

$$B = P^0 + (\Lambda + m_S + m_E + m_{I_A} + m_{I_S})T \tag{2.73}$$

is a uniform bound for the solution functions of (2.2). □

As a consequence of the local stability properties, the boundedness of the solutions of the mathematical model (2.2) and the absence of periodic solutions, we conclude that the steady-state solutions are globally asymptotically stable.

Before closing this section, we provide a standard sensitivity analysis of the basic reproductive number with respect to the model parameters. To that end, for each parameter ϕ of the model, define the constant

$$A_\phi = \frac{\phi}{\mathcal{R}_0}\frac{\partial \mathcal{R}_0}{\partial \phi}. \tag{2.74}$$

Notice then that

$$A_\alpha = 1, \qquad A_\Lambda = \frac{\Lambda}{\Lambda + m_S}, \tag{2.75}$$

$$A_{m_S} = \frac{m_S}{\Lambda + m_S}, \qquad A_\delta = -\frac{\delta}{\delta + \epsilon + \mu + \zeta}, \tag{2.76}$$

$$A_\epsilon = -\frac{\epsilon}{\delta + \epsilon + \mu + \zeta}, \qquad A_\zeta = -\frac{\zeta}{\delta + \epsilon + \mu + \zeta}, \tag{2.77}$$

$$A_\omega = -\frac{\omega}{\omega + \mu}, \tag{2.78}$$

and

$$A_\mu = -\frac{\mu(\omega + 2\mu + \delta + \epsilon + \zeta)}{(\delta + \epsilon + \mu + \zeta)(\omega + \mu)}. \tag{2.79}$$

Observe that only A_α, A_Λ and A_{m_S} are positive. We conclude that the basic reproductive number is sensitive only to the model parameters α, Λ and m_S.

3. Results

In this section, we introduce a finite-difference scheme to approximate the solutions of (2.2). The methodology will be designed using the nonstandard approach popularized by Mickens in various of his seminal papers and monographs [31–33]. As the most important results, we will establish the main theoretical properties of our discretization, namely, the consistency, the stability and the convergence. Moreover, We will prove the capability of our scheme to preserve the positivity of the solutions, the constant solutions and their stability.

For the sake of convenience, agree that $I_n = \{1, \ldots, n\}$ and $\bar{I}_n = I_n \cup \{0\}$, for each $n \in \mathbb{N}$. We will approximate the solutions of our epidemiological model on a finite interval of time $[0, T]$, where $T \geq 0$. Let $N \in \mathbb{N}$, and fix a regular partition of the interval $[0, T]$ of the form

$$0 = t_0 \leq t_1 < \ldots < t_n < \ldots < t_N = T, \tag{3.1}$$

for each $n \in \bar{I}_N$. For convenience, the associated partition norm will be represented by Δt where, obviously, $\Delta t = T/N$ is a positive real number. We will use the lower-case symbols s, v, e, i_A, q, i_S, r and p to represent numerical approximations to the exact values of the functions S, V, E, I_A, Q, I_S, R and P, respectively. Moreover, if w is any of the lower-case symbols, then we will convey that $w^n = w(t_n)$, for each $n \in \bar{I}_N$. Furthermore, we introduce the following linear discrete operator:

$$\hat{\delta}_t w^n = \frac{w^{n+1} - w^n}{\Delta t}. \tag{3.2}$$

It is well known that this operator provides a consistent approximation to the derivative if W at the point t_n, with consistency order equal to one in time. Alternatively, it also yields a first-order consistent approximation of the derivative of W with respect to t at the time t_{n+1}.

Using this nomenclature, the finite-difference scheme employed to approximate the solutions of the system (2.2) at time t_n is given by the algebraic nonlinear system of equations

$$\begin{aligned}
\hat{\delta}_t s^n &= \Lambda + m_S + \sigma r^n - \alpha s^{n+1} e^{n+1} + \tau v^n - (\omega + \mu) s^{n+1},\\
\hat{\delta}_t v^n &= \omega s^n - (\tau + \mu) v^{n+1},\\
\hat{\delta}_t e^n &= m_E + \alpha s^n e^n - (\zeta + \epsilon + \delta + \mu) e^{n+1},\\
\hat{\delta}_t i_A^n &= m_{I_A} + \delta e^n - (\eta + \mu) i_A^{n+1},\\
\hat{\delta}_t q^n &= \zeta e^n + \kappa i_S^n - (\iota + \upsilon + \mu) q^{n+1},\\
\hat{\delta}_t i_S^n &= m_{I_S} + \epsilon e^n - (\kappa + \rho + \theta + \mu) i_S^{n+1},\\
\hat{\delta}_t r^n &= \iota q^n + \theta i_S^n + \eta i_A^n - (\sigma + \mu) r^{n+1}.
\end{aligned} \tag{3.3}$$

Obviously, this is a nonstandard discretization in the sense that the approximations provided for some terms in the scheme are provided in a non-local manner. The numerical model is a two-step system which will be theoretically analyzed in this section. To that end, it is important to notice that the discrete model (3.3) can be alternatively expressed in explicit form. After some algebraic manipulations, the finite-difference scheme can be equivalently rewritten as

$$\begin{aligned}
s^{n+1} &= \frac{s^n + (\Lambda + m_S + \sigma r^n + \tau v^n)\Delta t}{1 + (\alpha e^{n+1} + \omega + \mu)\Delta t},\\
v^{n+1} &= \frac{v^n + \omega s^n \Delta t}{1 + (\tau + \mu)\Delta t},\\
e^{n+1} &= \frac{e^n + (m_E + \alpha s^n e^n)\Delta t}{1 + (\zeta + \epsilon + \delta + \mu)\Delta t},\\
i_A^{n+1} &= \frac{i_A^n + (m_{I_A} + \delta e^n)\Delta t}{1 + (\eta + \mu)\Delta t},\\
q^{n+1} &= \frac{q^n + (\zeta e^n + \kappa i_S^n)\Delta t}{1 + (\iota + \upsilon + \mu)\Delta t},\\
i_S^{n+1} &= \frac{i_S^n + (m_{I_S} + \epsilon e^n)\Delta t}{1 + (\kappa + \rho + \theta + \mu)\Delta t},\\
r^{n+1} &= \frac{r^n + (\iota q^n + \theta i_S^n + \eta i_A^n)\Delta t}{1 + (\sigma + \mu)\Delta t}.
\end{aligned} \tag{3.4}$$

From this discussion, it is obvious that the discrete model (3.3) is a semi-explicit algebraic system. We just need to point out that s^{n+1} is given in terms of e^{n+1} as the first equation of (3.4) shows. However, this shortcoming can be saved calculating firstly e^{n+1} from the third equation, and the obtaining s^{n+1} from

the first identity of (3.4). Moreover, the following theoretical result is also straightforward. The reader will notice that this is the discrete version of Theorem 4.

Theorem 6. *If the initial conditions S^0, V^0, E^0, Q^0, I_A^0, I_S^0 and R^0 are non-negative, then the discrete system (3.3) has a unique solution, and all the solution functions are non-negative.*

Proof. If $n = 0$, then $s^0 = S^0$, $v^0 = V^0$, $e^0 = E^0$, $i_A^0 = I_A^0$, $q^0 = Q^0$, $i_S^0 = I_S^0$ and $r^0 = R^0$ are non-negative numbers by hypothesis. Now, suppose that the conclusion of this result is true for some $n \in \bar{I}_{N-1}$. Under these circumstances, the right-hand sides of the identities in (3.4) are non-negative. As a consequence, the approximations at time t_{n+1} are also non-negative, and the conclusion of this theorem follows by induction. □

Our next step is to obtain a discrete form of the inequality (2.72). To that end, let us suppose that the initial conditions are all non-negative. As a consequence of the previous theorem, the numerical solutions are likewise non-negative. Add together the equations in the discrete system (3.3) and simplify terms. It is easy check that if $n \in \bar{I}_{N-1}$, then

$$\begin{aligned}\hat{\delta}_t p^n &= \Lambda + m_S + m_E + m_{I_A} + m_{I_S} - \mu p^{n+1} - \rho i_S^{n+1} \\ &\quad - \nu q^{n+1} + \sigma(r^n - r^{n+1}) + \tau(v^n - v^{n+1}) \\ &\quad + \omega(s^n - s^{n+1}) + (\delta + \epsilon + \zeta)(e^n - e^{n+1}) \\ &\quad + (\kappa + \theta)(i_S^n - i_S^{n+1}) + \eta(i_A^n - i_A^{n+1}) \\ &\quad + \iota(p^n - q^{n+1}) + \alpha(s^n e^n - s^{n+1} e^{n+1}). \end{aligned} \tag{3.5}$$

Let $k \in I_N$, and take the sum on both sides of this equation for n between 0 and $k-1$. Using the formula for telescoping sums, simplifying algebraically, rearranging terms, recalling that the solutions of the discrete model (3.3) are non-negative and using the fact that $t_k = k\Delta t$, we obtain the following upper bound for the total population at the time t_k:

$$\begin{aligned} p^k &\le p^0 + (\Lambda + m_S + m_E + m_{I_A} + m_{I_S})t_k \\ &\quad + \Delta t\Big[\sigma r^0 + \tau v^0 + \omega s^0 + (\delta + \epsilon + \zeta)e^0 \\ &\quad + (\kappa + \theta)i_S^0 + \eta i_A^0 + \iota p^0 + \alpha s^0 e^0\Big]. \end{aligned} \tag{3.6}$$

Observe that the continuous estimate (2.72) is recovered from this last inequality when we let $\Delta t \to 0$. Moreover, we have the following discrete version of Theorem 5.

Theorem 7. *Suppose that the initial conditions S^0, V^0, E^0, Q^0, I_A^0, I_S^0 and R^0 are non-negative. Then the non-negative number*

$$\begin{aligned} b &= p^0 + (\Lambda + m_S + m_E + m_{I_A} + m_{I_S})T \\ &\quad + \Delta t\Big[\sigma r^0 + \tau v^0 + \omega s^0 + (\delta + \epsilon + \zeta)e^0 \\ &\quad + (\kappa + \theta)i_S^0 + \eta i_A^0 + \iota p^0 + \alpha s^0 e^0\Big]. \end{aligned} \tag{3.7}$$

is a uniform bound for the solutions of model (3.3). □

The following theorem establishes that the disease-free and the endemic equilibrium solutions are also constant solutions of the numerical model (3.3). Moreover, their stability properties are also preserved in the discrete scenario.

Theorem 8. *The points P_{DFE} and P_{EE} are constant solutions of the numerical model (3.3). Moreover, the following hold:*

- *The point P_{DFE} is locally asymptotically stable if $\mathcal{R}_0 < 1$, and unstable if $\mathcal{R}_0 > 1$.*
- *The point P_{EE} is locally asymptotically stable if $\mathcal{R}_0 < 1$, and unstable if $\mathcal{R}_0 > 1$.*

Proof. The points are constant solutions of (3.3) follows after a simple substitution in that system. On the other hand, the local stability properties of the numerical model are satisfied in view that the Jacobian matrix of the discrete system (3.3) is the same as that of the continuous model (2.2). □

Next we establish the numerical properties of our finite-difference scheme. More precisely, we will prove that the numerical scheme (3.3) is consistent, stable and convergent. To that end, let us define the differential operators

$$\begin{aligned} \mathcal{L}_S &= \frac{dS}{dt} - \Lambda - m_S - \sigma R + \alpha SE - \tau V + (\omega + \mu)S, \\ \mathcal{L}_V &= \frac{dV}{dt} - \omega S + (\tau + \mu)V, \\ \mathcal{L}_E &= \frac{dE}{dt} - m_E - \alpha SE + (\zeta + \epsilon + \delta + \mu)E, \\ \mathcal{L}_{I_A} &= \frac{dI_A}{dt} - m_{I_A} - \delta E + (\eta + \mu)I_A, \\ \mathcal{L}_Q &= \frac{dQ}{dt} - \zeta E - \kappa I_S + (\iota + \upsilon + \mu)Q, \\ \mathcal{L}_{I_S} &= \frac{dI_S}{dt} - m_{I_S} - \epsilon E + (\kappa + \rho + \theta + \mu)I_S, \\ \mathcal{L}_R &= \frac{dR}{dt} - \iota Q - \theta I_S - \eta I_A + (\sigma + \mu)R. \end{aligned} \tag{3.8}$$

Obviously, these continuous operators are defined for each $t \in [0, T]$. For each $n \in \bar{I}_{N-1}$ and W being any of the solution functions of (2.2), agree that $\mathcal{L}_W^n = \mathcal{L}_W(t_n)$. On the other hand, define also the difference operators

$$\begin{aligned} L_S^n &= \hat{\delta}_t S^n - \Lambda - m_S - \sigma R^n + \alpha S^{n+1} E^n - \tau V^n \\ &\quad + (\omega + \mu)S^{n+1}, \\ L_V^n &= \hat{\delta}_t V^n - \omega S^n + (\tau + \mu)V^{n+1}, \\ L_E^n &= \hat{\delta}_t E^n - m_E - \alpha S^n E^n + (\zeta + \epsilon + \delta + \mu)E^{n+1}, \\ L_{I_A}^n &= \hat{\delta}_t I_A^n - m_{I_A} - \delta E^n + (\eta + \mu)I_A^{n+1}, \\ L_Q^n &= \hat{\delta}_t Q^n - \zeta E^n - \kappa I_S^n + (\iota + \upsilon + \mu)Q^{n+1}, \\ L_{I_S}^n &= \hat{\delta}_t I_S^n - m_{I_S} - \epsilon E^n + (\kappa + \rho + \theta + \mu)I_S^{n+1}, \\ L_R^n &= \hat{\delta}_t R^n - \iota Q^n - \theta I_S^n - \eta I_A^n + (\sigma + \mu)R^{n+1}. \end{aligned} \tag{3.9}$$

Let us define now

$$\mathcal{L}^n = (\mathcal{L}_S^n, \mathcal{L}_V^n, \mathcal{L}_E^n, \mathcal{L}_{I_A}^n, \mathcal{L}_Q^n, \mathcal{L}_{I_S}^n, \mathcal{L}_R^n), \tag{3.10}$$

$$L^n = (L_S^n, L_V^n, L_E^n, L_{I_A}^n, L_Q^n, L_{I_S}^n, L_R^n), \tag{3.11}$$

for each $n \in \bar{I}_{N-1}$. In the following, we will use $\|\cdot\|_1$ and $\|\cdot\|_\infty$ to denote, respectively, the L^1-norm and the infinity norm in $\mathbb{R}^7$. More precisely, if $\xi = (\xi_1, \dots \xi_7) \in \mathbb{R}^7$, then

$$\|\xi\|_1 = \sum_{i=1}^{7} |\xi_i|, \tag{3.12}$$

$$\|\xi\|_\infty = \max\{|\xi_i| : i \in I_7\}. \tag{3.13}$$

Moreover, we introduce the norm

$$|||\mathcal{L} - L|||_\infty = \max\left\{\|\mathcal{L}^n - L^n\|_\infty : n \in \bar{I}_{N-1}\right\}. \tag{3.14}$$

Using this nomenclature, we will prove firstly the consistency of the finite-difference method (3.3).

Theorem 9. *If $S, V, E, I_A, Q, I_S, R : [0, T] \to \mathbb{R}$ are of class $\mathcal{C}^2([0, T])$, then there exists a constant $C \ge 0$ which is independent of Δt, such that $|||\mathcal{L} - L|||_\infty \le C\Delta t$.*

Proof. Let $n \in \bar{I}_{N-1}$. Using the regularity of the function E, it follows that this function is bounded on $[0,T]$ by some non-negative constant K_E. Moreover, since S is of class $\mathcal{C}^2([0,T])$, Taylor's theorem readily guarantees that there exist constants $C_1', C_2' \geq 0$ which are independent of Δt, with the property that

$$\left|\frac{dS^n}{dt} - \hat{\delta}_t S^n\right| \leq C_1' \Delta t, \tag{3.15}$$

$$\left|S^n - S^{n+1}\right| \leq C_2' \Delta t, \tag{3.16}$$

for each $n \in \bar{I}_{N-1}$. As a consequence of these inequalities, algebraic simplifications and the triangle inequality, it follows that

$$\begin{aligned} |\mathcal{L}_S^n - L_S^n| &\leq \left|\frac{dS^n}{dt} - \hat{\delta}_t S^n\right| + \alpha |E^n| \left|S^n - S^{n+1}\right| \\ &\quad + (\omega+\mu)\left|S^n - S^{n+1}\right| \\ &\leq C_1' \Delta t + (\alpha K_E + \omega + \mu) C_2' \Delta t \\ &= C_S \Delta t, \end{aligned} \tag{3.17}$$

for each $n \in \bar{I}_{N-1}$. Here,

$$C_S = C_1' + (\alpha K_E + \omega + \mu) C_2', \tag{3.18}$$

which is a non-negative constant that is independent of Δt. It follows then that $\|\mathcal{L}_S - L_S\|_\infty \leq C_S \Delta t$. In similar fashion, it is possible to show that there exist constants $C_W \geq 0$ which are independent of Δt for $W = V, E, I_A, Q, I_S, R$, such that the inequality $\|\mathcal{L}_W - L_W\| \leq C_W \Delta t$ is satisfied. Now, if we define the non-negative constant

$$C = \max\{C_S, C_V, C_E, C_{I_A}, C_Q, C_{I_S}, C_R\}, \tag{3.19}$$

then the constant C is independent of Δt and it satisfies the conclusion of this theorem, as desired. □

Next, we turn our attention to the stability and convergence properties of the finite-difference scheme (3.3). The following discrete form of Gronwall's inequality will be needed.

Lemma 1 (Pen-Yu [34])**.** *Let $(\omega^n)_{n=0}^N$ and $(\rho^n)_{n=0}^N$ be finite sequences of nonnegative mesh functions, and suppose that there exists $C \geq 0$ such that*

$$\omega^k \leq \rho^k + C\tau \sum_{n=0}^{k-1} \omega^k, \quad \forall k \in I_{N-1}. \tag{3.20}$$

Then $\omega^n \leq \rho^n e^{Cn\tau}$ for each $n \in \bar{I}_N$. □

To establish the stability property, we will consider two sets of non-negative initial conditions for the finite-difference scheme, which we will denote respectively by

$$L^0 = (S^0, V^0, E^0, I_A^0, Q^0, I_S^0, R^0), \tag{3.21}$$

$$\tilde{L}^0 = (\tilde{S}^0, \tilde{V}^0, \tilde{E}^0, \tilde{I}_A^0, \tilde{Q}^0, \tilde{I}_S^0, \tilde{R}^0). \tag{3.22}$$

According to Theorem 6, the discrete model (3.3) yields non-negative solutions for each of these solutions. These solutions will be denoted respectively by $(L^n)_{n=0}^N$ and $(\tilde{L}^n)_{n=0}^N$, where

$$L^n = (s^n, v^n, e^n, i_A^n, q^n, i_S^n, r^n), \tag{3.23}$$

$$\tilde{L}^n = (\tilde{s}^n, \tilde{v}^n, \tilde{e}^n, \tilde{i}_A^n, \tilde{q}^n, \tilde{i}_S^n, \tilde{r}^n). \tag{3.24}$$

Moreover, we will agree that $\xi_w^n = w^n - \tilde{w}^n$, for each $n \in \bar{I}_N$ and $w = s, v, e, i_A, q, i_S, r$. This nomenclature will be used in the following theorem.

Theorem 10. *Let L^0 and $\tilde{L}^0$ be non-negative initial conditions for the model (3.3), and suppose that $(L^n)_{n=0}^N$ and $(\tilde{L}^n)_{n=0}^N$ are the respective solutions. If Δt is sufficiently small, then there is a constant $K > 0$ such that $\xi^n \leq K\xi^0$, for each $n \in \bar{I}_N$. Here,*

$$\xi^n = |\xi_s^n| + |\xi_v^n| + |\xi_e^n| + |\xi_{i_A}^n| + |\xi_q^n| + |\xi_{i_S}^n| + |\xi_r^n|. \tag{3.25}$$

Proof. For the sake of convenience, we will let $\Xi^n = L^n - \tilde{L}^n$, for each $n \in \bar{I}_N$. It is obvious that

$$\Xi^n = (\xi_S^n, \xi_v^n, \xi_e^n, \xi_{i_A}^n, \xi_q^n, \xi_{i_S}^n, \xi_r^n) \tag{3.26}$$

is satisfied for each $n \in \bar{I}_N$. Moreover, after simplification and some additional algebraic steps, it is possible to show the sequence $(\Xi^n)_{n=0}^N$ satisfies the system of algebraic equations

$$\begin{aligned} \hat{\delta}_t \xi_s^n &= \sigma \xi_r^n - \alpha(s^{n+1}\xi_e^n - \xi_s^{n+1}\tilde{e}^n) + \tau \xi_v^n - (\omega+\mu)\xi_s^{n+1}, \\ \hat{\delta}_t \xi_v^n &= \omega \xi_s^n - (\tau+\mu)\xi_v^{n+1}, \\ \hat{\delta}_t \xi_e^n &= \alpha(s^n \xi_e^n - \xi_s^n \tilde{e}^n) - (\zeta + \epsilon + \delta + \mu)\xi_e^{n+1}, \\ \hat{\delta}_t \xi_{i_A}^n &= \delta \xi_e^n - (\eta+\mu)\xi_{i_A}^{n+1}, \\ \hat{\delta}_t \xi_q^n &= \zeta \xi_e^n + \kappa \xi_{i_S}^n - (\iota + \upsilon + \mu)\xi_q^{n+1}, \\ \hat{\delta}_t \xi_{i_S}^n &= \epsilon \xi_e^n - (\kappa + \rho + \theta + \mu)\xi_{i_S}^{n+1}, \\ \hat{\delta}_t \xi_r^n &= \iota \xi_q^n + \theta \xi_{i_S}^n + \eta \xi_{i_A}^n - (\sigma+\mu)\xi_r^{n+1}. \end{aligned} \tag{3.27}$$

Let $m \in \bar{I}_N$, and assume that $C_p \geq 0$ is the uniform bound for the solution functions of (3.3). Take absolute value on both sides of the first equation of the discrete system (3.27), groups similar terms algebraically and use the triangle inequality to obtain

$$\frac{|\xi_s^{n+1}| - |\xi_s^n|}{\Delta t} \leq \sigma |\xi_r^n| + \alpha C_p |\xi_e^n| + \tau |\xi_v^n| + C_s' |\xi_s^{n+1}|, \tag{3.28}$$

for each $n \in \bar{I}_{N-1}$. Here, $C_s' = \alpha C_p + \omega + \mu$. Multiplying both sides of this inequality by Δt, summing on both sides for all n from 0 to $m-1$, using the formula for telescoping sums and rearranging terms, we obtain that

$$|\xi_s^m| \leq |\xi_s^0| + \Delta t \sum_{n=0}^{m-1} \left[\sigma |\xi_r^n| + \alpha C_p |\xi_e^n| + \tau |\xi_v^n| + C_s' |\xi_s^{n+1}|\right]. \tag{3.29}$$

In turn, if we let

$$C_s'' = \sigma + \alpha C_p + \tau + C_s', \tag{3.30}$$

then

$$\begin{aligned} (1 - C_s' \Delta t)|\xi_s^m| &\leq |\xi_s^0| + \Delta t \sum_{n=0}^{m-1} \Big[\sigma |\xi_r^n| + \alpha C_p |\xi_e^n| \\ &\quad + \tau |\xi_v^n| + C_s' |\xi_s^n|\Big] \\ &\leq |\xi_s^0| + C_s'' \Delta t \sum_{n=0}^{m-1} [|\xi_r^n| + |\xi_e^n| + |\xi_v^n| + |\xi_r^s|], \end{aligned} \tag{3.31}$$

for each $m \in \bar{I}_N$. In similar fashion, we may use the remaining equations in (3.27) to show that there exist non-negative constants C_w' and C_w'' for each $w = v, e, i_A, q, i_S, r$, such that

$$(1 - C_v' \Delta t)|\xi_v^m| \leq |\xi_v^0| + C_v'' \Delta t \sum_{n=0}^{m-1} [|\xi_s^n| + |\xi_v^n|], \tag{3.32}$$

$$(1 - C_e' \Delta t)|\xi_e^m| \leq |\xi_e^0| + C_e'' \Delta t \sum_{n=0}^{m-1} [|\xi_s^n| + |\xi_e^n|], \tag{3.33}$$

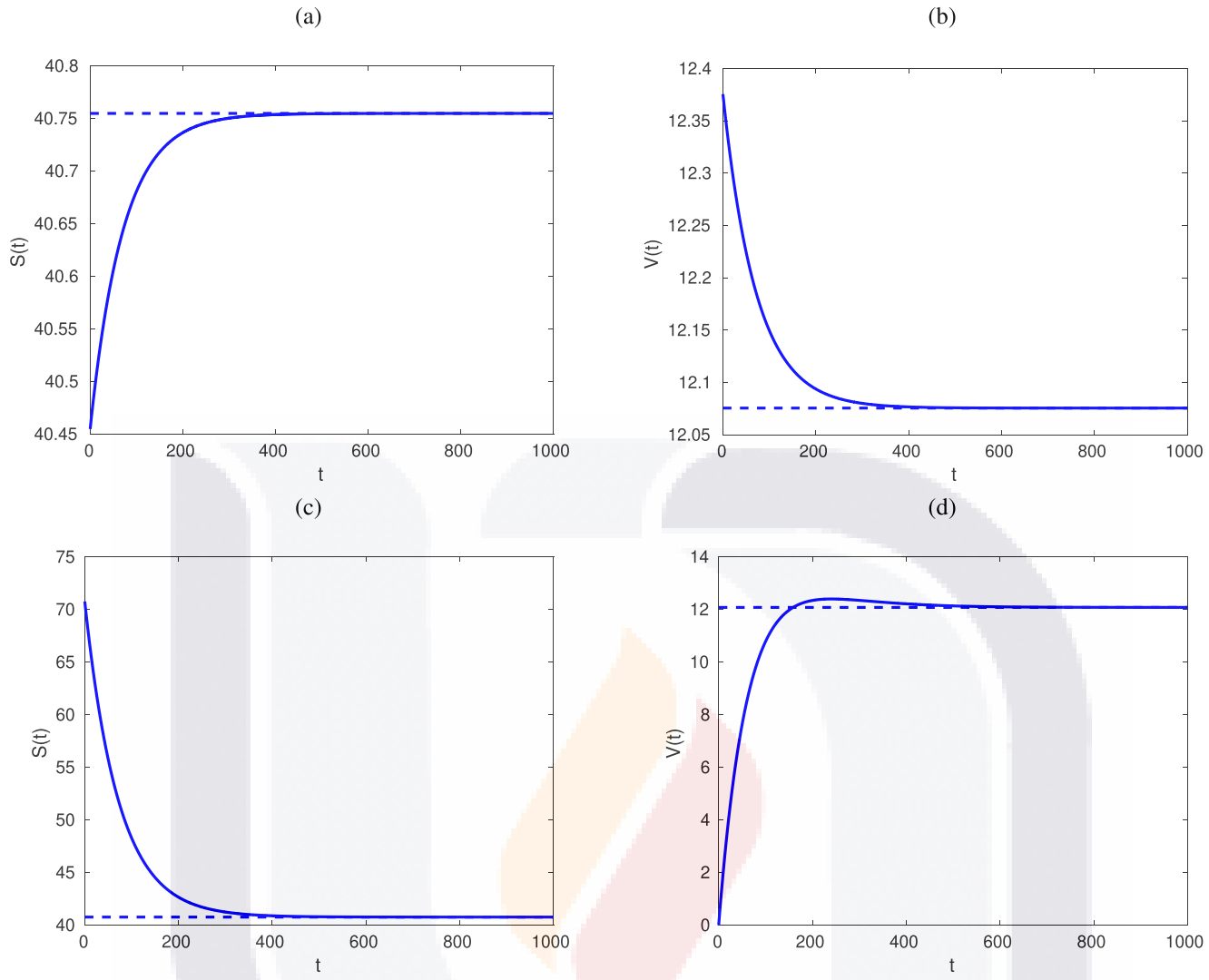

Fig. 2. Graphs of the temporal behavior of the sub-population of susceptible (first column) and the sub-population of vaccinated (second column) in the mathematical model (2.2). We employed the parameter values in Table 2, along with the initial conditions given by data set 1 (first row) and data set 2 (second row) in Table 3. The dashed lines represent the theoretical steady-state solutions for the disease-free scenario.

$$(1-C'_{i_A}\Delta t)|\xi^m_{i_A}| \leq |\xi^0_{i_A}| + C''_{i_A}\Delta t\sum_{n=0}^{m-1}\Big[|\xi^n_e| + |\xi^n_{i_A}|\Big], \tag{3.34}$$

$$(1-C'_q\Delta t)|\xi^m_q| \leq |\xi^0_q| + C''_q\Delta t\sum_{n=0}^{m-1}\Big[|\xi^n_e| + |\xi^n_{i_S}| + |\xi^n_q|\Big], \tag{3.35}$$

$$(1-C'_{i_S}\Delta t)|\xi^m_{i_S}| \leq |\xi^0_{i_S}| + C''_{i_S}\Delta t\sum_{n=0}^{m-1}\Big[|\xi^n_e| + |\xi^n_{i_S}|\Big], \tag{3.36}$$

and

$$\begin{aligned}(1-C'_r\Delta t)|\xi^m_r| \quad &\leq |\xi^0_r| + C''_r\Delta t\textstyle\sum_{n=0}^{m-1}\Big[|\xi^n_{i_S}| + |\xi^n_{i_A}| \\ &\quad + |\xi^n_q| + |\xi^n_r|\Big].\end{aligned} \tag{3.37}$$

Let $\Delta t > 0$ be sufficiently small so that $1 - C'_w\Delta t > 0$, for each $w = s, v, e, i_A, q, i_S, r$, and let $C > 0$ satisfy $C < 1 - C'_w\Delta t$, for each w. Adding the inequalities (3.31)–(3.37) and letting

$$C'' = C''_s + C''_v + C''_e + C''_{i_A} + C''_q + C''_{i_S} + C''_r, \tag{3.38}$$

we obtain that

$$C\xi^m \leq \xi^0 + C''\Delta t\sum_{n=0}^{m-1}\xi^n \tag{3.39}$$

Finally, we use Lemma 1 to establish that $\xi^n \leq K\xi^0$, where $K = C^{-1}\exp(C''T/C)$, for each $n \in \bar{I}_N$. The conclusion of this theorem readily follows from this fact. □

In terms of the nomenclature employed in the proof of the previous theorem, observe that the conclusion can be rewritten as $\|\Xi^n\|_1 \leq K\|\Xi^0\|_1$, for each $n \in \bar{I}_N$.

Our final theoretical result summarizes the convergence property of the finite-difference method (3.3). We omit the proof in view that it is similar to that of Theorem 10. We just need to point out that ξ^n_w is the difference between the exact solution W^n and the numerical approximation w^n, for each $n \in \bar{I}_N$ and $W = V, E, I_A, Q, I_S, R$. The consistency property of the computer method is also required to bound the local truncation error, along with the discrete form of Gronwall's inequality.

Theorem 11. *Suppose that the solutions of problem (2.2) are of class $\mathcal{C}^2([0,T])$. For sufficiently small values of Δt, the solutions of the dis-*

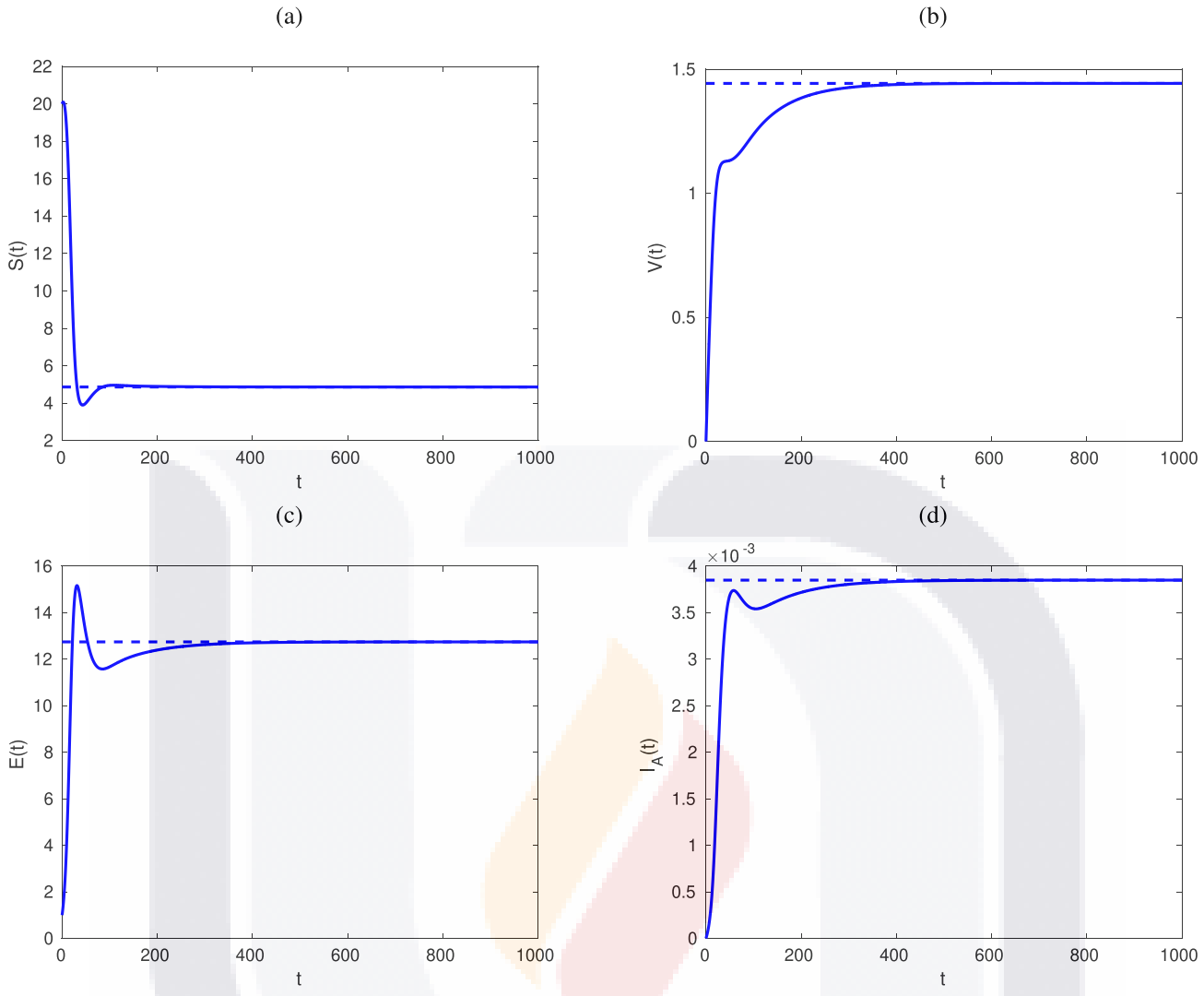

Fig. 3. Graphs of the temporal behavior of the sub-populations of (a) susceptible, (b) vaccinated, (c) exposed and (d) asymptomatic infected individuals in a population modeled by (2.2). We employed the parameter values in Table 2, along with the initial conditions given by data set 3 3. The dashed lines represent the theoretical steady-state solutions for the endemic scenario.

crete model (2.2) converge in the L^1-norm to the exact solution with order of convergence equal to Δt. □

Before closing this section, we present computer simulations which confirm the validity of some of the analytical results derived in this work. Our simulations have been carried out with the Matlab code provided in Appendix A. It is worth pointing out that the computational implementation is relatively simple, which is yet another important advantage of the approach introduced in the present manuscript. It is worth pointing out that the parameter values will be those in Table 2, and that some of those values wer taken from [35].

Example 1. In our first example, we will confirm the local stability properties of the disease-free equilibrium solution. To that end, we will employ the parameter values in Table 2 along with the data set 1 from Table 3. Under these circumstances, Figure 2 shows the dynamics of the solution for (a) the susceptible population and (b) the vaccinated population with respect to time, over the time period $[0, 250]$. The results confirm the stability of the disease-free equilibrium solution. It is worth pointing out that the value of the basic reproductive number is equal to 171.12. Moreover, the dashed

Table 2
Values of the parameters used in the various computational experiments presented in this manuscript.

Parameter	Value
α	0.01
δ	1.6728×10^{-5}
ϵ	0.0101
ζ	0.02798
η	0.04478
θ	0.0101
ι	0.0045
κ	0.0368
Λ	0.06
μ	0.0106
ρ	0.004
σ	0.0668
τ	0.0002
υ	3.2084×10^{-4}
ω	0.0032
m_S	0
m_E	0
m_{I_A}	0
m_{I_S}	0

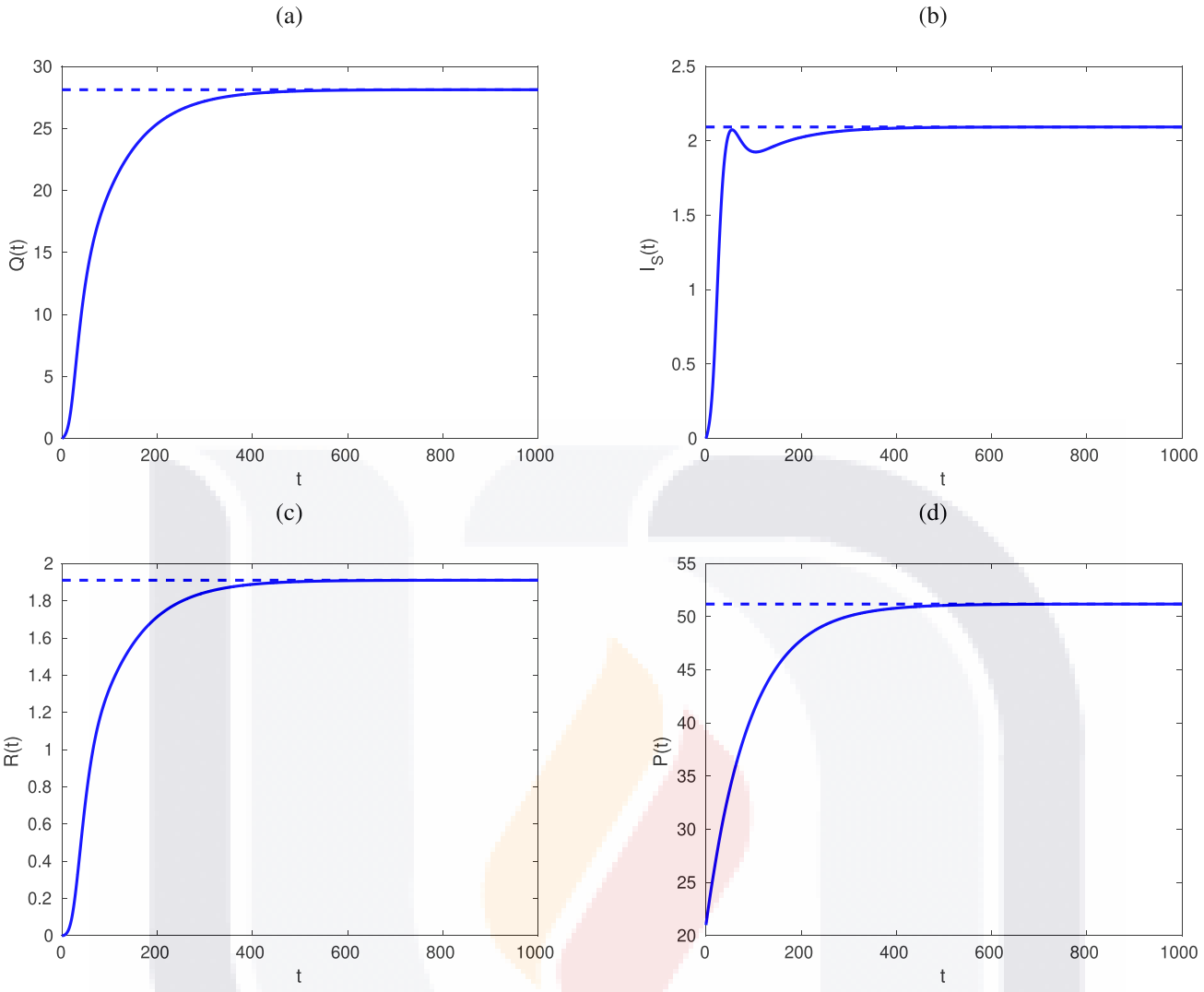

Fig. 4. Graphs of the temporal behavior of the sub-populations of (a) quarantined, (b) symptomatic infected, (c) recovered and (d) total population of individuals in a system modeled by (2.2). We employed the parameter values in Table 2, along with the initial conditions given by data set 3 3. The dashed lines represent the theoretical steady-state solutions for the endemic scenario.

Table 3
Initial conditions used in the numerical experiments of this manuscript.

	Data		
Parameter	Set 1	Set 2	Set 3
S^0	$S_0 - 0.3$	$S_0 + 30$	20
V^0	$V_0 + 0.3$	0	0
E^0	0	0	1
I_A^0	0	0	0
Q^0	0	0	0
I_S^0	0	0	0
R^0	0	0	0

line represents the value of the equilibrium point. Obviously, the solutions tend to reach those values as t tends to infinity. In turn, (c) and (d) show, respectively, the susceptible population and the vaccinated individuals as functions of time, for $t \in [0, 1000]$. We employed data set 2 from Table 3 in this case. Again, these sub-populations converge asymptotically to the steady-state solutions. So, whether the initial conditions are close to or far from the equilibrium solutions of the system (2.2), the numerical solutions converge to these values as time increases. This is in agreement with the analytical results. Moreover, the simulations show that the numerical method preserves the equilibria and their stability, as expected from the theoretical analysis. □

Example 2. In this example, we consider the endemic case and show once more that the finite-difference scheme is capable of preserving the steady-state solutions and their stabilities. Moreover, we provide computational proof that the endemic equilibrium is globally asymptotically stable as proved in the previous section. To that end, consider the parameter values given in Table 2, along with the initial conditions under data set 3 of Table 3. The results are provided in Figure 3 as time-dependent graphs of (a) susceptible, (b) vaccinated, (c) exposed and (d) asymptomatic infected, and in Figure 4 as graphs of (a) quarantined, (b) symptomatic infected, (c) recovered and (d) total population, for $t \in [0, 1000]$. For convenience, the theoretical endemic equilibrium values are plotted as dashed lines. The results show that the solutions tend to their equilibrium values as time in-

creases. This is in obvious agreement with the theoretical results derived in this work. □

4. Conclusions

In this work, we investigated both analytically and numerically a compartmental epidemiological model which describes the propagation of a disease among a human population. The model is intended to describe the propagation of COVID-19, but it can be used to any other disease which satisfies the epidemiological hypotheses used in this work. Among the distinctive features of the model, we considered various compartments: susceptible, exposed, asymptomatic and symptomatic infected, quarantined, recovered and vaccinated individuals. We supposed also that population migration is possible in the mathematical model. Analytically, we obtained the steady-state solutions of the model, and determined conditions for their local stability. The basic reproductive number was determined using the next generation matrix, and we established the existence and uniqueness of non-negative solutions. Also, we provided an upper bound for the solutions functions, and the analysis of parametric sensitivity was theoretically carried out.

As one of the most important results of our study, we proposed a finite-difference method to approximate the solutions of our mathematical model. This computational technique was designed using the nonstandard approach proposed by R. E. Mickens. An explicit form of the scheme was provide, and we established the existence and uniqueness of non-negative solutions for this mathematical model. We showed that the computational scheme has the same steady-state solutions as the continuous model and, moreover, the stability properties are also preserved by our discretization. We proved that the discrete model is a consistent discretization of the epidemiological model, and the conditional stability and convergence properties were derived using a discrete form of Gronwall's inequality. Here, it is worth pointing out that many nonstandard techniques are usually presented in the literature without providing these numerical properties. However, we established them mathematically in the present manuscript. Computationally, we obtained various simulations to illustrate the performance of our scheme. The results showed that the method identifies correctly the steady-state solutions and, moreover, it is also able to reproduce the stability properties of the continuous model. Our simulations show additionally that the scheme is capable or preserving the non-negativity and the boundedness of the solutions, in agreement with out theoretical results.

It is important to point out that the discretization proposed in this work is first order accurate in the temporal variable. As one of the reviewers pointed out, this numerical accuracy may not be satisfactory in the practice, in particular when dynamical simulations are performed. Other approaches may have the advantage of providing an accuracy of higher order, like the family of Runge–Kutta methods for systems of ordinary differential equations, which is a family of stable and convergent techniques. However, those approaches may not be able to preserve the positivity and boundedness of the solutions, or may not be able to preserve the equilibria and their stability. Nevertheless, in the case that they can preserve those features, the present methodology has its simplicity as one of the advantages. As the appendix shows, the present methodology is relatively easy to implement even for a scientist with little knowledge in computer programming.

On the other hand, as one of the anonymous reviewers of this manuscript pointed out, it is important to mention that there exist various reports available in the literature of third-order methods for time-dependent nonlinear partial differential equations in which the convergence and the stability have been analyzed. For example, there are reports on fully discrete Fourier collocation spectral methods for the 3-D viscous Burgers equation [36], high-order multi-step numerical schemes for two-dimensional incompressible Navier–Stokes equations [37], high-order exponential time-differencing numerical schemes for no-slope-selection epitaxial thin-film models with energy stability [38], third-order BDF energy-stable linear schemes for the no-slope-selection thin film model [39] and BDF-type energy-stable schemes for the Cahn–Hilliard equation [40].

Finally, as the same reviewer pointed out, there are various reports in which some logarithmic energy potential has been introduced for reaction-diffusion equations or other related gradient flows. In such way, the preservation of the positivity of the solutions has been ensured. As examples, we can mention some numerical works for the Poisson–Nernst–Planck system [41], a ternary Cahn–Hilliard system with the singular interfacial parameters [42], the three-component Cahn–Hilliard-type model for macromolecular microsphere composite hydrogels [43], the binary fluid-surfactant system [44], a liquid thin-film coarsening model [45], the Poisson–Nernst–Planck–Cahn–Hilliard equations with steric interactions [46], the Cahn–Hilliard equation with variable interfacial parameters [47], the Cahn–Hilliard equation with a Flory–Huggins–Degennes energy [48], he Cahn-Hilliard equation with logarithmic potential [49] and a reaction-diffusion system with detailed balance [50,51]. The authors of the present manuscript are not aware whether an entropy could be introduced in the epidemiological mathematical model (2.2), in order to guarantee the preservation of the positivity of the numerical solutions.

Funding

One of the authors (J.E.M.-D.) was funded by the National Council of Science and Technology of Mexico through grant A1-S-45928.

Data statement

The data that support the findings of this study are available from the corresponding author, J.E.M.-D., upon reasonable request.

Conflict of interest statement

The authors declare no potential conflict of interest.

Declaration of Competing Interest

The authors declare that they have no known competing financial interests or personal relationships that could have appeared to influence the work reported in this paper.

Acknowledgment

The authors wish to thank the anonymous reviewers and the associated editor in charge of handling this manuscript for their invaluable comments and suggestions.

Appendix A. Matlab code

```
function [t,s,v,e,q,iA,iS,r]=epidemic
 alpha=0.01;
 delta=1.6728e-5;
 epsilon=0.0101;
 zeta=0.02798;
 eta=0.04478;
 theta=0.0101;
 iota=0.0045;
 kappa=0.0368;
 Lambda=0.06;
 mu=0.0106;
 rho=0.004;
 sigma=0.0668;
 tau=0.0002;
 upsilon=3.2084e-4;
 omega=0.0032;

 mS=0;
 mE=0;
 mIA=0;
 mIS=0;

 S0=0.5;
 V0=0;
 E0=0.2;
 Q0=0.1;
 IA0=0.2;
 IS0=0.1;
 R0=0;

 T=150;
 Deltat=0.01;

 t=0:Deltat:T;

 s=zeros(size(t));
 v=zeros(size(t));
 e=zeros(size(t));
 q=zeros(size(t));
 iA=zeros(size(t));
 iS=zeros(size(t));
 r=zeros(size(t));

 s(1)=S0;
 v(1)=V0;
 e(1)=E0;
 q(1)=Q0;
 iA(1)=IA0;
 iS(1)=IS0;
 r(1)=R0;

 N=length(t)-1;

 for n=1:N
 e(n+1)=(e(n)+(mE+alpha*s(n)*e(n))*Deltat)/(1+(
     zeta+epsilon+delta+mu)*Deltat);
 s(n+1)=(s(n)+(Lambda+mS+sigma*r(n)+tau*v(n))*
     Deltat)/(1+(alpha*e(n+1)+omega+mu)*Deltat);
 v(n+1)=(v(n)+omega*s(n)*Deltat)/(1+(tau+mu)*
     Deltat);
 iA(n+1)=(iA(n)+(mIA+delta*e(n))*Deltat)/(1+(eta+
     mu)*Deltat);
 q(n+1)=(q(n)+(zeta*e(n)+kappa*iS(n))*Deltat)
     /(1+(iota+upsilon+mu)*Deltat);
 iS(n+1)=(iS(n)+(mIS+epsilon*e(n))*Deltat)/(1+(
     kappa+rho+theta+mu)*Deltat);
 r(n+1)=(r(n)+(iota*q(n)+theta*iS(n)+eta*iA(n))*
     Deltat)/(1+(sigma+mu)*Deltat);
 end
 p=s+v+e+iA+iS+q+r;
end
```

References

[1] B. Briones Aguirre, Metodología de la investigación en epidemiología, Martínez Montaño MLC, Briones Rojas R, Cortés Riveroll JGR. Metodología de la investigación para el área de la salud. Access-Medicina (2013).
[2] P. Elliot, J.C. Wakefield, N.G. Best, D.J. Briggs, et al., Spatial epidemiology: methods and applications, Oxford University Press, 2000.
[3] H. King, Green sickness: Hippocrates, galen and the origins of the ædisease of virginsg, International Journal of the Classical Tradition 2 (3) (1996) 372–387.
[4] D. Rosselli, Epidemiología de las pandemias, Medicina (Bogotá) 42 (2) (2020).
[5] F. Brauer, P. Van den Driessche, J. Wu, L.J. Allen, Mathematical epidemiology, volume 1945, Springer, 2008.
[6] G.B. Libotte, F.S. Lobato, G.M. Platt, A.J.S. Neto, Determination of an optimal control strategy for vaccine administration in covid-19 pandemic treatment, Computer methods and programs in biomedicine 196 (2020) 105664.
[7] F. Brauer, Mathematical epidemiology: Past, present, and future, Infectious Disease Modelling 2 (2) (2017) 113–127.
[8] L.B.R. Sánchez, H.S. Vargas, P.Á.G. Llanes, H.O. Ferrer, M.C.J. Ricardo, J.M. Quintana, Y.C. Mota, S.L. Choy, Predicción temprana de la covid-19 en cuba con el modelo seir, Anales de la Academia de Ciencias de Cuba 10 (2) (2020) 883.
[9] H.H. Weiss, The SIR model and the foundations of public health, Materials matematics (2013) 1–17.
[10] P. Montagnon, A stochastic SIR model on a graph with epidemiological and population dynamics occurring over the same time scale, Journal of Mathematical Biology 79 (1) (2019) 31–62.
[11] F. Brauer, C. Castillo-Chavez, Z. Feng, Mathematical models in epidemiology, volume 32, Springer, 2019.
[12] J.C. Blackwood, L.M. Childs, An introduction to compartmental modeling for the budding infectious, disease modeler (2018).
[13] G. Albi, L. Pareschi, M. Zanella, Control with uncertain data of socially structured compartmental epidemic models, Journal of Mathematical Biology 82 (7) (2021) 1–41.
[14] A. Viguerie, A. Veneziani, G. Lorenzo, D. Baroli, N. Aretz-Nellesen, A. Patton, T.E. Yankeelov, A. Reali, T.J. Hughes, F. Auricchio, Diffusion–reaction compartmental models formulated in a continuum mechanics framework: application to covid-19, mathematical analysis, and numerical study, Computational Mechanics 66 (5) (2020) 1131–1152.
[15] G. Ortigoza, F. Brauer, I. Neri, Modelling and simulating chikungunya spread with an unstructured triangular cellular automata, Infectious Disease Modelling 5 (2020) 197–220.
[16] A. Momoh, M. Ibrahim, I. Uwanta, S. Manga, Mathematical model for control of measles epidemiology, International Journal of Pure and Applied Mathematics 87 (5) (2013) 707–717.
[17] P. Widyaningsih, R.C. Affan, D.R.S. Saputro, A mathematical model for the epidemiology of diabetes mellitus with lifestyle and genetic factors, in: Journal of physics: conference series, volume 1028, IOP Publishing, 2018, p. 012110.
[18] G.P. Garnett, An introduction to mathematical models in sexually transmitted disease epidemiology, Sexually transmitted infections 78 (1) (2002) 7–12.
[19] S. Kim, A. Aurelio, E. Jung, Mathematical model and intervention strategies for mitigating tuberculosis in the philippines, Journal of theoretical biology 443 (2018) 100–112.
[20] A.F. Bezabih, G.K. Edessa, P.R. Koya, Mathematical epidemiology model analysis on the dynamics of covid-19 pandemic, American Journal of Applied Mathematics 8 (5) (2020) 247–256.
[21] Covid-19 map, ????, (????). https://coronavirus.jhu.edu/map.html.
[22] M. Dashtbali, M. Mirzaie, A compartmental model that predicts the effect of social distancing and vaccination on controlling covid-19, Scientific Reports 11 (1) (2021) 1–11.
[23] C.M. Batistela, D.P. Correa, Á.M. Bueno, J.R.C. Piqueira, SIRSi compartmental model for COVID-19 pandemic with immunity loss, Chaos, Solitons & Fractals 142 (2021) 110388.
[24] K.S. Sharov, Creating and applying SIR modified compartmental model for calculation of COVID-19 lockdown efficiency, Chaos, Solitons & Fractals 141 (2020) 110295.

[25] J.K.K. Asamoah, Z. Jin, G.-Q. Sun, B. Seidu, E. Yankson, A. Abidemi, F. Oduro, S.E. Moore, E. Okyere, Sensitivity assessment and optimal economic evaluation of a new COVID-19 compartmental epidemic model with control interventions, Chaos, Solitons & Fractals 146 (2021) 110885.
[26] J. Arino, S. Portet, A simple model for COVID-19, Infectious Disease Modelling 5 (2020) 309–315.
[27] T.A. Biala, A. Khaliq, A fractional-order compartmental model for the spread of the covid-19 pandemic, Communications in Nonlinear Science and Numerical Simulation 98 (2021) 105764.
[28] W. Yang, D. Zhang, L. Peng, C. Zhuge, L. Hong, Rational evaluation of various epidemic models based on the covid-19 data of china, Epidemics 37 (2021) 100501.
[29] P. Van den Driessche, J. Watmough, Reproduction numbers and sub-threshold endemic equilibria for compartmental models of disease transmission, Mathematical biosciences 180 (1-2) (2002) 29–48.
[30] S. Barnett, Polynomials and linear control systems, Marcel Dekker, Inc., 1983.
[31] R.E. Mickens, Nonstandard finite difference schemes for differential equations, Journal of Difference Equations and Applications 8 (9) (2002) 823–847.
[32] R.E. Mickens, Nonstandard finite difference schemes for reaction-diffusion equations, Numerical Methods for Partial Differential Equations: An International Journal 15 (2) (1999) 201–214.
[33] R.E. Mickens, Applications of nonstandard finite difference schemes, World Scientific, 2000.
[34] K. Pen-Yu, Numerical methods for incompressible viscous flow, Scientia Sinica 20 (1977) 287–304.
[35] I. Ahmed, G.U. Modu, A. Yusuf, P. Kumam, I. Yusuf, A mathematical model of Coronavirus Disease (COVID-19) containing asymptomatic and symptomatic classes, Results in physics 21 (2021) 103776.
[36] S. Gottlieb, C. Wang, Stability and convergence analysis of fully discrete fourier collocation spectral method for 3-d viscous burgers equation, Journal of Scientific Computing 53 (1) (2012) 102–128.
[37] K. Cheng, C. Wang, Long time stability of high order multistep numerical schemes for two-dimensional incompressible navier–stokes equations, SIAM Journal on Numerical Analysis 54 (5) (2016) 3123–3144.
[38] K. Cheng, Z. Qiao, C. Wang, A third order exponential time differencing numerical scheme for no-slope-selection epitaxial thin film model with energy stability, Journal of Scientific Computing 81 (1) (2019) 154–185.
[39] Y. Hao, Q. Huang, C. Wang, A third order bdf energy stable linear scheme for the no-slope-selection thin film model, Communications in computational physics 29 (3) (2021).
[40] K. Cheng, C. Wang, S.M. Wise, Y. Wu, A third order accurate in time, bdf-type energy stable scheme for the, cahn-hilliard equation (2021).
[41] C. Liu, C. Wang, S. Wise, X. Yue, S. Zhou, A positivity-preserving, energy stable and convergent numerical scheme for the poisson-nernst-planck system, Mathematics of Computation 90 (331) (2021) 2071–2106.
[42] L. Dong, C. Wang, S.M. Wise, Z. Zhang, A positivity-preserving, energy stable scheme for a ternary cahn-hilliard system with the singular interfacial parameters, Journal of Computational Physics 442 (2021) 110451.
[43] M. Yuan, W. Chen, C. Wang, S.M. Wise, Z. Zhang, An energy stable finite element scheme for the three-component cahn–hilliard-type model for macromolecular microsphere composite hydrogels, Journal of Scientific Computing 87 (3) (2021) 1–30.
[44] Y. QIN, C. WANG, Z. ZHANG, A positivity-preserving and convergent numerical scheme for the binary fluid-surfactant system, International Journal of Numerical Analysis & Modeling 18 (3) (2021).
[45] J. Zhang, C. Wang, S.M. Wise, Z. Zhang, Structure-preserving, energy stable numerical schemes for a liquid thin film coarsening model, SIAM Journal on Scientific Computing 43 (2) (2021) A1248–A1272.
[46] Y. Qian, C. Wang, S. Zhou, A positive and energy stable numerical scheme for the poisson–nernst–planck–cahn–hilliard equations with steric interactions, Journal of Computational Physics 426 (2021) 109908.
[47] L. Dong, A positivity-preserving second-order bdf scheme for the cahn-hilliard equation with variable interfacial parameters, Communications in Computational Physics 28 (3) (2020) 967–998.
[48] L. Dong, C. Wang, H. Zhang, Z. Zhang, A positivity-preserving, energy stable and convergent numerical scheme for the cahn–hilliard equation with a flory–huggins–degennes energy, Communications in Mathematical Sciences 17 (4) (2019) 921–939.
[49] W. Chen, C. Wang, X. Wang, S.M. Wise, Positivity-preserving, energy stable numerical schemes for the cahn-hilliard equation with logarithmic potential, Journal of Computational Physics: X 3 (2019) 100031.
[50] C. Liu, C. Wang, Y. Wang, S.M. Wise, Convergence analysis of the variational operator splitting scheme for a reaction-diffusion system with detailed balance, SIAM Journal on Numerical Analysis 60 (2) (2022) 781–803.
[51] C. Liu, C. Wang, Y. Wang, A structure-preserving, operator splitting scheme for reaction-diffusion equations with detailed balance, Journal of Computational Physics 436 (2021) 110253.

2. A multiconsistent computational methodology to resolve a diffusive epidemiological system with effects of migration, vaccination and quarantine

2.1 Introduction

This chapter extends the previous framework to a spatial setting. The model now consists of a system of nonlinear parabolic partial differential equations that track seven interacting subpopulations (susceptible, exposed, asymptomatic and symptomatic infected, quarantined, recovered, and vaccinated) while accounting for diffusion in space and migration between locations. The scientific aim is to design a numerical method that respects the model's dynamics and is robust for large-scale simulations.

A non-local, linearly implicit nonstandard finite-difference scheme is introduced. In suitable regimes the matrices behind the method are M-matrices, which supports positivity and monotonicity properties. The analysis proves that the method identifies the equilibria of the PDE model and preserves their local asymptotic stability; the reproduction number is computed with the next-generation technique. Moreover, the scheme is consistent, stable, and convergent—first order in time and second order in space—providing a practical balance between accuracy and structure preservation.

Implementation details are also discussed. The discrete systems at each time step are solved with a biconjugate-gradients-stabilized solver, and the experiments verify positivity, stability, and agreement with theory in both disease-free and endemic regimes.

2.2 Article 2

Computer Methods and Programs in Biomedicine 236 (2023) 107526

Contents lists available at ScienceDirect

Computer Methods and Programs in Biomedicine

journal homepage: www.elsevier.com/locate/cmpb

A multiconsistent computational methodology to resolve a diffusive epidemiological system with effects of migration, vaccination and quarantine

Jorge E. Herrera-Serrano[a,b], José A. Guerrero-Díaz-de-León[c], Iliana E. Medina-Ramírez[d], Jorge E. Macías-Díaz[e,f,*]

[a] Basic Sciences Faculty, Aguascalientes Autonomous University, Ave. Universidad 940, Ciudad Universitaria, Aguascalientes, Ags. 201000, Mexico
[b] Academic Direction of Information Technologies and Mechatronics, Technological University of the North of Aguascalientes, Ave. Universidad 1001, La Estación Rincón, Rincón de Romos, Ags. 20400, Mexico
[c] Department of Statistics, Aguascalientes Autonomous University, Ave. Universidad 940, Ciudad Universitaria, Aguascalientes, Ags. 20100, Mexico
[d] Department of Chemistry, Aguascalientes Autonomous University, Ave. Universidad 940, Ciudad Universitaria, Aguascalientes, Ags. 20100, Mexico
[e] Department of Mathematics and Didactics of Mathematics, School of Digital Technologies, Tallinn University, Narva Rd. 25, 10120 Tallinn, Estonia
[f] Department of Mathematics and Physics, Aguascalientes Autonomous University, Ave. Universidad 940, Ciudad Universitaria, Aguascalientes, Ags. 20100, Mexico

ARTICLE INFO

Article history:
Received 31 January 2023
Revised 21 March 2023
Accepted 2 April 2023

2020 MSC:
39A14
35L53
65M06
92D30

Keywords:
nonlinear parabolic systems of partial differential equations
compartmental epidemiological model
nonstandard computer method
non-singular inverse-positive matrices
nonlinear analysis of convergence and stability
computational simulations

ABSTRACT

Background: We provide a compartmental model for the transmission of some contagious illnesses in a population. The model is based on partial differential equations, and takes into account seven subpopulations which are, concretely, susceptible, exposed, infected (asymptomatic or symptomatic), quarantined, recovered and vaccinated individuals along with migration. The goal is to propose and analyze an efficient computer method which resembles the dynamical properties of the epidemiological model.

Materials and methods: A non-local approach is utilized for finding approximate solutions for the mathematical model. To that end, a non-standard finite-difference technique is introduced. The finite-difference scheme is a linearly implicit model which may be rewritten using a suitable matrix. Under suitable circumstances, the matrices representing the methodology are M-matrices.

Results: Analytically, the local asymptotic stability of the constant solutions is investigated and the next generation matrix technique is employed to calculate the reproduction number. Computationally, the dynamical consistency of the method and the numerical efficiency are investigated rigorously. The method is thoroughly examined for its convergence, stability, and consistency.

Conclusions: The theoretical analysis of the method shows that it is able to maintain the positivity of its solutions and identify equilibria. The method's local asymptotic stability properties are similar to those of the continuous system. The analysis concludes that the numerical model is convergent, stable and consistent, with linear order of convergence in the temporal domain and quadratic order of convergence in the spatial variables. A computer implementation is used to confirm the mathematical properties, and it confirms the ability in our scheme to preserve positivity, and identify equilibrium solutions and their local asymptotic stability.

1. Introduction

During the final months in 2019, humanity began a struggle against a new virus called SARS-CoV-2, which is a pathogen that has caused almost 6.7 million human casualties around the world until January 2023 [1]. This disease is known also as COVID-19, and it will be in the history annals along with others pandemics such as the black plague, the smallpox and the Spanish flu among many others [2]. It is worth mentioning that COVID-19 has not been as

* Corresponding author at Department of Mathematics and Physics, Aguascalientes Autonomous University, 940 University Ave, Aguascalientes 20100, Mexico.
E-mail addresses: jorge.herrera@edu.uaa.mx (J.E. Herrera-Serrano), jaguerrero@correo.uaa.mx (J.A. Guerrero-Díaz-de-León), iemedina@correo.uaa.mx (I.E. Medina-Ramírez), jorge.macias_diaz@tlu.ee, jemacias@correo.uaa.mx (J.E. Macías-Díaz).

https://doi.org/10.1016/j.cmpb.2023.107526
0169-2607/

deadly in comparison to other illnesses [3–5]. The above situation may be due to the fact that the population has better health and sanitation conditions nowadays. In addition, it may be due to the great advances in technology within the health sector [6,7]. In that sense, humankind has been fortunate enough to be in a time when the mortal consequences of the current pandemic have been minimized by many factors.

In Mexico, the initial confirmed of the existence of COVID-19 was reported on February 28th, 2020. The individual was an Italian citizen residing in the country [8]. Just a few weeks later, the federal government of this country announced the first victim of the disease on March 18, 2020 [8]. Based on the world panorama, the government decided to start a quarantine period, in which all the activities of a non-essential nature would be carried out at the distance. Furthermore, certain mandatory precautions were put in place, including regularly washing hands, using facial masks, and keeping a personal separation of at least 1.5 meters from others. Although these measures lasted for several months, it was impossible to maintain them for a long period. Later on, it was decided to employ a traffic-light system for the control of the disease: depending on the color of the traffic light, certain tasks were allowed or prohibited [9]. From the beginning of the disease to January 2023, almost 331,000 people have died in this country. In fact, January 2021 was the month reporting the most deaths with almost 33,000 individuals, representing around 10% of the total deaths to this day [10].

As we mentioned above, all the countries around the world suffered a lot of harsh consequences derived from this new disease. According to data from Johns Hopkins University [1], some nations have suffered to a greater or lesser degree. However, one thing is very clear: since vaccinations began, COVID-19-related deaths have drastically decreased [11]. As we previously pointed out, a possible reason why this pandemic was not as deadly as others may be because of the technological progress in the field of medicine (which is abysmal compared to the situation some centuries ago [2]). And it is a fact that the vaccines against the SARS-CoV-2 virus were developed in record time [12], something that perhaps would not have been possible many years ago. In addition, the vaccine has been effective for all detected variants [13]. Despite the fact that we already have the vaccine and that the number of infections and deaths have decreased by a large percentage, it is very important to continue understanding the dynamics of this and other lethal disease, and be ready when the next pandemic hits [14].

Surely, COVID-19 is not be the first nor will be the last disease to attack humanity. Thus, scientists must be ready to face the next pandemic. Specifically, experts in the field of epidemiology are continually refining and assessing their techniques and pushing the boundaries of the field, to be ready for the potential outbreak of subsequent illnesses [15]. It is worth remembering that epidemiology is the field in science which studies occurrences, spreading and causes of illnesses within human populations [16,17]. This branch of science has experienced an increased popularity in recent years due to the many diseases that have afflicted the human population. Among those diseases, we can mention malaria [18], the H1N1 flu [19,20] and currently COVID-19 [21]. Moreover, epidemiology and mathematics have come together to support this cause. In fact, mathematical modeling and simulation have been tools used to a great extent, in order to generate a general description of the spreading of a disease. In such way, mathematical epidemiology tries to predict the behavior of a disease in a population of human individuals.

Within the frame of mathematical epidemiology, the so-called compartment-based models have become a widely used technique to represent the behavior of the spreading of a specific disease within a population [22]. These models are adapted depending on the characteristics of the disease under study [23]. In the scientific literature, there are a number of basic compartmental models available such as the SIR (susceptible-infected-recovered) model [24], as well as more complex models such as the SEIQR which includes the quarantine compartment [25]. It is worth noting that these models can be adjusted to enhance the explanations of the phenomena [26]. Usually, this type of models are expressed as nonlinear systems of ordinary differential equations [27], but it is also possible to employ partial [28] or stochastic [29] differential equations to that end. In particular, the advantage of using partial differential equations is that they allow for modeling using two or more independent variables, like space and time. In light of this advantage, this manuscript presents a mathematical model using partial differential equations to simulate the propagation of COVID-19 within some human population, taking into account various realistic factors.

The aim of this study is to develop a general model that can be used to prescribe the transmission mechanisms for various illnesses, including COVID-19. The mathematical model will consider the presence of diffusion in two spatial variables, and various mechanisms of reaction will be taken into account. To that end, various interactions between population compartments will be considered, and we will use partial differential equations for a precise mathematical description of the model in the spatial and temporal variables. More specifically, our community is divided into sub-populations of vaccinated, recovered, quarantined, asymptomatic and symptomatic infected, exposed, and susceptible individuals. The model is a rather complex system which cannot be solved exactly in general, that is why the need to provide a numerical methodology to simulate it is justified. This paper is focused on presenting a computer scheme to simulate the dynamics in our epidemiological model. The mathematical analysis of the properties of the scheme will be discussed in detail, and various simulations will be conducted to provide examples.

Methodologically, the computer technique used in this work is based on a non-standard approach. It is worth pointing out that this approach was popularized by Ronald E. Mickens in various manuscripts [30], and various other authors have applied it successfully to solve numerically many mathematical problems [31,32], including some complex epidemiological models [33] and some other mathematical problems [34–37]. The present methodology follows a non-local perspective, which presents the advantage of being able to conserve the positive character of the numerical solutions. This is an important fact in view that the functions involved in our model represent population sizes or densities. Moreover, this approach results in a linear discretization of the model. In such way, the computer implementation of the scheme is relatively easy to carry out, though the theoretical analysis of the computer model is still challenging. However, we are able to establish mathematically the most important properties of the scheme. In particular, the consistency, the stability and the convergence of the methodology are proved rigorously, and some computational simulations verify the validity of many of our theoretical results.

This manuscript is organized as follows. In Section 2, we introduce the mathematical models investigated in this work. In a first stage, a continuous model based in partial differential equations is deduced from epidemiological assumptions. In such way, a system of seven nonlinear partial differential equations is obtained assuming the presence of spatial diffusion. Initial and boundary conditions are imposed on the boundary of the two-dimensional spatial domain. In addition, a computer method is derived from the continuous model using a finite-difference methodology. For the sake of computational convenience, the scheme is presented as a vector system which can be easily implemented in a computer. Section 3 establishes the most important analytical and numerical results. Analytically, we obtain the basic reproduction number using the next generation matrix method, and we

determine the disease-free and the endemic equilibria. Using nonlinear arguments, the local asymptotic stability of the equilibrium points is elucidated. Numerically, the computer method is thoroughly analyzed. In particular, we show that the method is capable of preserving the positivity, the equilibrium points and their local asymptotic stability under the same conditions for which they hold in the continuous case. Moreover, the consistency, the stability and the convergence of the scheme are theoretically established. Some computer simulations provided therein confirm our theoretical results. This work closes with some concluding remarks.

2. Methods

2.1. Epidemiological model

In this initial stage, a compartment mathematical model is introduced to depict the spreading of a sickness based on epidemiological assumptions. We will have in mind a group of people who are prone to catching some infectious disease. The variable $P(\mathbf{x}, t)$ symbolizes the number of people at time $t \geq 0$ and a spatial point $\mathbf{x} = (x, y) \in \mathbb{R}^2$. The specific vulnerable society is also divided into different sub-groups or categories:

- V - Vaccinated category.
- S - Susceptible category.
- E - Exposed category.
- I_S - Symptomatic infected category.
- I_A - Asymptomatic infected category.
- Q - Quarantined category.
- R - Recovered category.

Therefore, the following equation is fulfilled at any point $\mathbf{x} \in \Omega$ and any time $t \geq 0$:

$$P = S + E + I_A + I_S + Q + R + V. \tag{2.1}$$

To make the epidemiological model more accurate, this study considers constant rates of migration into the population. Those parameters are represented by m_S, m_V, m_E, m_{IA}, m_Q, m_{I_S}, and m_R, respectively, which indicate the number of individuals moving into the categories of vaccinated, susceptible, exposed, symptomatic, asymptomatic, quarantined, and recovered people.

All the terms will have non-negative real numbers. The population is assumed to have death and birth rates, represented with constants μ and Λ respectively. Three scenarios are considered in which susceptible individuals can become exposed. The first of which is when these persons get in touch with exposed subjects. This happens at a transmission velocity equal to α. A second case is if they are in contact with asymptomatic individual at a rate β. This scenario is supported by the fact that some diseases produce no symptoms on some individuals, but those subjects are carriers of the pathogen. The last case occurs when individuals have contact with people who are already infected by the disease, in which case the propagation will have a rate equal γ. We will assume also that there is a vaccine available to control the propagation. More specifically, susceptible individuals will be vaccinated at a rate represented by ω. To produce an even more realistic scenario, we also suppose that the vaccines are not 100% effective and, in some cases, the individuals may lose their immunity. To accomplish that, vaccinated people will become susceptible one more time at a rate given by the value of the constant τ.

Exposed individuals have three potential outcomes. One option is to quarantine, either when they know they are infected, or simply for precautionary measures. This occurs at a rate represented by ζ. The other two options are becoming asymptomatic infected or symptomatic infected, at rates δ and ϵ, respectively. It is important to mention here that we assume that the individuals do the test and the proofs report that they are positive for the infectious disease. Some people may or may not have symptoms, and this obviously depends strongly on the particular type of illness under study. In fact, we suppose that asymptomatic people recover at rate of η by natural causes.

Additionally, the population inside the symptomatic category will be transferred to the confined state at a rate of κ. It is important to note that the quarantined state can be assumed for mild or severe symptoms. However, depending on whether they were quarantined or symptomatic, they can only transition to the recovered condition at a rate of ι or θ, respectively. We will use υ to indicate the rates at which quarantined individuals succumb to the infectious disease, and ρ for the people who die as a consequence of the illness. In addition, since the body does not acquire a permanent immunity to the illness, individuals who have recovered may re-enter the susceptible class at a rate of σ. For easy reference, the epidemiological parameters employed herein are displayed in Table 1.

Table 1
Symbols used and their corresponding definitions for comprehending all the interconnections within the proposed model.

Parameter	Description
m_S	Rate of immigration individuals to susceptible class.
m_V	Rate of immigration individuals to vaccinated class.
m_E	Rate of immigration individuals to exposed class.
m_{I_S}	Rate of immigration individuals to symptomatic infected class.
m_{I_A}	Rate of immigration individuals to asymptomatic infected class.
m_Q	Rate of immigration individuals to quarantine class.
m_R	Rate of immigration individuals to recovered class.
Λ	Rate of recruitment for individuals prone to contracting the disease.
τ	Proportion of individuals to susceptible category from vaccinated.
ω	Proportion of individuals to vaccinated category from susceptible.
α	Proportion of contact enclosed by exposed and susceptible category.
γ	Proportion of contact enclosed by susceptible and symptomatic category.
β	Proportion of contact enclosed by susceptible and asymptomatic category.
ζ	Proportion of individuals from exposed to quarantine category.
ϵ	Proportion of individuals from exposed to symptomatic infected category.
δ	Proportion of individuals to asymptomatic infected category from exposed.
η	Proportion of individuals from asymptomatic infected to recover category.
ι	Proportion of individuals from quarantine to recover category.
υ	Deaths for the disease in quarantine category.
κ	Proportion of individuals from symptomatic infected to quarantine category.
ρ	Deaths for the disease in symptomatic infected category.
θ	Proportion of recovery individuals from symptomatic infected category.
σ	Proportion of individuals who lost immunity and return to susceptible category.
μ	Deaths due to causes unrelated to the disease.

A visually convenient flowchart is shown in Fig. 1, which depicts the epidemiological postulation discussed in this work. These assumptions are used to simulate the propagation of the illness. Mathematically, we present the next system of nonlinear partial differential equations:

$$\frac{\partial S}{\partial t} = \Lambda + m_S + \sigma R - \alpha SE - \beta SI_A - \gamma SI_S + \tau V - (\omega + \mu)S + d_S \nabla^2 S,$$
$$\frac{\partial V}{\partial t} = m_V + \omega S - (\tau + \mu)V + d_V \nabla^2 V,$$
$$\frac{\partial E}{\partial t} = m_E + \alpha SE + \beta SI_A + \gamma SI_S - (\zeta + \epsilon + \delta + \mu)E + d_E \nabla^2 E,$$
$$\frac{\partial I_A}{\partial t} = m_{I_A} + \delta E - (\eta + \mu)I_A + d_{I_A} \nabla^2 I_A,$$

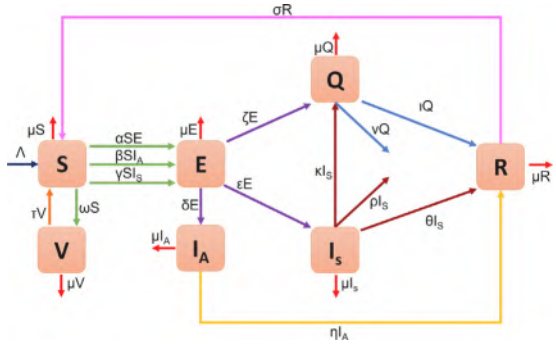

Fig. 1. A flowchart that graphically illustrates mechanisms involved in the transmission of a disease, as supposed in the present manuscript.

$$\begin{aligned}
\frac{\partial Q}{\partial t} &= m_Q + \zeta E + \kappa I_S - (\iota + \upsilon + \mu)Q + d_Q \nabla^2 Q,\\
\frac{\partial I_S}{\partial t} &= m_{I_S} + \epsilon E - (\kappa + \rho + \theta + \mu)I_S + d_{I_S} \nabla^2 I_S,\\
\frac{\partial R}{\partial t} &= m_R + \iota Q + \theta I_S + \eta I_A - (\sigma + \mu)R + d_R \nabla^2 R.
\end{aligned} \tag{2.2}$$

Obviously, the constants d_S, d_V, d_E, d_{I_A}, d_Q, d_{I_S} and d_R represent non-negative diffusion coefficients.

The set of equations presented here is a nonlinearly coupled system of differential equations in partial derivatives that are defined on a particular domain in space and time. The seven functions in the model are all real functions, and the domain of definition is an open, bounded subset of a two-dimensional space. So, this is defined as $(\mathbf{x}, t) \in \Omega \times [0, \infty)$ where $\Omega \in \mathbb{R}^2$. Additionally, we will add homogeneous Dirichlet data at the boundary of Ω, along with conditions at the time $t = 0$. To be more specific, we will assume that the following requirements are satisfied:

$$\begin{cases} U(\mathbf{x}, 0) = U^0(\mathbf{x}), & \forall \mathbf{x} \in \Omega,\\ U(\mathbf{x}, t) = 0, & \forall (\mathbf{x}, t) \in \partial\Omega \times [0, \infty). \end{cases} \tag{2.3}$$

Let us use the function U as any of the operators S, V, E, I_A, Q, I_S, or R, and S^0, V^0, E^0, I_A^0, Q^0, I_S^0, and R^0 are real-valued functions defined in our domain Ω. Moreover, the symbol $\partial\Omega$ is used to represent the boundary of Ω.

2.2. Computer method

Next, we present a numerical method using discrete operators to approximate the solutions of the epidemiological proposed model 2.2. It is worthy to mention that the steps followed to reduce the mathematical model to a numerical one were inspired by the use of the non-standard technique popularized by R. E. Mickens in various of his influential articles [30,38,39]. For the sake of convenience, we will approximate the numeric model within some fixed temporal period, namely, within the set $[0, T]$ for $T \in \mathbb{R}^+$. From the spatial point of view, we shall focus just on one rectangle-related domain denoted by $\Omega = [a, b] \times [c, d]$. Let us use $M, N, K \in \mathbb{N}$ to represent amount of subintervals for the variables x, y and t, respectively. Fix now uniform partitions of the form

$$\begin{aligned}
&a = x_0 < x_1 < x_2 < \ldots < x_m < \ldots < x_{M-1} < x_M = b,\\
&c = y_0 < y_1 < y_2 < \ldots < y_n < \ldots < x_{N-1} < y_N = d,\\
&0 = t_0 < t_1 < t_2 < \ldots < t_k < \ldots < t_{K-1} < t_K = T.
\end{aligned} \tag{2.4}$$

For convenience, the associated partition norms in the x, y and t variables will be the positive real numbers $\Delta x = (b - a)/M$, $\Delta y = (d - c)/N$ and $\Delta t = T/N$, respectively. Obviously, all of them are positive real numbers. Now, we set up the discrete terminology that is required for approximating the dynamics for the differential system (2.2). In a discrete setting, the continuous functions S, E, I_A, I_S, Q, R, V, and P shall be represented in the sequel by the lower-case letters s, e, i_A, i_S, q, r, v, and p, respectively. Assume that $U = S, E, I_S, I_A, Q, R, V$ and $u = s, e, i_S, i_A, q, r, v$. In what follows, we will agree that

$$U_{m,n}^k = U(x_m, y_n, t_k), \tag{2.5}$$

where $m = 0, 1, 2, \ldots, M-1, M$, $n = 0, 1, 2, \ldots, N-1, N$, $k = 0, 1, 2 \ldots, K-1, K$. Moreover, we introduce the following discrete finite-difference linear operators:

$$\hat{\sigma}_x u_{m,n}^k = u_{m-1,n}^k + u_{m+1,n}^k, \tag{2.6}$$

$$\hat{\sigma}_y u_{m,n}^k = u_{m,n-1}^k + u_{m,n+1}^k, \tag{2.7}$$

$$\hat{\mu}_t u_{m,n}^k = \frac{u_{m,n}^k + u_{m,n}^{k+1}}{2}, \tag{2.8}$$

$$\hat{\delta}_t u_{m,n}^k = \frac{1}{\Delta t}(u_{m,n}^{k+1} - u_{m,n}^k), \tag{2.9}$$

$$\hat{\delta}_y^2 u_{m,n}^k = \frac{1}{(\Delta y)^2}(u_{m,n-1}^k - 2u_{m,n}^k + u_{m,n+1}^k), \tag{2.10}$$

$$\hat{\delta}_x^2 u_{m,n}^k = \frac{1}{(\Delta x)^2}(u_{m-1,n}^k - 2u_{m,n}^k + u_{m+1,n}^k). \tag{2.11}$$

Needless to mention that operators (2.9)–(2.11) provide a consistent approximation to suitable continuous differential operators. The fully discretized methodology used to approximation the discretized solutions uses the discrete nomenclature used in this stage (2.2) at time t_k and spatial node (x_m, y_n). Concretely, the method is provided by the equations in the algebraic coupled nonlinear system

$$\begin{aligned}
\hat{\delta}_t s_{m,n}^k &= \Lambda + m_S + \sigma r_{m,n}^k - \alpha s_{m,n}^{k+1} e_{m,n}^k - \beta s_{m,n}^{k+1} i_{A_{m,n}}^k - \gamma s_{m,n}^{k+1} i_{S_{m,n}}^k\\
&\quad + \tau v_{m,n}^k - (\omega + \mu) s_{m,n}^{k+1} + d_S(\hat{\delta}_x^2 + \hat{\delta}_y^2)\hat{\mu}_t s_{m,n}^k,\\
\hat{\delta}_t v_{m,n}^k &= m_V + \omega s_{m,n}^k - (\tau + \mu) v_{m,n}^{k+1} + d_V(\hat{\delta}_x^2 + \hat{\delta}_y^2)\hat{\mu}_t v_{m,n}^k,\\
\hat{\delta}_t e_{m,n}^k &= m_E + \alpha s_{m,n}^k e_{m,n}^k + \beta s_{m,n}^k i_{A_{m,n}}^k + \gamma s_{m,n}^k i_{S_{m,n}}^k\\
&\quad - (\zeta + \epsilon + \delta + \mu) e_{m,n}^{k+1} + d_E(\hat{\delta}_x^2 + \hat{\delta}_y^2)\hat{\mu}_t e_{m,n}^k,\\
\hat{\delta}_t i_{A_{m,n}}^k &= m_{I_A} + \delta e_{m,n}^k - (\eta + \mu) i_{A_{m,n}}^{k+1} + d_{i_A}(\hat{\delta}_x^2 + \hat{\delta}_y^2)\hat{\mu}_t i_{A_{m,n}}^k,\\
\hat{\delta}_t q_{m,n}^k &= m_Q + \zeta e_{m,n}^k + \kappa i_{S_{m,n}}^k - (\iota + \upsilon + \mu) q_{m,n}^{k+1}\\
&\quad + d_Q(\hat{\delta}_x^2 + \hat{\delta}_y^2)\hat{\mu}_t q_{m,n}^k,\\
\hat{\delta}_t i_{S_{m,n}}^k &= m_{I_S} + \epsilon e_{m,n}^k - (\mu + \theta + \rho + \kappa) i_{S_{m,n}}^{k+1} + d_{i_S}(\hat{\delta}_x^2 + \hat{\delta}_y^2)\hat{\mu}_t i_{S_{m,n}}^k,\\
\hat{\delta}_t r_{m,n}^k &= m_R + \iota q_{m,n}^k + \theta i_{S_{m,n}}^k + \eta i_{A_{m,n}}^k - (\sigma + \mu) r_{m,n}^{k+1}\\
&\quad + d_R(\hat{\delta}_x^2 + \hat{\delta}_y^2)\hat{\mu}_t r_{m,n}^k.
\end{aligned} \tag{2.12}$$

It is clear that this discretization is nonstandard because it provides non-local approximations for some terms in the scheme. On the edge of Ω, discrete homogeneous Dirichlet conditions will then be applied. To put it another way, we shall impose discrete initial-boundary constraints as follows:

$$\begin{cases} u_{m,n}^0 = U_{m,n}^0, & \forall m = 1, 2, \ldots, M-1,\\ & \forall n = 1, 2, \ldots, N-1,\\ u_{m,n}^k = 0, & \forall k = 0, 1, 2, \ldots, K-1, K \text{ and}\\ & \big[\forall (m, 0), (m, N),\ m = 0, 1, 2, \ldots, M-1, M, \text{ or}\\ & \forall (0, n), (M, n),\ n = 0, 1, \ldots, N-1, N\big]. \end{cases} \tag{2.13}$$

Notice that the algebraic system (2.12) can be presented in linear form as follows:

$$\begin{aligned}
\mathbf{b}^{s}_{m,n,k} &= \mathbf{a}^{s}_{m,n,k}s^{k+1}_{m,n} - R^{s}_{x}s^{k+1}_{m+1,n} - R^{s}_{x}s^{k+1}_{m-1,n} - R^{s}_{y}s^{k+1}_{m,n+1} - R^{s}_{y}s^{k+1}_{m,n-1},\\
\mathbf{b}^{v}_{m,n,k} &= \mathbf{a}^{v}_{m,n,k}v^{k+1}_{m,n} - R^{v}_{x}v^{k+1}_{m+1,n} - R^{v}_{x}v^{k+1}_{m-1,n} - R^{v}_{y}v^{k+1}_{m,n+1} - R^{v}_{y}v^{k+1}_{m,n-1},\\
\mathbf{b}^{e}_{m,n,k} &= \mathbf{a}^{e}_{m,n,k}e^{k+1}_{m,n} - R^{e}_{x}e^{k+1}_{m+1,n} - R^{e}_{x}e^{k+1}_{m-1,n} - R^{e}_{y}e^{k+1}_{m,n+1} - R^{e}_{y}e^{k+1}_{m,n-1},\\
\mathbf{b}^{i_A}_{m,n,k} &= \mathbf{a}^{i_A}_{m,n,k}i^{k+1}_{Am,n} - R^{i_A}_{x}i^{k+1}_{Am+1,n} - R^{i_A}_{x}i^{k+1}_{Am-1,n} - R^{i_A}_{y}i^{k+1}_{Am,n+1} - R^{i_A}_{y}i^{k+1}_{Am,n-1},\\
\mathbf{b}^{q}_{m,n,k} &= \mathbf{a}^{q}_{m,n,k}q^{k+1}_{m,n} - R^{q}_{x}q^{k+1}_{m+1,n} - R^{q}_{x}q^{k+1}_{m-1,n} - R^{q}_{y}q^{k+1}_{m,n+1} - R^{q}_{y}q^{k+1}_{m,n-1},\\
\mathbf{b}^{i_S}_{m,n,k} &= \mathbf{a}^{i_S}_{m,n,k}i^{k+1}_{Sm,n} - R^{i_S}_{x}i^{k+1}_{Sm+1,n} - R^{i_S}_{x}i^{k+1}_{Sm-1,n} - R^{i_S}_{y}i^{k+1}_{Sm,n+1} - R^{i_S}_{y}i^{k+1}_{Sm,n-1},\\
\mathbf{b}^{r}_{m,n,k} &= \mathbf{a}^{r}_{m,n,k}r^{k+1}_{m,n} - R^{r}_{x}r^{k+1}_{m+1,n} - R^{r}_{x}r^{k+1}_{m-1,n} - R^{r}_{y}r^{k+1}_{m,n+1} - R^{r}_{y}r^{k+1}_{m,n-1},
\end{aligned} \tag{2.14}$$

where

$$\begin{aligned}
\mathbf{a}^{s}_{m,n,k} &= 1 + 2R^{s}_{x} + 2R^{s}_{y} + \Delta t(\alpha e^{k}_{m,n} + \beta i^{k}_{A_{m,n}} + \gamma i^{k}_{S_{m,n}} + \omega + \mu),\\
\mathbf{a}^{v}_{m,n,k} &= 1 + 2R^{v}_{x} + 2R^{v}_{y} + \Delta t(\tau + \mu),\\
\mathbf{a}^{e}_{m,n,k} &= 1 + 2R^{e}_{x} + 2R^{e}_{y} + \Delta t(\zeta + \epsilon + \delta + \mu),\\
\mathbf{a}^{i_A}_{m,n,k} &= 1 + 2R^{i_A}_{x} + 2R^{i_A}_{y} + \Delta t(\eta + \mu),\\
\mathbf{a}^{q}_{m,n,k} &= 1 + 2R^{q}_{x} + 2R^{q}_{y} + \Delta t(\iota + \upsilon + \mu),\\
\mathbf{a}^{i_S}_{m,n,k} &= 1 + 2R^{i_S}_{x} + 2R^{i_S}_{y} + \Delta t(\kappa + \rho + \theta + \mu),\\
\mathbf{a}^{r}_{m,n,k} &= 1 + 2R^{r}_{x} + 2R^{r}_{y} + \Delta t(\sigma + \mu).
\end{aligned} \tag{2.15}$$

and

$$\begin{aligned}
\mathbf{b}^{s}_{m,n,k} &= \Delta t\left(\Lambda + m_S + \sigma r^{k}_{m,n} + \tau v^{k}_{m,n}\right) + \hat{D}_s s^{k}_{m,n},\\
\mathbf{b}^{v}_{m,n,k} &= \Delta t\left(m_V + \omega s^{k}_{m,n}\right) + \hat{D}_v v^{k}_{m,n},\\
\mathbf{b}^{e}_{m,n,k} &= \Delta t\left(m_E + \alpha s^{k}_{m,n}e^{k}_{m,n} + \beta s^{k}_{m,n}i^{k}_{Am,n} + \gamma s^{k}_{m,n}i^{k}_{Sm,n}\right) + \hat{D}_e e^{k}_{m,n},\\
\mathbf{b}^{i_A}_{m,n,k} &= \Delta t\left(m_{I_A} + \delta e^{k}_{m,n}\right) + \hat{D}_{i_A} i^{k}_{Am,n},\\
\mathbf{b}^{q}_{m,n,k} &= \Delta t\left(m_Q + \zeta e^{k}_{m,n} + \kappa i^{k}_{Sm,n}\right) + \hat{D}_q q^{k}_{m,n},\\
\mathbf{b}^{i_S}_{m,n,k} &= \Delta t\left(m_{I_S} + \epsilon e^{k}_{m,n}\right) + \hat{D}_{i_S} i^{k}_{Sm,n},\\
\mathbf{b}^{r}_{m,n,k} &= \Delta t\left(m_R + \iota q^{k}_{m,n} + \theta i^{k}_{Sm,n} + \eta i^{k}_{Am,n}\right) + \hat{D}_r r^{k}_{m,n}.
\end{aligned} \tag{2.16}$$

Moreover, we used the computational parameters and operators

$$\begin{aligned}
R^{u}_{x} &= \frac{d_u}{2}\frac{\Delta t}{(\Delta x)^2},\\
R^{u}_{y} &= \frac{d_u}{2}\frac{\Delta t}{(\Delta y)^2},\\
\hat{D}_u u^{k}_{m,n} &= \left[(1 - 2R^{u}_{x} - 2R^{u}_{y}) + R^{u}_{x}\hat{\sigma}_x + R_y\hat{\sigma}_y\right]u^{k}_{m,n}.
\end{aligned} \tag{2.17}$$

In the numerical model, each recursive equation can be expressed in vector form alternatively as

$$A^{u}_{k}\mathbf{u}^{k+1} = \mathbf{b}^{u}_{k}, \tag{2.18}$$

where $\mathbf{u}^{k+1}$ and $\mathbf{b}^{u}_{k}$ are, respectively, the real vectors of length equal to $(M+1)(N+1)$ given by

$$\begin{aligned}
\mathbf{u}^{k+1} = (&u^{k+1}_{0,0}, u^{k+1}_{0,1}, \cdots, u^{k+1}_{0,N}, u^{k+1}_{1,0}, u^{k+1}_{1,1}, \ldots, u^{k+1}_{1,N},\\
&\cdots, u^{k+1}_{M,0}, u^{k+1}_{M,1}, \cdots, u^{k+1}_{M,N}),
\end{aligned} \tag{2.19}$$

and

$$\begin{aligned}
\mathbf{b}^{u}_{k} = (&\underbrace{0, 0, \ldots, 0, 0}_{(N+1)\text{-times}},\\
&0, b^{u}_{1,1,k}, \ldots, b^{u}_{1,N-1,k}, 0,\\
&0, b^{u}_{2,1,k}, \ldots, b^{u}_{2,N-1,k}, 0,\\
&\vdots\\
&0, b^{u}_{M-1,1,k}, \ldots, b^{u}_{M-1,N-1,k}, 0,\\
&\underbrace{0, 0, \ldots, 0, 0}_{(n+1)\text{-times}}),
\end{aligned} \tag{2.20}$$

for each $k = 0, 1, 2, \ldots, K-1$ and u any of the discrete functions s, e, i_A, i_S, q, r or v. Moreover, the matrix A^{u}_{k} is the square block matrix with number of rows equal to $(N+1)(M+1)$, given as

$$A^{u}_{k} = \begin{pmatrix}
\boxed{I} & 0 & 0 & 0 & \cdots & 0 & 0 & 0\\
\boxed{E^u} & \boxed{D^{u}_{k}} & \boxed{E^u} & 0 & \cdots & 0 & 0 & 0\\
0 & \boxed{E^u} & \boxed{D^{u}_{k}} & \boxed{E^u} & \cdots & 0 & 0 & 0\\
\vdots & \vdots & \vdots & \vdots & \ddots & \vdots & \vdots & \vdots\\
0 & 0 & 0 & 0 & \cdots & \boxed{E^u} & \boxed{D^{u}_{k}} & \boxed{E^u}\\
0 & 0 & 0 & 0 & \cdots & 0 & 0 & \boxed{I}
\end{pmatrix}. \tag{2.21}$$

The identity matrix is indicated by I and it is has dimension $N+1$. The matrices D^{u}_{k}, E^u both have similar size as I, and are, respectively, the tridiagonal and diagonal matrices given below:

$$D^{u}_{k} = \begin{pmatrix}
1 & 0 & 0 & 0 & \cdots & 0 & 0 & 0\\
-R^{u}_{y} & \mathbf{a}^{u}_{m,1,k} & -R^{u}_{y} & 0 & \cdots & 0 & 0 & 0\\
0 & -R^{u}_{y} & \mathbf{a}^{u}_{m,2,k} & -R^{u}_{y} & \cdots & 0 & 0 & 0\\
\vdots & \vdots & \vdots & \vdots & \ddots & \vdots & \vdots & \vdots\\
0 & 0 & 0 & 0 & \cdots & -R^{u}_{y} & \mathbf{a}^{u}_{m,n-1,k} & -R^{u}_{y}\\
0 & 0 & 0 & 0 & \cdots & 0 & 0 & 1
\end{pmatrix} \tag{2.22}$$

and

$$E^{u} = \begin{pmatrix}
0 & 0 & 0 & \cdots & 0 & 0\\
0 & -R^{u}_{x} & 0 & \cdots & 0 & 0\\
0 & 0 & -R^{u}_{x} & \cdots & 0 & 0\\
\vdots & \vdots & \vdots & \ddots & \vdots & \vdots\\
0 & 0 & 0 & \cdots & -R^{u}_{x} & 0\\
0 & 0 & 0 & \cdots & 0 & 0
\end{pmatrix} \tag{2.23}$$

It is important to realize that the identity matrix appears at the beginning and at the end of the main diagonal of matrix A. This inclusion is to account for the homogeneous Dirichlet data at the vertical boundaries. Observe that other of the remaining entries on the main diagonal of matrix A^{u}_{k} are equal to 1. These entries are associated to the homogeneous Dirichlet boundary data at the horizontal boundaries of Ω. All remaining entries obviously correspond to the discretization at the inner nodes of the spatial domain.

In the case that $e^{k}_{m,n}$, $i^{k}_{A_{m,n}}$ and $i^{k}_{S_{m,n}}$ are non-negative, it is worth noting that each of the matrices A^{u}_{k} is an M-matrix, for each $k = 0, 1, \ldots, K-1$, and u being r, s, q, e, i_S, i_A or v. The term *M-matrix* refers to a real and square matrix M which satisfies the criteria listed below [40]:

1. The off-diagonal components are negative numbers.
2. Entries of the principal diagonal are all positive.
3. The matrix is strictly diagonally dominant.

As a matter of fact, these type of matrices have the property of being non-singular and having positive real numbers as entries in their inverses [40]. The non-negativity preservation for the approximations obtained through the computer methodology will be demonstrated by utilizing the previously stated property on M-matrices. Evidently, this is a crucial aspect of the numerical model, given that the solutions for the continuous system correspond to population sizes.

3. Results

In this section, we showcase the key analytical and numerical outcomes linked to the epidemiological model (2.2) and its non-standard discretization (2.12). We provide a fresh start by deriving rigorously some results on the analytical solutions for our mathematical model.

3.1. Analytical outcomes

In a first stage, the equilibrium solutions for system (2.2) will be derived. First, we determine the equilibrium that exists when there is no sickness, which is a steady-state solution to the mathematical model. In particular, this implies that $E = I_A = I_S = Q = R = 0$. As a consequence, the epidemiological model leads to the following algebraic system of equations:

$$\begin{aligned} \Lambda + m_S + \tau V - S(\mu + \omega) &= 0, \\ m_V + \omega S - V(\mu + \tau) &= 0. \end{aligned} \tag{3.1}$$

From this system, we can find the constants S and V algebraically. This leads us to calculate the equilibrium point for the case without sickness, which is

$$P_{DFE} = (S_0, V_0, 0, 0, 0, 0, 0), \tag{3.2}$$

where

$$\begin{aligned} S_0 &= \frac{(\mu + \tau)(\Lambda + m_S) + \tau m_V}{\mu(\mu + \omega + \tau)}, \\ V_0 &= \frac{(\mu + \omega)m_V + \omega(m_S + \Lambda)}{\mu(\mu + \omega + \tau)}. \end{aligned} \tag{3.3}$$

Next, we calculate the basic reproduction number of (2.2). This number is denoted by $\mathscr{R}_0$. To that end, we will apply the technique of the next generation matrix. In that way,

$$\mathscr{R}_0 = \rho(FV^{-1}). \tag{3.4}$$

The largest absolute value of an eigenvalue is represented by the symbol ρ, which stands for the spectral radius operator of a matrix [41]. To find our matrices F and V, we focus on the compartments in the mathematical model that impact the spreading, concretely, the exposed, asymptomatic, quarantined, and symptomatic individuals. Their behavior is controlled by the following system:

$$\begin{aligned} \frac{\partial E}{\partial t} &= m_E + \alpha SE + \beta SI_A + \gamma SI_S - (\zeta + \epsilon + \delta + \mu)E + d_E \nabla^2 E, \\ \frac{\partial I_A}{\partial t} &= m_{I_A} + \delta E - (\eta + \mu)I_A + d_{I_A} \nabla^2 I_A, \\ \frac{\partial Q}{\partial t} &= m_Q + \zeta E + \kappa I_S - (\iota + \upsilon + \mu)Q + d_Q \nabla^2 Q, \\ \frac{\partial I_S}{\partial t} &= m_{I_S} + \epsilon E - (\kappa + \rho + \theta + \mu)I_S + d_{I_S} \nabla^2 I_S. \end{aligned} \tag{3.5}$$

Using results derived in [42,43], the determination of the basic reproductive number can be obtained by omitting the diffusion terms in system (3.5). In that way, the system of PDEs becomes a mathematical model consisting of the simpler model

$$\begin{aligned} \frac{dE}{dt} &= m_E + \alpha SE + \beta SI_A + \gamma SI_S - (\zeta + \epsilon + \delta + \mu)E, \\ \frac{dI_A}{dt} &= m_{I_A} + \delta E - (\eta + \mu)I_A, \\ \frac{dQ}{dt} &= m_Q + \zeta E + \kappa I_S - (\iota + \upsilon + \mu)Q, \\ \frac{dI_S}{dt} &= m_{I_S} + \epsilon E - (\kappa + \rho + \theta + \mu)I_S. \end{aligned} \tag{3.6}$$

From (3.6), we introduce two vectors. The first is denoted by $\mathscr{F}$, and it considers only those terms where infection exists. The second will be represented by $\mathscr{V}$, and will contain all the remaining terms with opposite sign. More precisely, let us define

$$\mathscr{F} = \begin{pmatrix} \alpha SE + \beta SI_A + \gamma SI_S \\ 0 \\ 0 \\ 0 \end{pmatrix} \tag{3.7}$$

and

$$\mathscr{V} = \begin{pmatrix} -m_E + (\zeta + \epsilon + \delta + \mu)E \\ -m_{I_A} - \delta E + (\eta + \mu)I_A \\ -m_Q - \zeta E - \kappa I_S + (\iota + \upsilon + \mu)Q \\ -m_{I_S} - \epsilon E + (\kappa + \rho + \theta + \mu)I_S \end{pmatrix}. \tag{3.8}$$

Let V and F represent, respectively, the Jacobians associated to the vectors $\mathscr{V}$ and $\mathscr{F}$ calculated on the constant solution where the disease does not exists. Thus, we find that

$$F = \begin{pmatrix} \alpha S & \beta S & 0 & \gamma S \\ 0 & 0 & 0 & 0 \\ 0 & 0 & 0 & 0 \\ 0 & 0 & 0 & 0 \end{pmatrix} \tag{3.9}$$

and

$$V_J = \begin{pmatrix} \zeta + \epsilon + \delta + \mu & 0 & 0 & 0 \\ -\delta & \eta + \mu & 0 & 0 \\ -\zeta & 0 & \iota + \upsilon + \mu & -\kappa \\ -\epsilon & 0 & 0 & \kappa + \rho + \theta + \mu \end{pmatrix}. \tag{3.10}$$

As a consequence,

$$FV^{-1} = \begin{pmatrix} g_{11} & g_{12} & 0 & g_{14} \\ 0 & 0 & 0 & 0 \\ 0 & 0 & 0 & 0 \\ 0 & 0 & 0 & 0 \end{pmatrix}, \tag{3.11}$$

where g_{11}, g_{12} and g_{14} are real numbers that depend on the model parameters. As a consequence, the basic reproductive number satisfies $\mathscr{R}_0 = |g_{11}|$ or, more precisely,

$$\mathscr{R}_0 = \frac{S_0[((\kappa + \mu + \rho + \theta)(\alpha(\eta + \mu) + \beta\delta)) + \epsilon\gamma(\eta + \mu)]}{(\eta + \mu)(\delta + \epsilon + \mu + \zeta)(\kappa + \mu + \rho + \theta)}. \tag{3.12}$$

Here, we may substitute the value for $S = S_0$ from (3.3) into (3.12). Thus, only constants from the proposed model will be used to generate the expression for $\mathscr{R}_0$. Theorem 1 presents the study on the local asymptotic stability of this constant solution.

Theorem 1. *The equilibrium of the model (2.2) in the case when the disease is absent is locally asymptotically stable whenever* $\mathscr{R}_0 < 1$. □

Proof. The Jacobian matrix is represented by J, and evaluated for the system (2.2) when the disease is not present. After some calculations, it can be readily checked that J is given by

$$J = \begin{pmatrix} J_{11} & \tau & -\alpha S & -\beta S & 0 & -\gamma S & \sigma \\ \omega & J_{22} & 0 & 0 & 0 & 0 & 0 \\ \alpha E + \beta I_A + \gamma I_S & 0 & J_{33} & 0 & 0 & 0 & 0 \\ 0 & 0 & \delta & J_{44} & 0 & 0 & 0 \\ 0 & 0 & \zeta & 0 & J_{55} & \kappa & 0 \\ 0 & 0 & \epsilon & 0 & 0 & J_{66} & 0 \\ 0 & 0 & 0 & \eta & \iota & \theta & J_{77} \end{pmatrix}, \tag{3.13}$$

where

$$\begin{aligned} J_{11} &= -\alpha E - \beta I_A - \gamma I_S - (\omega + \mu), \\ J_{22} &= -(\tau + \mu), \\ J_{33} &= \alpha S - (\zeta + \epsilon + \delta + \mu), \end{aligned}$$

$$J_{44} = -(\eta + \mu),$$
$$J_{55} = -(\iota + \upsilon + \mu),$$
$$J_{66} = -(\kappa + \rho + \theta + \mu),$$
$$J_{77} = -(\sigma + \mu). \tag{3.14}$$

Suppose that λ is any complex eigenvalue of J. It is straightforward to verify that $M = J - \lambda I$, with

$$M = \begin{pmatrix} M_{11} & \tau & -\alpha S & -\beta S & 0 & -\gamma S & \sigma \\ \omega & M_{22} & 0 & 0 & 0 & 0 & 0 \\ \alpha E + \beta I_A + \gamma I_S & 0 & M_{33} & 0 & 0 & 0 & 0 \\ 0 & 0 & \delta & M_{44} & 0 & 0 & 0 \\ 0 & 0 & \zeta & 0 & M_{55} & \kappa & 0 \\ 0 & 0 & \epsilon & 0 & 0 & M_{66} & 0 \\ 0 & 0 & 0 & \eta & \iota & \theta & M_{77} \end{pmatrix}. \tag{3.15}$$

In this equation, we observe the following conventions:

$$M_{11} = -\alpha E - \beta I_A - \gamma I_S - (\omega + \mu) - \lambda,$$
$$M_{22} = -(\tau + \mu) - \lambda,$$
$$M_{33} = \alpha S - (\zeta + \epsilon + \delta + \mu) - \lambda,$$
$$M_{44} = -(\mu + \eta) - \lambda,$$
$$M_{55} = -(\mu + \upsilon + \iota) - \lambda,$$
$$M_{66} = -(\mu + \rho + \kappa + \theta) - \lambda,$$
$$M_{77} = -(\mu + \sigma) - \lambda. \tag{3.16}$$

It is possible to verify through the use of the properties for determinants that

$$\det M = (M_{11}M_{22} - \omega\tau)M_{33}M_{44}M_{55}M_{66}M_{77}. \tag{3.17}$$

Equating the determinant to zero and performing some adequate mathematical calculations yields

$$\lambda_1 = \alpha\left[\frac{(\mu + \tau)(\Lambda + m_S) + \tau m_v}{\mu(\mu + \omega + \tau)}\right] - (\zeta + \epsilon + \delta + \mu),$$
$$\lambda_2 = -(\eta + \mu),$$
$$\lambda_3 = -(\iota + \upsilon + \mu),$$
$$\lambda_4 = -(\kappa + \rho + \theta + \mu),$$
$$\lambda_5 = -(\mu + \sigma). \tag{3.18}$$

Notice that λ_2, λ_3, λ_4 and λ_5 are negative. Moreover, λ_1 is also negative if $\mathscr{R}_0 < 1$ (see Appendix A for the calculations). The missing eigenvalues will be calculated by utilizing the expression of a second order polynomial, that is,

$$\lambda^2 + (\omega + \tau + 2\mu)\lambda + \mu(\mu + \tau + \omega)\mu = 0. \tag{3.19}$$

More precisely,

$$\lambda_{6,7} = \frac{-(\omega + \tau + 2\mu) \pm \sqrt{\omega^2 + \tau^2 + \omega\tau}}{2}. \tag{3.20}$$

As a result, λ_6 and λ_7 are negative. To summarize our findings, if $\mathscr{R}_0 < 1$, than all eigenvalues are negative, whence the conclusion of this proposition follows. □

To determine the endemic equilibrium solution, let us suppose a constant solution for (2.2). This solution will take the expression $R(t) = R^*$, $I_S(t) = I_S^*$, $Q(t) = Q^*$, $I_A(t) = I_A^*$, $V(t) = V^*$, $E(t) = E^*$ and $S(t) = S^*$. Here, S^*, E^*, V^*, I_A^*, Q^*, I_S^* and R^* are numbers which are greater than or equal to zero. Conveniently agree that

$$P_{EE} = (S^*, V^*, E^*, I_A^*, Q^*, I_S^*, R^*). \tag{3.21}$$

Under these circumstances, the main model (2.2) can be changed to a particular algebraic system. It is possible to check that those solutions satisfy the implicit system

$$S^* = \frac{\Lambda + m_S + \sigma R^* + \tau V^*}{\mu + \omega + \alpha E^* + \beta I_A^* + \gamma I_S^*},$$
$$V^* = \frac{m_V + S^*\omega}{\mu + \tau},$$
$$E^* = \frac{m_E + \beta S^* I_A^* + \gamma S^* I_S^*}{\delta + \epsilon + \mu + \zeta - \alpha S^*},$$
$$I_A^* = \frac{m_{I_A} + \delta E^*}{\eta + \mu},$$
$$Q^* = \frac{m_Q + \kappa^* I_S + \zeta E^*}{\iota + \mu + \upsilon},$$
$$I_S^* = \frac{m_{I_S} + \epsilon E^*}{\kappa + \mu + \rho + \theta},$$
$$R^* = \frac{m_R + \eta I_A^* + \iota Q^* + \theta I_S^*}{\mu + \sigma}. \tag{3.22}$$

An explicit form of the solutions is available using software for symbolic algebra. We have not presented those solutions in view that their expressions are too long to be provided herein.

We state now the local asymptotic stability property for our point P_{EE} in our next theorem. The demonstration is similar to that for Theorem 1 and, thus, to avoid duplication of arguments, we omit the proof here.

Theorem 2. *In the system (2.2), local asymptotic stability for the endemic constant solution is observed when $\mathscr{R}_0 > 1$.* □

Before closing this stage of our work, we provide the parametric sensitivity analysis for system (2.2). The next expression is used in order to calculate it:

$$A_\phi = \frac{\phi}{\mathscr{R}_0}\frac{\partial \mathscr{R}_0}{\partial \phi}. \tag{3.23}$$

Notice then that

$$A_\alpha = \frac{(\kappa + \mu + \rho + \theta)(\eta + \mu)\alpha}{(\beta\delta + \alpha(\eta + \mu))(\kappa + \mu + \rho + \theta) + \epsilon\gamma(\mu + \eta)},$$
$$A_\beta = \frac{\beta\delta(\kappa + \mu + \rho + \theta)}{(\beta\delta + \alpha(\eta + \mu))(\kappa + \mu + \rho + \theta) + \epsilon\gamma(\eta + \mu)},$$
$$A_\gamma = \frac{\epsilon\gamma(\eta + \mu)}{(\beta\delta + \alpha(\eta + \mu))(\kappa + \mu + \rho + \theta) + \epsilon\gamma(\eta + \mu)},$$
$$A_\eta = \frac{-\beta\delta\eta(\kappa + \mu + \rho + \theta)}{(\eta + \mu)(\epsilon\gamma(\eta + \mu) + (\alpha\eta + \alpha\mu + \beta\delta)(\kappa + \mu + \rho + \theta)},$$
$$A_{m_V} = \frac{m_V\tau}{m_V\tau + (\Lambda + m_S)(\mu + \tau)},$$
$$A_\Lambda = \frac{\Lambda(\mu + \tau)}{m_V\tau + (\Lambda + m_S)(\mu + \tau)},$$
$$A_\omega = \frac{-\omega}{\mu + \omega + \tau},$$
$$A_\zeta = \frac{-\zeta}{\delta + \epsilon + \mu + \zeta},$$
$$A_{m_S} = \frac{m_S(\mu + \tau)}{m_V\tau(\Lambda + m_S)(\mu + \tau)}. \tag{3.24}$$

Observe that the constants A_α, A_β, A_γ, A_{m_V}, A_Λ and A_{m_S} are positive numbers. It can be checked also that A_τ, A_ϵ and A_δ are positive. The expressions for these values have been omitted in view that they are too long to be presented herein. The constants A_η, A_ζ and A_ω are negative, and so are A_μ, A_κ, A_ρ and A_θ. The remaining constants A_ϕ are not presented here, but they are actually equal to zero. From this sensitivity analysis, we deduce that $\mathscr{R}_0$ is sensitive to values of the variables α, β, γ, δ, ϵ, Λ, τ, m_S and m_V.

3.2. Numerical outcomes

We outline in this section the most significant theoretical findings related to the computational approach (2.12). To demonstrate the accuracy of the analytical and numerical properties of our

models, some simulations will be performed. The first result confirms the presence of positive solutions for the computer method (2.12).

Theorem 3. *Suppose that* $S^0, V^0, E^0, I_A^0, Q^0, I_S^0, R^0 : \Omega \to \mathbb{R}$ *are non-negative. If*

$$2R_x^u + 2R_y^u < 1 \tag{3.25}$$

for each $u = s, e, i_A, q, i_S, r, v$, *then the solution functions obtained through the computational method (2.12) are also non-negative.*

Proof. This proof will make use of an inductive argument. For this purpose, note that the initial approximations $u_{m,n}^0$ are all non-negative because the initial data are non-negative, for each $u = s, e, i_A, q, i_S, r, v$. So, assume that it is true that $u_{m,n}^k \geq 0$ for some $k \in \mathbb{N} \cup \{0\}$, for all $m = 0, 1, \ldots, M$ and $n = 0, 1, \ldots, N$, and all grid functions $u = s, e, i_A, q, i_S, r, v$. This implies that all the matrices A_k^u are M-matrices and, moreover, the components of all the vectors $\mathbf{b}_{m,n,k}^u$ are non-negative numbers by virtue of the fact that the inequality (3.25) is satisfied. The positivity property of the inverses of M-matrices and the identity (2.18) assure now that the real vector

$$\mathbf{u}^{k+1} = (A_k^u)^{-1}\mathbf{b}_k^u \tag{3.26}$$

is non-negative, for each $u = s, e, i_A, q, i_S, r, v$. The conclusion follows then from mathematical induction. □

Our next result establishes that the finite-difference method (2.12) has the same equilibrium solutions as those from the mathematical model (2.2). Additionally, the numerical approach keeps the stability characteristics of such equilibrium solutions.

Theorem 4. *The equilibrium solutions for the computer method (2.12) are* P_{DFE} *and* P_{EE}. *Moreover,*

(a) *if* $\mathscr{R}_0 < 1$, P_{DFE} *is locally asymptotically stable.*
(b) *when* $\mathscr{R}_0 > 1$, P_{EE} *is locally asymptotically stable.*

Proof. This result is reached by noting that the nonlinear analysis of the computer method (2.12) is exactly the same as that of the mathematical model (2.2). □

Considering this results, the proposed computer method presented in this report is a dynamically consistent discretization of the epidemiological system (2.2). Only the numerical properties for our method need to be established now. The consistency of the finite-difference method will then be discussed in a first step. We introduce the next continuous operators in order to examine the consistency:

$$\begin{aligned}
{}_S\mathscr{L} &= \frac{\partial S}{\partial t} - \Lambda - m_S - \sigma R + \alpha SE + \beta SI_A + \gamma SI_S \\
&\quad - \tau V + (\omega + \mu)S - d_S\nabla^2 S, \\
{}_V\mathscr{L} &= \frac{\partial V}{\partial t} - m_V - \omega S + (\tau + \mu)V - d_V\nabla^2 V, \\
{}_E\mathscr{L} &= \frac{\partial E}{\partial t} - m_E - \alpha SE - \beta SI_A - \gamma SI_S \\
&\quad + (\zeta + \epsilon + \delta + \mu)E - d_E\nabla^2 E, \\
{}_{I_A}\mathscr{L} &= \frac{\partial I_A}{\partial t} - m_{I_A} - \delta E + (\eta + \mu)I_A - d_{I_A}\nabla^2 I_A, \\
{}_Q\mathscr{L} &= \frac{\partial Q}{\partial t} - m_Q - \zeta E - \kappa I_S + (\iota + \upsilon + \mu)Q - d_Q\nabla^2 Q, \\
{}_{I_S}\mathscr{L} &= \frac{\partial I_S}{\partial t} - m_{I_S} - \epsilon E + (\kappa + \rho + \theta + \mu)I_S - d_{I_S}\nabla^2 I_S, \\
{}_R\mathscr{L} &= \frac{\partial R}{\partial t} - m_R - \iota Q - \theta I_S - \eta I_A + (\sigma + \mu)R - d_R\nabla^2 R.
\end{aligned} \tag{3.27}$$

All these operators are considered functions of $(\mathbf{x}, t)$. For simplification purposes, agree that ${}_U\mathscr{L}_{m,n}^{k+1} = \mathscr{L}(x_m, y_n, t_k)$, for each $U = S, V, E, I_A, Q, I_S, R$, $m = 0, 1, \ldots, M$, $n = 0, 1, \ldots, N$ and $k = 0, 1, \ldots, K-1$.

Let us consider also the following discrete operators, for $k = 0, 1, 2, \ldots, K-1$, $m = 0, 1, 2, \ldots, M$ and $n = 0, 1, 2, \ldots, N$:

$$\begin{aligned}
{}_SL_{m,n}^{k+1} &= \hat{\delta}_t S_{m,n}^{k+1} - \Lambda - m_S - \delta R_{m,n}^k + \alpha S_{m,n}^{k+1}E_{m,n}^k + \beta S_{m,n}^{k+1}I_{A_{m,n}}^k \\
&\quad + \gamma S_{m,n}^{k+1}I_{S_{m,n}}^k - \tau V_{m,n}^k - (\omega + \mu)S_{m,n}^{k+1} - \hat{\nabla}_s^2 S_{m,n}^{k+1}, \\
{}_VL_{m,n}^{k+1} &= \hat{\delta}_t V_{m,n}^{k+1} - m_V - \omega S_{m,n}^k + (\tau + \mu)V_{m,n}^{k+1} - \hat{\nabla}_v^2 V_{m,n}^{k+1}, \\
{}_EL_{m,n}^{k+1} &= \hat{\delta}_t E_{m,n}^{k+1} - m_E - \alpha S_{m,n}^k E_{m,n}^{k+1} - \beta S_{m,n}^k I_{A_{m,n}}^k - \gamma S_{m,n}^k I_{S_{m,n}^k} \\
&\quad + (\zeta + \epsilon + \delta + \mu)E_{m,n}^{k+1} - \hat{\nabla}_e^2 E_{m,n}^{k+1}, \\
{}_{I_A}L_{m,n}^{k+1} &= \hat{\delta}_t I_{A_{m,n}}^{k+1} - m_{I_A} - \delta E_{m,n}^k + (\eta + \mu)I_{A_{m,n}}^{k+1} - \hat{\nabla}_{i_A}^2 I_{A_{m,n}}^{k+1}, \\
{}_QL_{m,n}^{k+1} &= \hat{\delta}_t Q_{m,n}^{k+1} - m_Q - \zeta E_{m,n}^k - \kappa I_{S_{m,n}^k} + (\iota + \upsilon + \mu)Q_{m,n}^k - \hat{\nabla}_q^2 Q_{m,n}^{k+1}, \\
{}_{I_S}L_{m,n}^{k+1} &= \hat{\delta}_t I_{S_{m,n}}^{k+1} - m_{I_S} - \epsilon E_{m,n}^k + (\kappa + \rho + \theta + \mu)I_{S_{m,n}}^{k+1} - \hat{\nabla}_{i_S}^2 I_{S_{m,n}}^{k+1}, \\
{}_RL_{m,n}^{k+1} &= \hat{\delta}_t R_{m,n}^{k+1} - m_R - \iota Q_{m,n}^k - \theta I_{S_{m,n}}^k - \eta I_{A_{m,n}}^k + (\sigma + \mu)R_{m,n}^{k+1} - \hat{\nabla}_r^2 R_{m,n}^{k+1}.
\end{aligned} \tag{3.28}$$

Here, we let

$$\hat{\nabla}_u^2 U_{m,n}^{k+1} = d_U(\hat{\delta}_x^2 + \hat{\delta}_y^2)\hat{\mu}_t U_{m,n}^k. \tag{3.29}$$

Theorem 5. *Suppose that* $S, E, I_A, I_S, Q, R, V \in \mathcal{C}_{x,t}^{4,2}(\overline{\Omega} \times [0, T])$. *Then there is some* $C \geq 0$ *independently from* Δt, Δx *and* Δy, *which satisfies*

$$\left|{}_U\mathscr{L}_{m,n}^{k+1} - {}_UL_{m,n}^{k+1}\right| \leq C(\Delta t + (\Delta x)^2 + (\Delta y)^2), \tag{3.30}$$

for all the indexes $m = 0, 1, 2, \ldots, M$, $n = 0, 1, 2, \ldots, N$ *and* $k = 0, 1, 2, \ldots, K-1$.

Proof. Notice that the triangle inequality and some algebraic simplifications yield

$$\begin{aligned}
\left|{}_S\mathscr{L}_{m,n}^{k+1} - {}_SL_{m,n}^{k+1}\right| &\leq \left|\frac{\partial S}{\partial t}(x_n, y_n, t_{k+1}) - \hat{\delta}_t S_{m,n}^{k+1}\right| \\
&\quad + (\alpha|E_{m,n}^k| + \beta|I_{A_{m,n}}^k| + \gamma|I_{S_{m,n}}^k| + \omega + \mu)\left|S_{m,n}^{k+1} - S_{m,n}^k\right| \\
&\quad + \left|\frac{\partial^2 S}{\partial x^2}(x_n, y_n, t_{k+1}) - \hat{\delta}_x^2 S_{m,n}^{k+1}\right| + \left|\frac{\partial^2 S}{\partial y^2}(x_n, y_n, t_{k+1}) - \hat{\delta}_y^2 S_{m,n}^{k+1}\right|,
\end{aligned} \tag{3.31}$$

for each $k = 0, 1, 2, \ldots, K-1$, $m = 0, 1, 2, \ldots, M$ and $n = 0, 1, 2, \ldots, N$. The regularity assumption on the functions implies that, for some $K_E, K_{I_A}, K_{I_S} \geq 0$ independently from Δt, Δx and Δy, the next relations hold:

$$\begin{aligned}
|E_{m,n}^k| &\leq K_E, \\
|I_{A_{m,n}}^k| &\leq K_{I_A}, \\
|I_{S_{m,n}}^k| &\leq K_{I_S},
\end{aligned} \tag{3.32}$$

for $k = 0, 1, 2, \ldots, K$, $m = 0, 1, 2, \ldots, M$ and $n = 0, 1, 2, \ldots, N$. Using Taylor's theorem, there are constants $C_1, C_2, C_3, C_4 \geq 0$ which are also independent from the computational parameters such that, for each k, m and n, the following are satisfied:

$$\begin{aligned}
\left|\frac{\partial S}{\partial t}(x_n, y_n, t_{k+1}) - \hat{\delta}_t S_{m,n}^{k+1}\right| &\leq C_1\Delta t, \\
\left|S_{m,n}^{k+1} - S_{m,n}^k\right| &\leq C_2\Delta t, \\
\left|\frac{\partial^2 S}{\partial x^2}(x_n, y_n, t_{k+1}) - \hat{\delta}_x^2\hat{\mu}_t S_{m,n}^k\right| &\leq C_3\left[\Delta t + (\Delta x)^2\right], \\
\left|\frac{\partial^2 S}{\partial y^2}(x_n, y_n, t_{k+1}) - \hat{\delta}_y^2\hat{\mu}_t S_{m,n}^k\right| &\leq C_4\left[\Delta t + (\Delta y)^2\right],
\end{aligned} \tag{3.33}$$

Let us define

$$C_S = \max\{C_1, (\alpha K_E + \beta K_{I_A}\gamma K_{I_S} + \omega + \mu)C_2, C_3, C_4\}. \tag{3.34}$$

It is obvious that $C_S \geq 0$ is independent from Δt, Δx and Δy. Moreover, the inequality (3.31) implies that

$$\left|{}_S\mathscr{L}^{k+1}_{m,n} - {}_SL^k_{m,n}\right| \leq C_S(\Delta t + (\Delta x)^2 + (\Delta y)^2), \tag{3.35}$$

for $k = 0, 1, 2, \ldots, K$, $m = 0, 1, 2, \ldots, M$ and $n = 0, 1, 2, \ldots, N$. Similarly, it is possible to verify that there are non-negative constants C_V, C_E, C_{I_A}, C_Q, C_{I_S} and C_R which are independent from the numerical step sizes, with the properties that the following inequalities hold uniformly over all k, m and n:

$$\begin{aligned}
\left|{}_V\mathscr{L}^{k+1}_{m,n} - {}_VL^{k+1}_{m,n}\right| &\leq C_V(\Delta t + (\Delta x)^2 + (\Delta y)^2),\\
\left|{}_E\mathscr{L}^{k+1}_{m,n} - {}_EL^{k+1}_{m,n}\right| &\leq C_E(\Delta t + (\Delta x)^2 + (\Delta y)^2),\\
\left|{}_{I_A}\mathscr{L}^{k+1}_{m,n} - {}_{I_A}L^{k+1}_{m,n}\right| &\leq C_{I_A}(\Delta t + (\Delta x)^2 + (\Delta y)^2),\\
\left|{}_Q\mathscr{L}^{k+1}_{m,n} - {}_QL^{k+1}_{m,n}\right| &\leq C_Q(\Delta t + (\Delta x)^2 + (\Delta y)^2),\\
\left|{}_{I_S}\mathscr{L}^{k+1}_{m,n} - {}_{I_S}L^{k+1}_{m,n}\right| &\leq C_{I_S}(\Delta t + (\Delta x)^2 + (\Delta y)^2),\\
\left|{}_R\mathscr{L}^{k+1}_{m,n} - {}_RL^{k+1}_{m,n}\right| &\leq C_R(\Delta t + (\Delta x)^2 + (\Delta y)^2).
\end{aligned} \tag{3.36}$$

If $C = \max\{C_S, C_V, C_E, C_{I_A}, C_Q, C_{I_S}, C_R\}$, then the conclusion of this result is readily satisfied. □

We now concentrate on the stability and convergence of model (2.12). The discrete form of Gronwall's inequality (a well-known result from analysis) will be essential in reaching those properties [44].

Lemma 1. *Let $(\rho^n)_{n=0}^N$ and $(\omega^n)_{n=0}^N$ be arrays of non-negative numbers, and let $C \geq 0$ satisfy*

$$\omega^k \leq \rho^k + C\tau\sum_{n=0}^{k-1}\omega^k, \quad \forall k \in \{1, \ldots, N\}. \tag{3.37}$$

Then $\omega^n \leq \rho^n e^{Cn\tau}$ for each $n \in \{0, 1, \ldots, N\}$. □

For the mathematical model, we take into consideration two sets of initial data (2.2). They will be represented, respectively, by

$$\begin{aligned}
P^0 &= (S^0, V^0, E^0, I_A^0, Q^0, I_S^0, R^0),\\
\tilde{P}^0 &= (\tilde{S}^0, \tilde{V}^0, \tilde{E}^0, \tilde{I}_A^0, \tilde{Q}^0, \tilde{I}_S^0, \tilde{R}^0).
\end{aligned} \tag{3.38}$$

The components of these vectors are obviously non-negative real functions with domain Ω. The numerical solutions corresponding to the initial data P^0 and $\tilde{P}^0$ will be denoted, respectively, by $p = (s, v, e, i_A, q, i_S, r)$ and $\tilde{p} = (\tilde{s}, \tilde{v}, \tilde{e}, \tilde{i}_A, \tilde{q}, \tilde{i}_S, \tilde{r})$. Notice that the former solution satisfies the computer method (2.12), while the latter satisfies the following system, for each $k = 0, 1, \ldots, K-1$, $m = 0, 1, \ldots, M$ and $n = 0, 1, \ldots, N$:

$$\begin{aligned}
\hat{\delta}_t\tilde{s}^k_{m,n} &= \Lambda + m_S + \sigma\tilde{r}^k_{m,n} - \alpha\tilde{s}^{k+1}_{m,n}\tilde{e}^k_{m,n} - \beta\tilde{s}^{k+1}_{m,n}\tilde{i}^k_{A_{m,n}} - \gamma s^{k+1}_{m,n}\tilde{i}^k_{S_{m,n}}\\
&\quad + \tau\tilde{v}^k_{m,n} - (\omega+\mu)\tilde{s}^{k+1}_{m,n} + \hat{\nabla}_s^2\tilde{s}^{k+1}_{m,n},\\
\hat{\delta}_t\tilde{v}^k_{m,n} &= m_V + \omega\tilde{s}^k_{m,n} - (\tau+\mu)\tilde{v}^{k+1}_{m,n} + \hat{\nabla}_v^2\tilde{v}^{k+1}_{m,n},\\
\hat{\delta}_t\tilde{e}^k_{m,n} &= m_E + \alpha\tilde{s}^k_{m,n}\tilde{e}^k_{m,n} + \beta\tilde{s}^k_{m,n}\tilde{i}^k_{A_{m,n}} + \gamma\tilde{s}^k_{m,n}\tilde{i}^k_{S_{m,n}}\\
&\quad - (\zeta+\epsilon+\delta+\mu)\tilde{e}^{k+1}_{m,n} + \hat{\nabla}_e^2\tilde{e}^{k+1}_{m,n},\\
\hat{\delta}_t\tilde{i}^k_{A_{m,n}} &= m_{I_A} + \delta\tilde{e}^k_{m,n} - (\eta+\mu)\tilde{i}^{k+1}_{A_{m,n}} + \hat{\nabla}_{i_A}^2\tilde{i}^{k+1}_{A_{m,n}},\\
\hat{\delta}_t\tilde{q}^k_{m,n} &= m_Q + \zeta\tilde{e}^k_{m,n} + \kappa\tilde{i}^k_{S_{m,n}} - (\iota+\upsilon+\mu)\tilde{q}^{k+1}_{m,n} + \hat{\nabla}_q^2\tilde{q}^{k+1}_{m,n},\\
\hat{\delta}_t\tilde{i}^k_{S_{m,n}} &= m_{I_S} + \epsilon\tilde{e}^k_{m,n} - (\kappa+\rho+\theta+\mu)\tilde{i}^{k+1}_{S_{m,n}} + \hat{\nabla}_{i_S}^2\tilde{i}^{k+1}_{S_{m,n}},
\end{aligned}$$

$$\hat{\delta}_t\tilde{r}^k_{m,n} = m_R + \iota\tilde{q}^k_{m,n} + \theta\tilde{i}^k_{S_{m,n}} + \eta\tilde{i}^k_{A_{m,n}} - (\sigma+\mu)\tilde{r}^{k+1}_{m,n} + \hat{\nabla}_r^2\tilde{r}^{k+1}_{m,n}. \tag{3.39}$$

For the sake of simplification, we introduce following numbers

$${}_u\varepsilon^k_{m,n} = u^k_{m,n} - \tilde{u}^k_{m,n}, \tag{3.40}$$

where $u = s, v, e, i_A, q, i_S, r$.

For the remainder of this manuscript, we will suppose that $S, E, I_A, I_S, Q, R, V \in \mathcal{C}^{4,2}_{x,t}(\overline{\Omega}\times[0,T])$. The subsequent theorem, which provides the stability features of the numerical model, will follow this notation (2.12). Moreover, we will require the following additional operators:

$$\hat{\delta}_x u^k_{m,n} = \frac{u^k_{m+1,n} - u^k_{m,n}}{\Delta x}, \tag{3.41}$$

$$\hat{\delta}_y u^k_{m,n} = \frac{u^k_{m,n+1} - u^k_{m,n}}{\Delta y}. \tag{3.42}$$

Additionally, we concur that the Euclidean norm of u and the inner product of u and v (when they are real vectors of the same size N) are, respectively,

$$\|u\|_2^2 = \sum_{i=1}^N |u_i|^2, \tag{3.43}$$

$$\langle u, v\rangle = \sum_{i=1}^N u_i v_i. \tag{3.44}$$

Using this notation, the Cauchy–Schwartz and Young's inequalities are given, respectively, by

$$|\langle u, v\rangle| \leq \|u\|_2\|v\|_2, \tag{3.45}$$

$$|\langle u, v\rangle| \leq \frac{1}{2}\|u\|_2^2 + \frac{1}{2}\|v\|_2^2. \tag{3.46}$$

Theorem 6. *Stability in the Euclidean norm of the computer methodology can be ensured whenever Δt is sufficiently small.*

Proof. In this proof, the parameter C will denote a non-negative constant which does not depend on the computational parameters, and which may be different in each case. Taking the difference between the first equation in system (2.12) and the first equation of (3.39), one readily shows that the next discrete equality holds:

$$\begin{aligned}
\hat{\delta}_{ts}\varepsilon^k &= \sigma_r\varepsilon^k - \gamma(s^{k+1}i^k_S - \tilde{s}^{k+1}\tilde{i}^k_S) + \tau_v\varepsilon^k\\
&\quad - (\omega+\mu)_s\varepsilon^{k+1} - \alpha(s^{k+1}e^k - \tilde{s}^{k+1}\tilde{e}^k_{m,n})\\
&\quad - \beta(s^{k+1}i^k_A - \tilde{s}^{k+1}\tilde{i}^k_A) + d_S(\hat{\delta}_x^2 + \hat{\delta}_y^2)\hat{\mu}_{ts}\varepsilon^k.
\end{aligned} \tag{3.47}$$

It is now possible to verify that the subsequent identities are satisfied:

$$2\Delta t\langle\hat{\delta}_{ts}\varepsilon^k, \hat{\mu}_{ts}\varepsilon^k\rangle = \|{}_s\varepsilon^{k+1}\|_2^2 - \|{}_s\varepsilon^k\|_2^2, \tag{3.48}$$

$$\langle(\hat{\delta}_x^2 + \hat{\delta}_y^2)\hat{\mu}_{ts}\varepsilon^k, \hat{\mu}_{ts}\varepsilon^k\rangle = -\left(\|\hat{\delta}_x\hat{\mu}_{ts}\varepsilon^k\|_2^2 + \|\hat{\delta}_y\hat{\mu}_{ts}\varepsilon^k\|_2^2\right). \tag{3.49}$$

Moreover, the following equations hold component-wise:

$$\begin{aligned}
s^{k+1}i^k_S - \tilde{s}^{k+1}\tilde{i}^k_S &= {}_s\varepsilon^{k+1}i^k_S - \tilde{s}^{k+1}{}_{i_S}\varepsilon^k,\\
s^{k+1}e^k - \tilde{s}^{k+1}\tilde{e}^k &= {}_s\varepsilon^{k+1}e^k - \tilde{s}^{k+1}{}_e\varepsilon^k,\\
s^{k+1}i^k_A - \tilde{s}^{k+1}\tilde{i}^k_A &= {}_s\varepsilon^{k+1}i^k_A - \tilde{s}^{k+1}{}_{i_A}\varepsilon^k.
\end{aligned} \tag{3.50}$$

Let then m be any number in $\{0, 1, \ldots, K-1\}$. Calculate summation among all the indexes $k \in \{0, 1, \ldots, m\}$ on both sides of (3.47), take then the product of $\hat{\mu}_{ts}\varepsilon^k$ on both ends and apply our last

identities. Rearranging terms algebraically, using telescoping sums and bounding from above, one obtains that

$$\begin{aligned}\|{}_s\varepsilon^{m+1}\|_2^2 \le \|{}_s\varepsilon^0\|_2^2 + 2\Delta t \sum_{k=0}^{m}\Big[&\langle \sigma_r \varepsilon^k, \hat{\mu}_{ts}\varepsilon^k\rangle - \gamma\langle {}_s\varepsilon^k i_s^k, \hat{\mu}_{ts}\varepsilon^k\rangle \\ &+ \gamma\langle \tilde{s}^{k+1}{}_{i_S}\varepsilon^k, \hat{\mu}_{ts}\varepsilon^k\rangle + \tau\langle {}_v\varepsilon^k, \hat{\mu}_{ts}\varepsilon^k\rangle \\ &- (\omega+\mu)\langle {}_s\varepsilon^{k+1}, \hat{\mu}_{ts}\varepsilon^k\rangle - \alpha\langle {}_s\varepsilon^{k+1}e^k, \hat{\mu}_{ts}\varepsilon^k\rangle \\ &+ \alpha\langle \tilde{s}^{k+1}{}_e\varepsilon^k, \hat{\mu}_{ts}\varepsilon^k\rangle - \beta\langle {}_s\varepsilon^{k+1}i_A^k, \hat{\mu}_{ts}\varepsilon^k\rangle \\ &\beta\langle \tilde{s}^{k+1}{}_{i_A}\varepsilon^k, \hat{\mu}_{ts}\varepsilon^k\rangle\Big]. \end{aligned} \tag{3.51}$$

Notice now that Young's inequality yields

$$\begin{aligned}\left|\langle {}_r\varepsilon^k, \hat{\mu}_{ts}\varepsilon^k\rangle\right| &\le \frac{1}{2}\left|\langle {}_r\varepsilon^k, {}_s\varepsilon^{k+1}\rangle\right| + \frac{1}{2}\left|\langle {}_r\varepsilon^k, {}_s\varepsilon^k\rangle\right| \\ &\le \frac{1}{2}\|{}_r\varepsilon^k\|_2^2 + \frac{1}{4}\|{}_s\varepsilon^{k+1}\|_2^2 + \frac{1}{4}\|{}_s\varepsilon^k\|_2^2 \\ &\le C\big(\|{}_r\varepsilon^k\|_2^2 + \hat{\mu}_t\|{}_s\varepsilon^k\|_2^2\big). \end{aligned} \tag{3.52}$$

Obviously, in this case, the constant C can be taken as $\frac{1}{2}$. On the contrary, the supposition that the solutions have an upper bound and an application of Young's inequality lead to

$$\begin{aligned}\left|\gamma\langle {}_s\varepsilon^k i_s^k, \hat{\mu}_{ts}\varepsilon^k\rangle\right| &\le \frac{\gamma}{2}\left|\langle {}_s\varepsilon^k i_s^k, {}_s\varepsilon^{k+1}\rangle\right| + \frac{\gamma}{2}\left|\langle {}_s\varepsilon^k i_s^k, {}_s\varepsilon^k\rangle\right| \\ &\le \frac{\gamma}{2}C\left|\langle {}_s\varepsilon^k, {}_s\varepsilon^{k+1}\rangle\right| + \frac{\gamma}{2}C\left|\langle {}_s\varepsilon^k, {}_s\varepsilon^k\rangle\right| \\ &\le C\hat{\mu}_t\|{}_s\varepsilon^k\|_2^2. \end{aligned} \tag{3.53}$$

In an analogue form, the following are readily obtained using the boundedness of the solutions and Young's inequality:

$$\begin{aligned}\left|\gamma\langle \tilde{s}^{k+1}{}_{i_S}\varepsilon^k, \hat{\mu}_{ts}\varepsilon^k\rangle\right| &\le C\big(\|{}_{i_S}\varepsilon^k\|_2^2 + \hat{\mu}_t\|{}_s\varepsilon^k\|_2^2\big), \\ \left|\tau\langle {}_v\varepsilon^k, \hat{\mu}_{ts}\varepsilon^k\rangle\right| &\le C\big(\|{}_v\varepsilon^k\|_2^2 + \hat{\mu}_t\|{}_s\varepsilon^k\|_2^2\big), \\ \left|(\omega+\mu)\langle {}_s\varepsilon^{k+1}, \hat{\mu}_{ts}\varepsilon^k\rangle\right| &\le C\hat{\mu}_t\|{}_s\varepsilon^k\|_2^2, \\ \left|\alpha\langle {}_s\varepsilon^{k+1}e^k, \hat{\mu}_{ts}\varepsilon^k\rangle\right| &\le C\hat{\mu}_t\|{}_s\varepsilon^k\|_2^2, \\ \left|\alpha\langle \tilde{s}^{k+1}{}_e\varepsilon^k, \hat{\mu}_{ts}\varepsilon^k\rangle\right| &\le C\big(\|{}_e\varepsilon^k\|_2^2 + \hat{\mu}_t\|{}_s\varepsilon^k\|_2^2\big), \\ \left|\beta\langle {}_s\varepsilon^{k+1}i_A^k, \hat{\mu}_{ts}\varepsilon^k\rangle\right| &\le C\hat{\mu}_t\|{}_s\varepsilon^k\|_2^2, \\ \left|\beta\langle \tilde{s}^{k+1}{}_{i_A}\varepsilon^k, \hat{\mu}_{ts}\varepsilon^k\rangle\right| &\le C\big(\|{}_{i_A}\varepsilon^k\|_2^2 + \hat{\mu}_t\|{}_s\varepsilon^k\|_2^2\big). \end{aligned} \tag{3.54}$$

Using these inequalities into (3.51), the validity of the inequality below can be readily demonstrated:

$$\hat{\mu}_t\|{}_s\varepsilon^m\|_2^2 \le \|{}_s\varepsilon^0\|_2^2 + C_s\Delta t\sum_{k=0}^{m}\sum_{w}\hat{\mu}_t\|{}_w\varepsilon^k\|_2^2 \tag{3.55}$$

Here, the second summation in (3.55) ranges over all the functions $w = s, v, e, i_A, q, i_S, r$, and C_s is a positive constant which does not depend on the computer parameters. Obviously, the last inequality was obtained by using the finite-difference associated to ${}_s\varepsilon^k$. Using the other discrete equations, we obtain the following inequalities in similar fashion:

$$\hat{\mu}_t\|{}_u\varepsilon^m\|_2^2 \le \|{}_u\varepsilon^0\|_2^2 + C_u\Delta t\sum_{k=0}^{m}\sum_{w}\hat{\mu}_t\|{}_w\varepsilon^k\|_2^2, \tag{3.56}$$

for each $u = s, v, e, i_A, q, i_S, r$ and $m \in \{0, 1, \ldots, K-1\}$. Adding these inequalities for all u, it follows that

$$\omega^m \le \rho + C\Delta t\sum_{k=0}^{m}\omega^k, \quad \forall m \in \{0, 1, \ldots, K\}. \tag{3.57}$$

Table 2
Common parameter values for the simulations in Section 3.3. The only parameters which vary in the experiments are m_S and m_E.

Paramater	Value	Paramater	Value
α	0.01	β	0
γ	0	δ	1.6728×10^{-5}
ϵ	0.0101	ζ	0.02798
η	0.04478	θ	0.0101
ι	0.0045	κ	0.0368
Λ	0.06	μ	0.0106
ρ	0.004	σ	0.0668
τ	0.0002	υ	3.2084×10^{-4}
ω	0.0032	d_S	1
d_V	1	d_E	1
d_{I_A}	1	d_Q	1
d_{I_S}	1	d_R	1
m_V	0.1	m_{I_A}	0
m_Q	0	m_{I_S}	0
m_R	0		

Here, we let

$$\rho = \sum_{w}\|{}_w\varepsilon^0\|_2^2, \tag{3.58}$$

$$\omega^k = \sum_{w}\hat{\mu}_t\|{}_w\varepsilon^k\|_2^2. \tag{3.59}$$

As a consequence from Lemma 1, if $\Delta t > 0$ is sufficiently small, then $\omega^m \le \rho e^{Cm\Delta t} \le \rho e^{CT}$, for each $k \in \{0, 1, \ldots, K\}$. Evidently, e^{CT} is a constant which does not depend on the computational parameters, and ρ depends on the differences between the initial conditions. The stability of the finite-difference method can now be established easily. □

The demonstration of the following proposition is analogue to that of Theorem 6. It is left out to prevent repetition.

Theorem 7. *If $S, E, I_A, I_S, Q, R, V \in \mathcal{C}^{4,2}_{x,t}(\overline{\Omega}\times[0,T])$ and Δt is small enough, then the approximations derived from the method (2.12) converge to the solution of the model (2.2) in the Euclidean norm, with convergence order $\mathcal{O}((\Delta x)^2 + (\Delta y)^2 + \Delta t)$.* □

3.3. Computer simulations

The objective of this stage is to demonstrate the analytical properties of mathematical model (2.2) through computer simulations and to confirm that computer method (2.12) can accurately capture the key dynamics of the continuous model. To do so, two sets of parameter values will be used, one with a basic reproductive number greater than 1 and the other with a value less than 1. The common parameter values used in all simulations are listed in Table 2. The value of parameter m_S will be altered to change the basic reproductive number. The migration rate of susceptible individuals will be adjusted to alter the basic reproductive number as follows:

- $m_S = 0.001$, in which case, $\mathscr{R}_0 < 1$.
- $m_S = 0.02$, which yields $\mathscr{R}_0 > 1$.

The rate of migration of exposed individuals will be taken into account to consider the disease-free and the endemic cases.

It is worthwhile mentioning that the values of the constants were chosen arbitrarily. Moreover, we will consider two examples in this section. In one of them, we will study the disease-free scenario, while the second example will investigate the endemic case. Computationally, we will let $\Omega = [0, 30]\times[0, 30]$, and let $\Delta_x = \Delta y = 1$ and $\Delta t = 0.1$. The computer method (2.12) was used to approximate the solutions of the epidemiological model

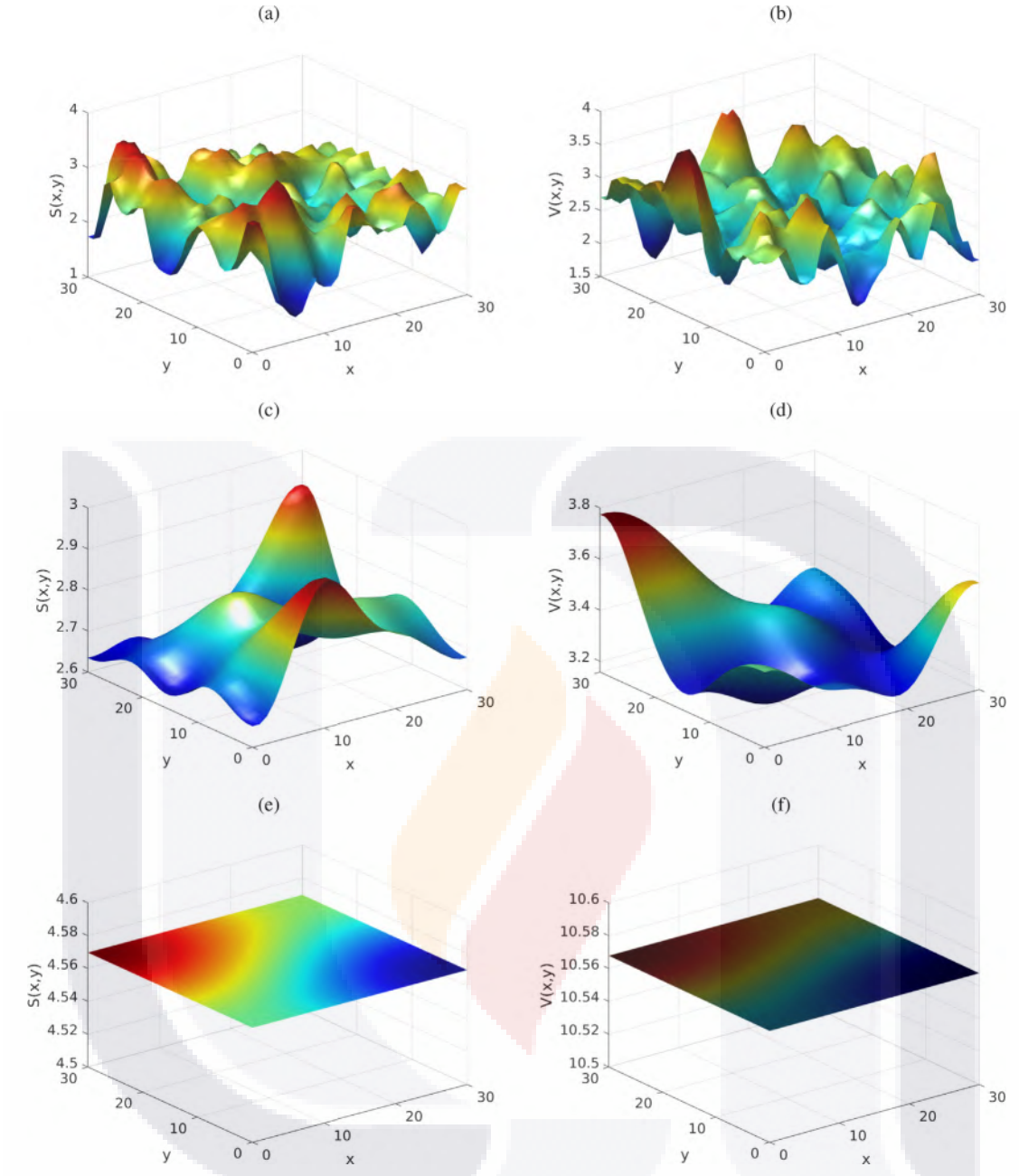

Fig. 2. Approximate solutions of the epidemiological model (2.2) versus the variables x and y at various instants of time. The left column shows approximate solutions for the function S, while the right column shows those for the function V. We used $t = 1$ (first row), $t = 10$ (second row) and $t = 500$ (third row). The approximations were obtained using the computer method (2.12) together with the parameter values in Table 2 and $m_S = 0.001$. All the initial populations are identically equal to zero, except for the susceptible and vaccinated, which were selected randomly in $[0, 5]$ using the function `rand` from Matlab.

(2.2). Obviously, the inequality (3.25) is satisfied, whence the computer method is solvable and yields non-negative solutions.

Example 1 (Disease-free case)**.** Throughout, we will assume that the initial populations of exposed, asymptomatic, symptomatic, quarantined and recovered individuals are all identically equal to zero. Meanwhile, the populations for susceptible and vaccinated individuals will be randomly selected in the interval $[0, 5]$, using the random number generator function `rand` from Matlab. Fix the values of the parameter as in Table 2, and let $m_E = 0$. Let us consider the case $\mathscr{R}_0 < 1$. More precisely, the basic reproductive number satisfies $\mathscr{R}_0 = 0.9393$ when $m_S = 0.001$. In this case, the disease-free equilibrium solution is the point $P_{DFE} = (S_0, V_0, 0, 0, 0, 0, 0)$, where

$$S_0 = 4.5741, \tag{3.60}$$

$$V_0 = 10.6145. \tag{3.61}$$

Figure 2 shows the results for our simulations at three different times. More precisely, the left column shows approximate solutions for the function S, while the right column shows those for the function V. We used $t = 1$ for the first row, $t = 10$ for the second row, and $t = 500$ for the third row. It is clear that the approximate solutions approach the equilibrium solutions as time approaches infinity, which is consistent with the theoretical outcomes for both

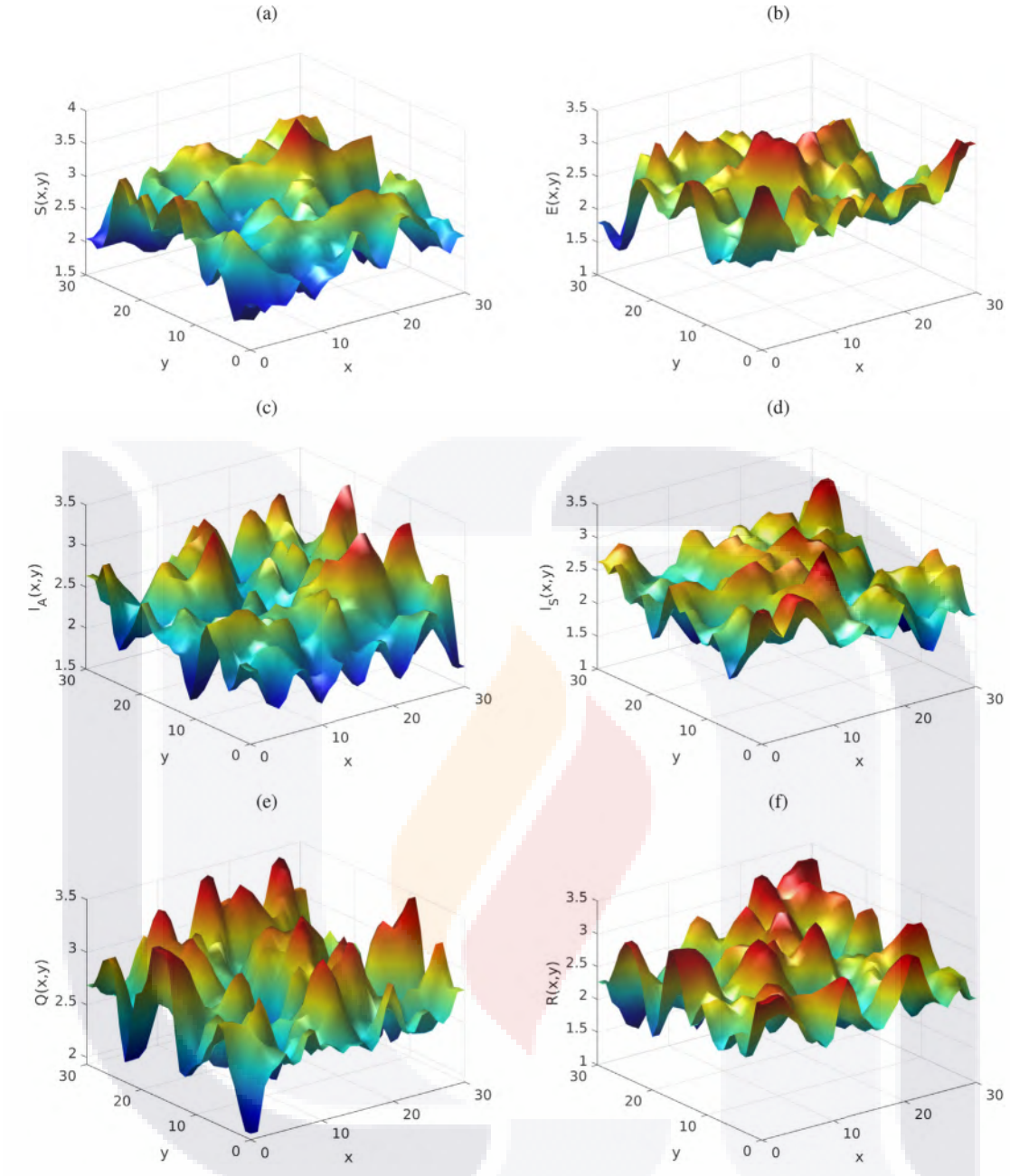

Fig. 3. Approximate solutions of the epidemiological model (2.2) versus the variables x and y at the time $t = 1$. The graphs correspond to the approximations to the functions (a) S, (b) E, (c) I_A, (d) I_S, (e) Q and (f) R. The approximations were obtained using the computer method (2.12) together with the parameter values in Table 2 and $m_S = 0.02$. All the initial populations were selected randomly in $[0, 5]$ using the function `rand` from Matlab.

the continuous and discrete models. Here, we must point out that we did not include graphs depicting the dynamical behavior of the other compartments in view that they are always equal to zero, as expected in the disease-free case. □

Example 2 (Endemic case)**.** In this computational experiment, we let all the initial populations sizes be randomly defined taking values in $[0, 5]$, and let $m_S = 0.02$ and $m_E = 0.1$. Under these circumstances, the basic reproductive number is equal to 1.2236, which means that $\mathscr{R}_0 > 1$. In this particular case, the epidemiological system has the theoretical endemic equilibrium solution $P_{EE} = (S^*, V^*, E^*, I_A^*, Q^*, I_S^*, R^*)$, where the components of this vector are

$$\begin{aligned} S^* &= 2.2959, \\ V^* &= 9.9395, \\ E^* &= 3.8853, \\ I_A^* &= 1.1736 \times 10^{-3}, \\ Q^* &= 8.5724, \\ I_S^* &= 6.3808 \times 10^{-1}, \\ R^* &= 5.8234 \times 10^{-1}. \end{aligned} \tag{3.62}$$

Figures 3, 4 and 5 show the results of our simulations at the times $t = 1$, $t = 10$ and $t = 1000$, respectively. For each figure, the graphs show the approximate solutions for (a) S, (b) E, (c) I_A, (d) I_S, (e) Q and (f) R, as functions of the variables x and y. The graphs were obtained using the computer method (2.12), and they show that the

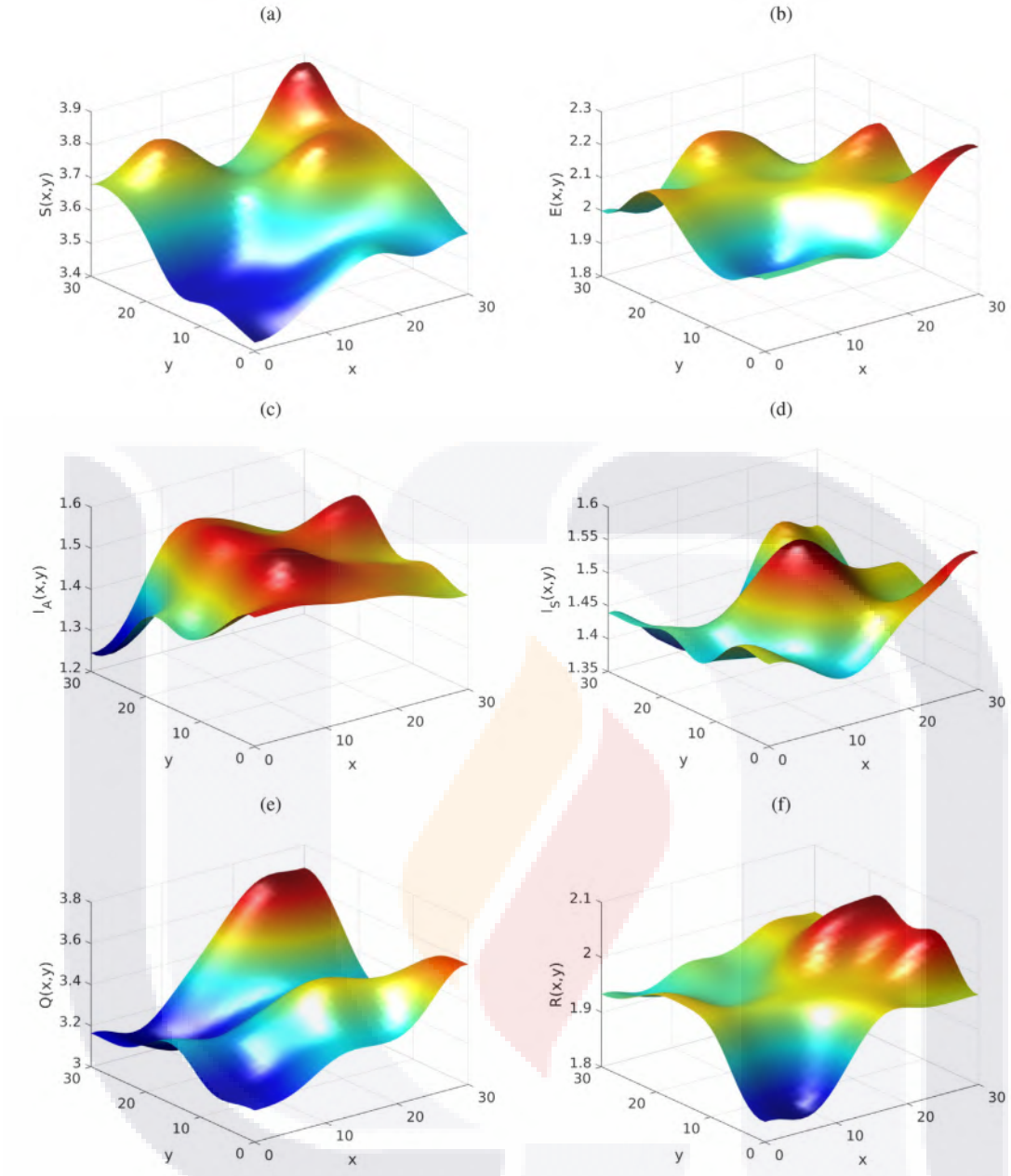

Fig. 4. Approximate solutions of the epidemiological model (2.2) versus the variables x and y at the time $t = 10$. The graphs correspond to the approximations to the functions (a) S, (b) E, (c) I_A, (d) I_S, (e) Q and (f) R. The approximations were obtained using the computer method (2.12) together with the parameter values in Table 2 and $m_S = 0.02$. All the initial populations were selected randomly in $[0, 5]$ using the function `rand` from Matlab.

solutions converge in time toward constant solutions. It is worthwhile to notice that each of these functions tends point-wisely to the corresponding component of the endemic equilibrium point. This outcome is consistent with the properties of both the continuous and discrete models analyzed in this study. To conserve space, the graphs for function V were omitted, but it's worth mentioning that the simulations also align well with the analytical prediction for the equilibrium solution. □

As a summary of our computer simulations, Figures 2–5 investigate the dynamics of propagation for the disease in both scenarios, namely, the disease-free and the endemic cases. Figure 2 considered the disease-free case by showing the evolution of the susceptible and the vaccinated compartments (which are the only compartments in that scenario). Starting from a random profile, that figure shows snapshots of the solutions at three different times for a human population confined on the two-dimensional square $[0, 30] \times [0, 30]$. The results show that both solutions tend toward two constants, namely, approximately 4.5741 for the susceptible, and 10.6145 for the vaccinated. This is in agreement with the theoretical value of the disease-free equilibrium point. On the other hand, the remaining figures consider the endemic case, each of them at three different and consecutive times. For each figure, we provide the snapshot of the solutions for (a) S, (b) E, (c) I_A, (d) I_S, (e) Q and (f) R over the same spatial domain as in the disease-free case. The results again show that the tendency of the solutions is to converge asymptotically toward constants. Those constants are the same as the endemic equilibrium solution, as predicted by our theoretical results.

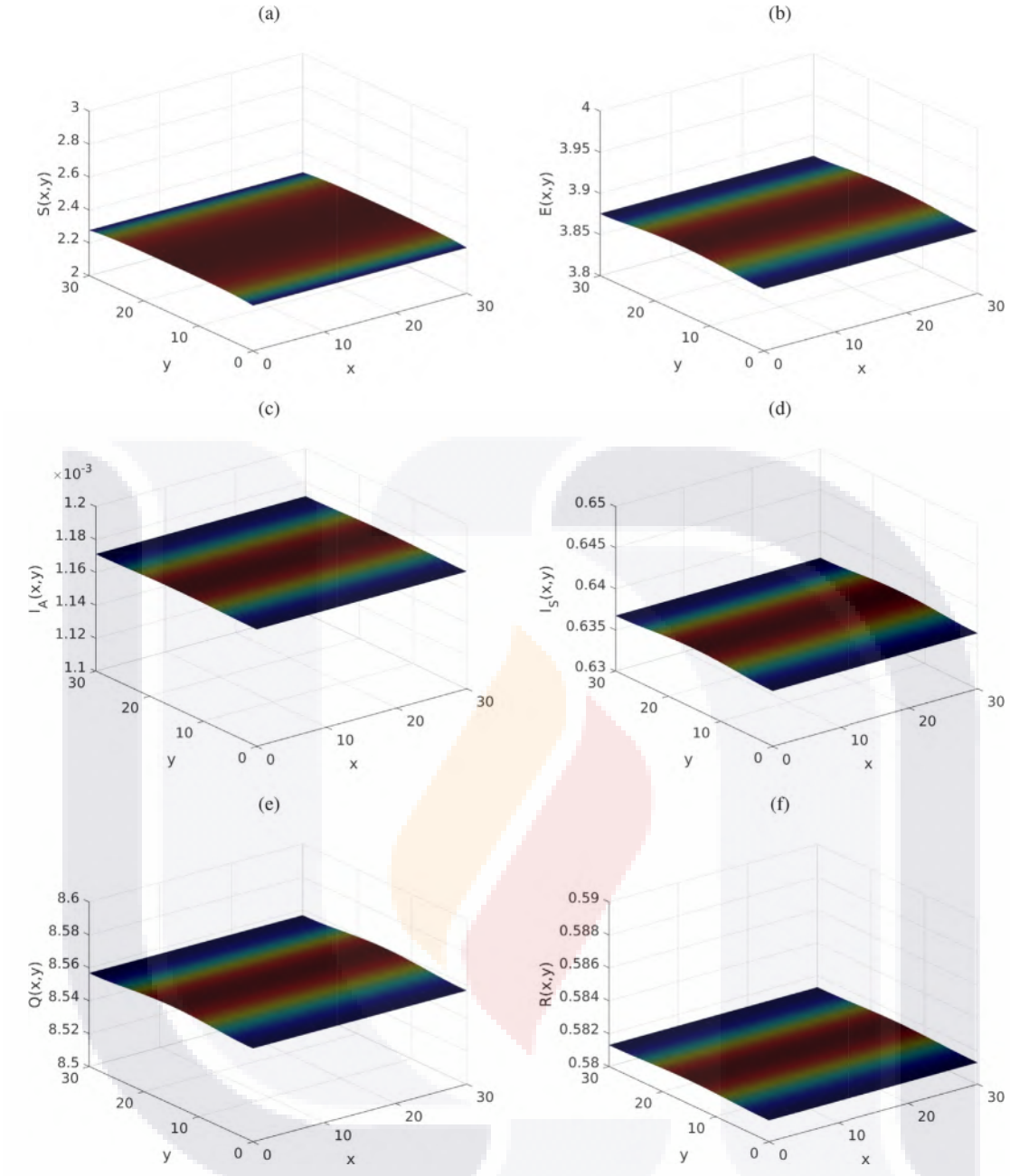

Fig. 5. Approximate solutions of the epidemiological model (2.2) versus the variables x and y at the time $t = 1000$. The graphs correspond to the approximations to the functions (a) S, (b) E, (c) I_A, (d) I_S, (e) Q and (f) R. The approximations were obtained using the computer method (2.12) together with the parameter values in Table 2 and $m_S = 0.02$. All the initial populations were selected randomly in $[0, 5]$ using the function `rand` from Matlab.

Before concluding this section, we want to emphasize that additional simulations were conducted using the computer methods. We do not present them here in order to avoid redundancy, but they confirm the analytical features of the epidemic model as well as the numerical properties of the computer method.

4. Conclusions

A mathematical epidemic system describing the spread of an infectious illness inside a population of individuals was presented in this study. It is a compartmental deterministic system that takes into account the presence of different types of individuals, such as susceptible, exposed, asymptomatic infected, symptomatic infected, quarantined, recovered and vaccinated, and various transmission mechanisms. It also includes migration and nonlinear interactions between compartments. To analyze the system, a unique computer method based on finite differences was proposed, which is a linear, discrete, two-step model that can be expressed in vector form. When conditions are met, the numerical model matrix is an M-matrix, ensuring positivity conservation. Analytically, the existence of equilibrium solutions in both cases endemic and disease-free was established, and the local asymptotic stability was determined, as well as calculate the basic reproduction number through the next-generation matrix approach. The computer method has various other desirable properties, such as preserving the equilibria and stability, and being a consistent, stable, and convergent method. The results of numerical simulations using this method showed the posi-

tivity conservation, stability, and agreement with the theoretical results.

The proposed model has equilibrium solutions in the continuous model and also in the discretized system and the method can preserve the local stability properties of these constant solutions. The computer method has been proven to be a consistent discretization of the continuous model with linear order of consistency in time and quadratic order of consistency in the spatial variables using Taylor's theorem. Additionally, the discretized model is conditionally stable in the Euclidean norm for small temporal step-size, and is a convergent technique with linear order convergence in time and quadratic order in both spatial variables, established through Gronwall's and Young's discretized inequality. The vector form of the method was implemented in Matlab and the linear systems were solved at each temporal step using the biconjugate gradients stabilized method. Numerical simulations showed positivity preservation and stability of the method, and the results were in agreement with the theory.

Before concluding this manuscript, it is important to discuss the future work that we plan to carry out. Although the proposed model in this study is quite complete, complex and robust, the goal is to make it as realistic as possible. Some research papers have utilized the Crowley–Martin model instead of a direct or linear spread of the disease. This model was initially designed for predator-prey models but has been adapted to epidemiological models effectively [45]. Furthermore, a treatment function rather than a direct cure of the infection has also been suggested in different studies [46]. Additionally, the model presented in this manuscript can be also scaled to a fractional case [47]. Various operators are used in that case, depending on whether the fractional derivative order is used in the temporal or the spacial variables. In the particular case of Riesz spatial derivatives, the applications seem to be more promising as various theoretical, numerical and physical results are already available for that scenario [48]. We expect to tackle these research avenues and others in the near future.

Declaration of Competing Interest

The authors declare no potential conflict of interest.

Acknowledgment

Beforehand, the authors wish to thank the anonymous reviewers and the associate editor in charge of handling this manuscript for their time and efforts.

Funding

The author for correspondence (J.E.M.-D.) wishes to acknowledge the financial support from the National Council of Science and Technology of Mexico via grant A1-S-45928.

Data statement

The data that support the findings of this study are available from the corresponding author, J.E.M.-D., upon reasonable request.

Institutional review

Not applicable.

Informed consent

Not applicable.

Appendix A.

In this appendix, we show that the eigenvalue λ_1 in the proof of Theorem 1 is negative whenever $\mathscr{R}_0 < 1$. For the sake of convenience, remember that the expressions for λ_1, S_0 and $\mathscr{R}_0$ are, respectively,

$$\lambda_1 = \alpha S_0 - (\zeta + \epsilon + \delta + \mu), \tag{A.1}$$

$$S_0 = \frac{(\mu+\tau)(\Lambda + m_S) + \tau m_v}{\mu(\mu+\omega+\tau)}, \tag{A.2}$$

$$\mathscr{R}_0 = \frac{S_0[((\kappa+\mu+\rho+\theta)(\alpha(\eta+\mu)+\beta\delta)) + \epsilon\gamma(\eta+\mu)]}{(\eta+\mu)(\delta+\epsilon+\mu+\zeta)(\kappa+\mu+\rho+\theta)}. \tag{A.3}$$

Solving for S_0 in this last equation, using the hypothesis that $\mathscr{R}_0 < 1$ and recalling that all the parameters are non-negative numbers, it follows that

$$\begin{aligned}
\alpha S_0 &= \frac{\alpha(\eta+\mu)(\delta+\epsilon+\mu+\zeta)(\kappa+\mu+\rho+\theta)\mathscr{R}_0}{(\kappa+\mu+\rho+\theta)(\alpha(\eta+\mu)+\beta\delta)+\epsilon\gamma(\eta+\mu)} \\
&\leq \frac{\alpha(\eta+\mu)(\delta+\epsilon+\mu+\zeta)(\kappa+\mu+\rho+\theta)\mathscr{R}_0}{(\kappa+\mu+\rho+\theta)(\alpha(\eta+\mu)+\beta\delta)} \\
&= \frac{\alpha(\eta+\mu)(\delta+\epsilon+\mu+\zeta)\mathscr{R}_0}{\alpha(\eta+\mu)+\beta\delta} \\
&\leq \frac{\alpha(\eta+\mu)(\delta+\epsilon+\mu+\zeta)\mathscr{R}_0}{\alpha(\eta+\mu)} \\
&\leq (\delta+\epsilon+\mu+\zeta)\mathscr{R}_0 \\
&< \delta+\epsilon+\mu+\zeta.
\end{aligned} \tag{A.4}$$

Subtracting the term $\delta+\epsilon+\mu+\zeta$ on both ends, we readily reach that $\lambda_1 < 0$, as desired.

References

[1] E. Dong, H. Du, L. Gardner, An interactive web-based dashboard to track COVID-19 in real time, The Lancet infectious diseases 20 (5) (2020) 533–534.
[2] D.M. Morens, P. Daszak, H. Markel, J.K. Taubenberger, Pandemic COVID-19 joins history's pandemic legion, MBio 11 (3) (2020) e00812–20.
[3] M. Martini, V. Gazzaniga, N.L. Bragazzi, I. Barberis, The spanish influenza pandemic: a lesson from history 100 years after 1918, Journal of preventive medicine and hygiene 60 (1) (2019) E64.
[4] P. Berche, Life and death of smallpox, La Presse Médicale 51 (3) (2022) 104117.
[5] R.W. Byard, A forensic evaluation of plague–a re-emerging infectious disease with biowarfare potential, Medicine, Science and the Law 60 (3) (2020) 200–205.
[6] R.K.R. Kummitha, Smart technologies for fighting pandemics: The techno-and human-driven approaches in controlling the virus transmission, Government Information Quarterly 37 (3) (2020) 101481.
[7] A. Kumar, P.K. Gupta, A. Srivastava, A review of modern technologies for tackling COVID-19 pandemic, Diabetes & Metabolic Syndrome: Clinical Research & Reviews 14 (4) (2020) 569–573.
[8] Dirección General de Epidemiología, Datos abiertos, 2015, https://www.gob.mx/salud/documentos/datos-abiertos-152127.
[9] J.L.R. Lozano, Protocolo del semáforo epidemiológico COVID-19 en méxico: una clasificación alternativa mediante el método flowsort.
[10] CONACYT, Mapa interactivo de COVID-19 méxico, 2020, https://datos.covid-19.conacyt.mx/#DOView.
[11] E.S. Rosenberg, V. Dorabawila, D. Easton, U.E. Bauer, J. Kumar, R. Hoen, D. Hoefer, M. Wu, E. Lutterloh, M.B. Conroy, et al., Covid-19 vaccine effectiveness in new york state, New England Journal of Medicine 386 (2) (2022) 116–127.
[12] T.T. Le, Z. Andreadakis, A. Kumar, R.G. Román, S. Tollefsen, M. Saville, S. Mayhew, et al., The COVID-19 vaccine development landscape, Nat Rev Drug Discov 19 (5) (2020) 305–306.
[13] N. Andrews, J. Stowe, F. Kirsebom, S. Toffa, T. Rickeard, E. Gallagher, C. Gower, M. Kall, N. Groves, A.-M. O'Connell, et al., Covid-19 vaccine effectiveness against the omicron (b. 1.1. 529) variant, New England Journal of Medicine 386 (16) (2022) 1532–1546.
[14] V.J. Lee, M. Ho, C.W. Kai, X. Aguilera, D. Heymann, A. Wilder-Smith, Epidemic preparedness in urban settings: new challenges and opportunities, The lancet infectious diseases 20 (5) (2020) 527–529.
[15] H. Ge, X. Wang, X. Yuan, G. Xiao, C. Wang, T. Deng, Q. Yuan, X. Xiao, The epidemiology and clinical information about COVID-19, European Journal of Clinical Microbiology & Infectious Diseases 39 (6) (2020) 1011–1019.

[16] M. Frérot, A. Lefebvre, S. Aho, P. Callier, K. Astruc, L.S. Aho Glélé, What is epidemiology? changing definitions of epidemiology 1978-2017, PloS one 13 (12) (2018) e0208442.
[17] J.L.L.n. Fernández, Metodología de la investigación epidemiológica, Editorial El Manual Moderno, 2022.
[18] H.S. Taffese, E. Hemming-Schroeder, C. Koepfli, G. Tesfaye, M.-c. Lee, J. Kazura, G.-Y. Yan, G.-F. Zhou, Malaria epidemiology and interventions in ethiopia from 2001 to 2016, Infectious diseases of poverty 7 (06) (2018) 1–9.
[19] L.P. Hariri, C.M. North, A.R. Shih, R.A. Israel, J.H. Maley, J.A. Villalba, V. Vinarsky, J. Rubin, D.A. Okin, A. Sclafani, et al., Lung histopathology in coronavirus disease 2019 as compared with severe acute respiratory sydrome and H1N1 influenza: a systematic review, Chest 159 (1) (2021) 73–84.
[20] A.C. Kalil, P.G. Thomas, Influenza virus-related critical illness: pathophysiology and epidemiology, Critical care 23 (1) (2019) 1–7.
[21] V.G. Da Costa, M.V. Saivish, D.E.R. Santos, R.F. de Lima Silva, M.L. Moreli, Comparative epidemiology between the 2009 h1n1 influenza and COVID-19 pandemics, Journal of Infection and Public Health 13 (12) (2020) 1797–1804.
[22] A. Ballesteros, A. Blasco, I. Gutierrez-Sagredo, Hamiltonian structure of compartmental epidemiological models, Physica D: Nonlinear Phenomena 413 (2020) 132656.
[23] B. Reyné, N. Saby, M.T. Sofonea, Principles of mathematical epidemiology and compartmental modelling application to COVID-19, Anaesthesia, Critical Care & Pain Medicine 41 (1) (2022) 101017.
[24] M. Vidal Ledo, R. Guinovart Díaz, W. Baldoquín Rodríguez, N.C. Valdivia Onega, W. Morales Lezca, Modelos matemáticos para el control epidemiológico, Educación Médica Superior 34 (2) (2020).
[25] Y. Zhang, B. Jiang, J. Yuan, Y. Tao, The impact of social distancing and epicenter lockdown on the COVID-19 epidemic in mainland china: A data-driven SEIQR model study, MedRxiv (2020).
[26] J.E. Herrera-Serrano, J.E. Macías-Díaz, I.E. Medina-Ramírez, J.A. Guerrero, An efficient nonstandard computer method to solve a compartmental epidemiological model for COVID-19 with vaccination and population migration, Computer Methods and Programs in Biomedicine (2022) 106920.
[27] A.P. Lemos-Paião, C.J. Silva, D.F.M. Torres, A new compartmental epidemiological model for COVID-19 with a case study of Portugal, Ecological Complexity 44 (2020) 100885.
[28] M. Grave, A.L. Coutinho, Adaptive mesh refinement and coarsening for diffusion–reaction epidemiological models, Computational Mechanics 67 (4) (2021) 1177–1199.
[29] M. Mahrouf, A. Boukhouima, H. Zine, E.M. Lotfi, D.F.M. Torres, N. Yousfi, Modeling and forecasting of COVID-19 spreading by delayed stochastic differential equations, Axioms 10 (1) (2021) 18.
[30] R.E. Mickens, Nonstandard finite difference schemes for differential equations, Journal of Difference Equations and Applications 8 (9) (2002) 823–847.
[31] J.E. Macías-Díaz, A. Szafrańska, Existence and uniqueness of monotone and bounded solutions for a finite-difference discretization à la Mickens of the generalized Burgers–Huxley equation, Journal of Difference Equations and Applications 20 (7) (2014) 989–1004.
[32] J.E. Macías-Díaz, I.E. Medina-Ramírez, A. Puri, Numerical treatment of the spherically symmetric solutions of a generalized Fisher–Kolmogorov–Petrovsky–Piscounov equation, Journal of computational and applied mathematics 231 (2) (2009) 851–868.
[33] M. Rafiq, J.E. Macias-Diaz, A. Raza, N. Ahmed, Design of a nonlinear model for the propagation of COVID-19 and its efficient nonstandard computational implementation, Applied Mathematical Modelling 89 (2021) 1835–1846.
[34] A. Cascone, A. Marigo, B. Piccoli, L. Rarità, Decentralized optimal routing for packets flow on data networks, Discrete Contin Dyn Syst Ser B 13 (1) (2010) 59–78.
[35] L. Rarità, I. Stamova, S. Tomasiello, Numerical schemes and genetic algorithms for the optimal control of a continuous model of supply chains, Applied Mathematics and Computation 388 (2021) 125464.
[36] A. Cascone, R. Manzo, B. Piccoli, L. Rarità, Optimization versus randomness for car traffic regulation, Physical Review E 78 (2) (2008) 026113.
[37] J.E. Macías-Díaz, S. Tomasiello, A differential quadrature-based approach à la Picard for systems of partial differential equations associated with fuzzy differential equations, Journal of Computational and Applied Mathematics 299 (2016) 15–23.
[38] R.E. Mickens, Nonstandard finite difference schemes for reaction-diffusion equations, Numerical Methods for Partial Differential Equations: An International Journal 15 (2) (1999) 201–214.
[39] R.E. Mickens, Applications of nonstandard finite difference schemes, World Scientific, 2000.
[40] R.J. Plemmons, M-matrix characterizations. i-nonsingular m-matrices, Linear Algebra and its applications 18 (2) (1977) 175–188.
[41] A.F. Brouwer, Why the spectral radius? an intuition-building introduction to the basic reproduction number, Bulletin of Mathematical Biology 84 (9) (2022) 1–26.
[42] C. Yang, J. Wang, Basic reproduction numbers for a class of reaction-diffusion epidemic models, Bulletin of mathematical biology 82 (8) (2020) 1–25.
[43] P. Van den Driessche, J. Watmough, Reproduction numbers and sub-threshold endemic equilibria for compartmental models of disease transmission, Mathematical biosciences 180 (1-2) (2002) 29–48.
[44] K. Pen-Yu, Numerical methods for incompressible viscous flow, Scientia Sinica 20 (1977) 287–304.
[45] A.P. Maiti, C. Jana, D.K. Maiti, A delayed eco-epidemiological model with nonlinear incidence rate and crowley–martin functional response for infected prey and predator, Nonlinear Dynamics 98 (2019) 1137–1167.
[46] A. Kumar, et al., Dynamic behavior of an SIR epidemic model along with time delay; crowley–martin type incidence rate and holling type II treatment rate, International Journal of Nonlinear Sciences and Numerical Simulation 20 (7-8) (2019) 757–771.
[47] R. Almeida, A.M.C. Brito da Cruz, N. Martins, M.T.T. Monteiro, An epidemiological MSEIR model described by the caputo fractional derivative, International journal of dynamics and control 7 (2019) 776–784.
[48] J.E. Macías-Díaz, On the solution of a riesz space-fractional nonlinear wave equation through an efficient and energy-invariant scheme, International Journal of Computer Mathematics 96 (2) (2019) 337–361.

Conclusions

Chapter 1. We introduced a linearly implicit NSFD discretization that preserves the key qualitative features of a diffusion–enhanced epidemic model with vaccination and quarantine. By designing the discrete operators so that their coefficient matrices possess an M–matrix structure, and by verifying consistency and stability, we obtained convergence together with biologically meaningful, positivity–preserving approximations. The computational experiments corroborate the analysis and illustrate the method's effectiveness across scenarios that include vaccination and quarantine interventions.

It is worth emphasizing that the proposed time discretization is first–order accurate. As a reviewer correctly noted, this temporal order may be insufficient for long–horizon dynamical studies. Higher–order alternatives—such as Runge–Kutta families for ODE subsystems—are well known to be stable and convergent; however, they do not automatically guarantee preservation of positivity, boundedness, or equilibrium invariance (nor the stability of those equilibria). In cases where such qualitative properties can be enforced with higher–order schemes, the present approach retains a practical advantage: simplicity. As shown in the appendix, our NSFD formulation is straightforward to implement even for users with modest programming experience.

Related literature documents third–order (and higher) schemes for time–dependent nonlinear PDEs with rigorous stability/convergence analyses, e.g., fully discrete Fourier–collocation spectral methods for the 3D viscous Burgers equation [50], high–order multistep schemes for the 2D incompressible Navier–Stokes equations [29], exponential time–differencing methods for no–slope–selection thin–film models with energy stability [28], third–order BDF energy–stable linear schemes for no–slope–selection thin films [52], and BDF–type energy–stable schemes for the Cahn–Hilliard equation [30].

A complementary line of work enforces positivity via logarithmic (or singular) energy potentials in reaction–diffusion systems and related gradient flows: see, for instance, positivity–preserving numerics for Poisson–Nernst–Planck systems [78], ternary Cahn–Hilliard models with singular interfacial parameters [41], three–component Cahn–Hilliard–type models for MMC hydrogels [120], binary fluid–surfactant systems [96], liquid thin–film coarsening [121], Poisson–Nernst–Planck–Cahn–Hilliard with steric interactions [95], Cahn–Hilliard with variable interfacial parameters [40], Flory–Huggins–de Gennes energies [42], logarithmic potentials [27], and reaction–diffusion with detailed balance [77, 76]. Whether an entropy structure of this type can be embedded into the epidemiological model (**??**) to *guarantee* discrete positivity remains, to our knowledge, an open question.

Chapter 2. We developed a diffusion–driven compartmental framework with vaccination and quarantine, analyzed its deterministic structure, and proposed a structure–preserving NSFD scheme aligned with the continuous model. On the analytical side, we identified the disease–free and endemic equilibria, derived the basic reproduction number $\mathscr{R}_0$ via the next–generation matrix formalism, and determined local stability thresholds around each steady state [109]. We also delineated an invariant, positively invariant region and verified nonnegativity of solutions. On the numerical side, the linearly implicit discretization yields coefficient matrices with M–matrix character; in conjunction with discrete Gronwall–type arguments, this ensures inverse positivity, step–size–dependent stability, and convergence of the scheme. Moreover, the discretization is equilibrium–consistent: steady states of the PDE model are inherited as constant solutions of the discrete dynamics, and their local stability properties are preserved under suitable conditions.

From a computational viewpoint, simulations in both disease–free and endemic regimes show trajectories converging toward the corresponding steady states, matching the theoretical predictions for thresholds determined by $\mathscr{R}_0$. Parametric explorations illustrate how vaccination, quarantine, and waning–immunity rates modulate $\mathscr{R}_0$ and the transient profiles, while grid/time–step refinements confirm first–order accuracy in time and second–order accuracy in space, consistent with the design of the scheme. The framework readily accommodates modeling extensions—space–dependent parameters, advective transport, spatially heterogeneous controls, or optimal–control interventions—without abandoning the emphasis on qualitative preservation. In summary, Chapter 2 complements the theory with a practical, reproducible computational pipeline that (i) respects the biology (positivity and invariance), (ii) mirrors the steady–state structure and its stability, and (iii) delivers provable consistency, stability, and convergence for the space–time discretization, thereby providing a reliable platform for scenario analysis and policy–relevant experimentation.

Bibliography

[1] Saeed Ahmad, Mati ur Rahman, and Muhammad Arfan. On the analysis of semi-analytical solutions of Hepatitis B epidemic model under the Caputo-Fabrizio operator. *Chaos, Solitons & Fractals*, 146:110892, 2021.

[2] Idris Ahmed, Goni Umar Modu, Abdullahi Yusuf, Poom Kumam, and Ibrahim Yusuf. A mathematical model of Coronavirus Disease (COVID-19) containing asymptomatic and symptomatic classes. *Results in physics*, 21:103776, 2021.

[3] Amani Alahmadi, Sarah Belet, Andrew Black, Deborah Cromer, Jennifer A Flegg, Thomas House, Pavithra Jayasundara, Jonathan M Keith, James M McCaw, Robert Moss, et al. Influencing public health policy with data-informed mathematical models of infectious diseases: Recent developments and new challenges. *Epidemics*, 32:100393, 2020.

[4] Muntasir Alam, KM Ariful Kabir, and Jun Tanimoto. Based on mathematical epidemiology and evolutionary game theory, which is more effective: quarantine or isolation policy? *Journal of Statistical Mechanics: Theory and Experiment*, 2020(3):033502, 2020.

[5] Giacomo Albi, Lorenzo Pareschi, and Mattia Zanella. Control with uncertain data of socially structured compartmental epidemic models. *Journal of Mathematical Biology*, 82(7):1–41, 2021.

[6] Marco A Amaral, Marcelo M de Oliveira, and Marco A Javarone. An epidemiological model with voluntary quarantine strategies governed by evolutionary game dynamics. *Chaos, Solitons & Fractals*, 143:110616, 2021.

[7] Nick Andrews, Julia Stowe, Freja Kirsebom, Samuel Toffa, Tim Rickeard, Eileen Gallagher, Charlotte Gower, Meaghan Kall, Natalie Groves, Anne-Marie O'Connell, et al. Covid-19 vaccine effectiveness against the omicron (b. 1.1. 529) variant. *New England Journal of Medicine*, 386(16):1532–1546, 2022.

[8] Nursanti Anggriani, Meksianis Z Ndii, Rika Amelia, Wahyu Suryaningrat, and Mochammad Andhika Aji Pratama. A mathematical covid-19 model considering asymptomatic and symptomatic classes with waning immunity. *Alexandria Engineering Journal*, 61(1):113–124, 2022.

[9] Julien Arino and Stéphanie Portet. A simple model for COVID-19. *Infectious Disease Modelling*, 5:309–315, 2020.

[10] Joshua Kiddy K Asamoah, Zhen Jin, Gui-Quan Sun, Baba Seidu, Ernest Yankson, Afeez Abidemi, FT Oduro, Stephen E Moore, and Eric Okyere. Sensitivity assessment and optimal economic evaluation of a new COVID-19 compartmental epidemic model with control interventions. *Chaos, Solitons & Fractals*, 146:110885, 2021.

[11] Shumaila Azam, Jorge E Macías-Díaz, Nauman Ahmed, Ilyas Khan, Muhammad S Iqbal, Muhammad Rafiq, Kottakkaran S Nisar, and Muhammad O Ahmad. Numerical modeling and theoretical analysis of a nonlinear advection-reaction epidemic system. *Computer Methods and Programs in Biomedicine*, 193:105429, 2020.

[12] Angel Ballesteros, Alfonso Blasco, and Ivan Gutierrez-Sagredo. Hamiltonian structure of compartmental epidemiological models. *Physica D: Nonlinear Phenomena*, 413:132656, 2020.

[13] Stephen Barnett. *Polynomials and linear control systems*. Marcel Dekker, Inc., 1983.

[14] Cristiane M Batistela, Diego PF Correa, Átila M Bueno, and José Roberto C Piqueira. SIRSi compartmental model for COVID-19 pandemic with immunity loss. *Chaos, Solitons & Fractals*, 142:110388, 2021.

[15] Patrick Berche. Life and death of smallpox. *La Presse Médicale*, 51(3):104117, 2022.

[16] Abayneh Fentie Bezabih, Geremew Kenassa Edessa, and Purnachandra Rao Koya. Mathematical epidemiology model analysis on the dynamics of covid-19 pandemic. *American Journal of Applied Mathematics*, 8(5):247–256, 2020.

[17] Toheeb A Biala and AQM Khaliq. A fractional-order compartmental model for the spread of the covid-19 pandemic. *Communications in Nonlinear Science and Numerical Simulation*, 98:105764, 2021.

[18] Julie C Blackwood and Lauren M Childs. An introduction to compartmental modeling for the budding infectious disease modeler. *Letters in Biomathematics*, 5(1):195–221, 2018.

[19] Fred Brauer. Compartmental models in epidemiology. *Mathematical epidemiology*, pages 19–79, 2008.

[20] Fred Brauer. Mathematical epidemiology: Past, present, and future. *Infectious Disease Modelling*, 2(2):113–127, 2017.

[21] Fred Brauer, Carlos Castillo-Chavez, and Zhilan Feng. *Mathematical models in epidemiology*, volume 32. Springer, 2019.

[22] Fred Brauer, Pauline Van den Driessche, Jianhong Wu, and Linda JS Allen. *Mathematical epidemiology*, volume 1945. Springer, 2008.

[23] B Briones Aguirre. Metodología de la investigación en epidemiología. *Martínez Montaño MLC, Briones Rojas R, Cortés Riveroll JGR. Metodología de la investigación para el área de la salud. Access-Medicina*, 2013.

[24] Andrew F Brouwer. Why the spectral radius? an intuition-building introduction to the basic reproduction number. *Bulletin of Mathematical Biology*, 84(9):1–26, 2022.

[25] Roger W Byard. A forensic evaluation of plague–a re-emerging infectious disease with biowarfare potential. *Medicine, Science and the Law*, 60(3):200–205, 2020.

[26] Johns Hopkins Coronavirus Resource Center. Covid-19 map, 2021.

[27] Wenbin Chen, Cheng Wang, Xiaoming Wang, and Steven M Wise. Positivity-preserving, energy stable numerical schemes for the cahn-hilliard equation with logarithmic potential. *Journal of Computational Physics: X*, 3:100031, 2019.

[28] Kelong Cheng, Zhonghua Qiao, and Cheng Wang. A third order exponential time differencing numerical scheme for no-slope-selection epitaxial thin film model with energy stability. *Journal of Scientific Computing*, 81(1):154–185, 2019.

[29] Kelong Cheng and Cheng Wang. Long time stability of high order multistep numerical schemes for two-dimensional incompressible navier–stokes equations. *SIAM Journal on Numerical Analysis*, 54(5):3123–3144, 2016.

[30] Kelong Cheng, Cheng Wang, Steven M Wise, and Yanmei Wu. A third order accurate in time, bdf-type energy stable scheme for the cahn-hilliard equation. *Numerical Mathematics: Theory, Methods and Applications*, 15(2), 2022.

[31] Philip Ciunkiewicz, W Brooke, M Rogers, and S Yanushkevich. Agent-based epidemiological modeling of COVID-19 in localized environments. *Computers in Biology and Medicine*, 144:105396, 2022.

[32] CONACYT. Mapa interactivo de covid-19 méxico, 2020.

[33] Renato M Cotta, Carolina P Naveira-Cotta, and Pierre Magal. Mathematical parameters of the COVID-19 epidemic in Brazil and evaluation of the impact of different public health measures. *Biology*, 9(8):220, 2020.

[34] Vivaldo Gomes Da Costa, Marielena Vogel Saivish, Dhullya Eduarda Resende Santos, Rebeca Francielle de Lima Silva, and Marcos Lázaro Moreli. Comparative epidemiology between the 2009 h1n1 influenza and covid-19 pandemics. *Journal of Infection and Public Health*, 13(12):1797–1804, 2020.

[35] Mohammadali Dashtbali and Mehdi Mirzaie. A compartmental model that predicts the effect of social distancing and vaccination on controlling covid-19. *Scientific Reports*, 11(1):1–11, 2021.

[36] Dirección General de Epidemiología. Datos abiertos, 2015.

[37] Odo Diekmann, JAP Heesterbeek, and Michael G Roberts. The construction of next-generation matrices for compartmental epidemic models. *Journal of the royal society interface*, 7(47):873–885, 2010.

[38] Klaus Dietz. The estimation of the basic reproduction number for infectious diseases. *Statistical methods in medical research*, 2(1):23–41, 1993.

[39] Ensheng Dong, Hongru Du, and Lauren Gardner. An interactive web-based dashboard to track covid-19 in real time. *The Lancet infectious diseases*, 20(5):533–534, 2020.

[40] Lixiu Dong. A positivity-preserving second-order bdf scheme for the cahn-hilliard equation with variable interfacial parameters. *Communications in Computational Physics*, 28(3):967–998, 2020.

[41] Lixiu Dong, Cheng Wang, Steven M Wise, and Zhengru Zhang. A positivity-preserving, energy stable scheme for a ternary cahn-hilliard system with the singular interfacial parameters. *Journal of Computational Physics*, 442:110451, 2021.

[42] Lixiu Dong, Cheng Wang, Hui Zhang, and Zhengru Zhang. A positivity-preserving, energy stable and convergent numerical scheme for the cahn–hilliard equation with a flory–huggins–degennes energy. *Communications in Mathematical Sciences*, 17(4):921–939, 2019.

[43] Preeti Dubey, Balram Dubey, and Uma S Dubey. An sir model with nonlinear incidence rate and holling type iii treatment rate. In *Applied Analysis in Biological and Physical Sciences: ICMBAA, Aligarh, India, June 2015*, pages 63–81. Springer, 2016.

[44] Adil El-Alami Laaroussi, Mostafa Rachik, and Mohamed Elhia. An optimal control problem for a spatiotemporal sir model. *International Journal of Dynamics and Control*, 6:384–397, 2018.

[45] Paul Elliot, Jon C Wakefield, Nicola G Best, David John Briggs, et al. *Spatial epidemiology: methods and applications.* Oxford University Press, 2000.

[46] Juan Luis Londoño Fernández. *Metodología de la investigación epidemiológica.* Editorial El Manual Moderno, 2022.

[47] Mathilde Frérot, Annick Lefebvre, Simon Aho, Patrick Callier, Karine Astruc, and Ludwig Serge Aho Glélé. What is epidemiology? changing definitions of epidemiology 1978-2017. *PloS one*, 13(12):e0208442, 2018.

[48] Geoff P Garnett. An introduction to mathematical models in sexually transmitted disease epidemiology. *Sexually transmitted infections*, 78(1):7–12, 2002.

[49] Huipeng Ge, Xiufen Wang, Xiangning Yuan, Gong Xiao, Chengzhi Wang, Tianci Deng, Qiongjing Yuan, and Xiangcheng Xiao. The epidemiology and clinical information about covid-19. *European Journal of Clinical Microbiology & Infectious Diseases*, 39(6):1011–1019, 2020.

[50] Sigal Gottlieb and Cheng Wang. Stability and convergence analysis of fully discrete fourier collocation spectral method for 3-d viscous burgers' equation. *Journal of Scientific Computing*, 53(1):102–128, 2012.

[51] Malú Grave and Alvaro LGA Coutinho. Adaptive mesh refinement and coarsening for diffusion–reaction epidemiological models. *Computational Mechanics*, 67(4):1177–1199, 2021.

[52] Yonghong Hao, Qiumei Huang, and Cheng Wang. A third order bdf energy stable linear scheme for the no-slope-selection thin film model. *Communications in computational physics*, 29(3), 2021.

[53] Lida P Hariri, Crystal M North, Angela R Shih, Rebecca A Israel, Jason H Maley, Julian A Villalba, Vladimir Vinarsky, Jonah Rubin, Daniel A Okin, Alyssa Sclafani, et al. Lung histopathology in coronavirus disease 2019 as compared with severe acute respiratory sydrome and H1N1 influenza: a systematic review. *Chest*, 159(1):73–84, 2021.

[54] Khalid Hattaf, Noura Yousfi, and Abdessamad Tridane. Mathematical analysis of a virus dynamics model with general incidence rate and cure rate. *Nonlinear Analysis: Real World Applications*, 13(4):1866–1872, 2012.

[55] Shaobo He, Yuexi Peng, and Kehui Sun. Seir modeling of the covid-19 and its dynamics. *Nonlinear dynamics*, 101:1667–1680, 2020.

[56] Jorge E Herrera-Serrano, José A Guerrero-Díaz-de León, Iliana E Medina-Ramírez, and Jorge E Macías-Díaz. A multiconsistent computational methodology to resolve a diffusive epidemiological system with effects of migration, vaccination and quarantine. *Computer Methods and Programs in Biomedicine*, 236:107526, 2023.

[57] Jorge E Herrera-Serrano, Jorge E Macías-Díaz, Iliana E Medina-Ramírez, and JA Guerrero. An efficient nonstandard computer method to solve a compartmental epidemiological model for covid-19 with vaccination and population migration. *Computer Methods and Programs in Biomedicine*, page 106920, 2022.

[58] João P Hespanha, Raphael Chinchilla, Ramon R Costa, Murat K Erdal, and Guosong Yang. Forecasting covid-19 cases based on a parameter-varying stochastic sir model. *Annual reviews in control*, 51:460–476, 2021.

[59] Herbert W Hethcote. Three basic epidemiological models. In *Applied Mathematical Ecology*, pages 119–144. Springer, 1989.

[60] Richard Horton. *The COVID-19 catastrophe: What's gone wrong and how to stop it happening again*. John Wiley & Sons, 2021.

[61] Amit Huppert and Guy Katriel. Mathematical modelling and prediction in infectious disease epidemiology. *Clinical microbiology and infection*, 19(11):999–1005, 2013.

[62] Chandan Jana, Atasi Patra Maiti, and Dilip Kumar Maiti. Complex dynamical behavior of a ratio-dependent eco-epidemic model with Holling type-II incidence rate in the presence of two delays. *Communications in Nonlinear Science and Numerical Simulation*, 110:106380, 2022.

[63] Atheer Jawad Kadhim and Azhar A Majeed. Epidemiological model involving two diseases in predator population with Holling type-II functional response. *International Journal of Nonlinear Analysis and Applications*, 12(2):2085–2107, 2021.

[64] Andre C Kalil and Paul G Thomas. Influenza virus-related critical illness: pathophysiology and epidemiology. *Critical care*, 23(1):1–7, 2019.

[65] Edward H Kaplan and Yew Sing Lee. How bad can it get? bounding worst case endemic heterogenous mixing models of HIV/AIDS. *Mathematical Biosciences*, 99(2):157–180, 1990.

[66] Muhammad Altaf Khan, Muhammad Ismail, Saif Ullah, and Muhammad Farhan. Fractional order sir model with generalized incidence rate. *AIMS Mathematics*, 5(3):1856–1880, 2020.

[67] Soyoung Kim, A Aurelio, and Eunok Jung. Mathematical model and intervention strategies for mitigating tuberculosis in the philippines. *Journal of theoretical biology*, 443:100–112, 2018.

[68] Helen King. Green sickness: Hippocrates, galen and the origins of the "disease of virgins". *International Journal of the Classical Tradition*, 2(3):372–387, 1996.

[69] Abhishek Kumar. Dynamic behavior of an SIR epidemic model along with time delay; Crowley–Martin type incidence rate and holling type II treatment rate. *International Journal of Nonlinear Sciences and Numerical Simulation*, 20(7-8):757–771, 2019.

[70] Aishwarya Kumar, Puneet Kumar Gupta, and Ankita Srivastava. A review of modern technologies for tackling covid-19 pandemic. *Diabetes & Metabolic Syndrome: Clinical Research & Reviews*, 14(4):569–573, 2020.

[71] Rama Krishna Reddy Kummitha. Smart technologies for fighting pandemics: The techno-and human-driven approaches in controlling the virus transmission. *Government Information Quarterly*, 37(3):101481, 2020.

[72] T Thanh Le, Zacharias Andreadakis, Arun Kumar, R Gómez Román, Stig Tollefsen, Melanie Saville, Stephen Mayhew, et al. The covid-19 vaccine development landscape. *Nat Rev Drug Discov*, 19(5):305–306, 2020.

[73] Vernon J Lee, Marc Ho, Chen Wen Kai, Ximena Aguilera, David Heymann, and Annelies Wilder-Smith. Epidemic preparedness in urban settings: new challenges and opportunities. *The lancet infectious diseases*, 20(5):527–529, 2020.

[74] Ana P Lemos-Paião, Cristiana J Silva, and Delfim FM Torres. A new compartmental epidemiological model for COVID-19 with a case study of Portugal. *Ecological Complexity*, 44:100885, 2020.

[75] Gustavo Barbosa Libotte, Fran Sérgio Lobato, Gustavo Mendes Platt, and Antônio J Silva Neto. Determination of an optimal control strategy for vaccine administration in covid-19 pandemic treatment. *Computer methods and programs in biomedicine*, 196:105664, 2020.

[76] Chun Liu, Cheng Wang, and Yiwei Wang. A structure-preserving, operator splitting scheme for reaction-diffusion equations with detailed balance. *Journal of Computational Physics*, 436:110253, 2021.

[77] Chun Liu, Cheng Wang, Yiwei Wang, and Steven M Wise. Convergence analysis of the variational operator splitting scheme for a reaction-diffusion system with detailed balance. *SIAM Journal on Numerical Analysis*, 60(2):781–803, 2022.

[78] Chun Liu, Cheng Wang, Steven Wise, Xingye Yue, and Shenggao Zhou. A positivity-preserving, energy stable and convergent numerical scheme for the poisson-nernst-planck system. *Mathematics of Computation*, 90(331):2071–2106, 2021.

[79] Alun L Lloyd and Robert M May. Spatial heterogeneity in epidemic models. *Journal of theoretical biology*, 179(1):1–11, 1996.

[80] Marouane Mahrouf, Adnane Boukhouima, Houssine Zine, El Mehdi Lotfi, Delfim FM Torres, and Noura Yousfi. Modeling and forecasting of COVID-19 spreading by delayed stochastic differential equations. *Axioms*, 10(1):18, 2021.

[81] Atasi Patra Maiti, Chandan Jana, and Dilip Kumar Maiti. A delayed eco-epidemiological model with nonlinear incidence rate and Crowley–Martin functional response for infected prey and predator. *Nonlinear Dynamics*, 98:1137–1167, 2019.

[82] Mariano Martini, Valentina Gazzaniga, Nicola Luigi Bragazzi, and Ilaria Barberis. The spanish influenza pandemic: a lesson from history 100 years after 1918. *Journal of preventive medicine and hygiene*, 60(1):E64, 2019.

[83] Ronald E Mickens. Nonstandard finite difference schemes for reaction-diffusion equations. *Numerical Methods for Partial Differential Equations: An International Journal*, 15(2):201–214, 1999.

[84] Ronald E Mickens. *Applications of nonstandard finite difference schemes*. World Scientific, 2000.

[85] Ronald E Mickens. Nonstandard finite difference schemes for differential equations. *Journal of Difference Equations and Applications*, 8(9):823–847, 2002.

[86] Hakimeh Mohammadi, Shahram Rezapour, and Mohammad Esmael Samei. A mathematical model for the spread of covid-19 with a fractional derivative. *Chaos, Solitons & Fractals*, 138:109949, 2020.

[87] AA Momoh, MO Ibrahim, IJ Uwanta, and SB Manga. Mathematical model for control of measles epidemiology. *International Journal of Pure and Applied Mathematics*, 87(5):707–717, 2013.

[88] Pierre Montagnon. A stochastic SIR model on a graph with epidemiological and population dynamics occurring over the same time scale. *Journal of Mathematical Biology*, 79(1):31–62, 2019.

[89] David M Morens, Peter Daszak, Howard Markel, and Jeffery K Taubenberger. Pandemic covid-19 joins history's pandemic legion. *MBio*, 11(3):e00812–20, 2020.

[90] Angelo Moretti and Caterina Santi. The need for reliable and timely data to contrast covid-19: What went wrong? *Available at SSRN 3633827*, 2020.

[91] Gerardo Ortigoza, Fred Brauer, and Iris Neri. Modelling and simulating chikungunya spread with an unstructured triangular cellular automata. *Infectious Disease Modelling*, 5:197–220, 2020.

[92] Kuo Pen-Yu. Numerical methods for incompressible viscous flow. *Scientia Sinica*, 20:287–304, 1977.

[93] Vinicius Piccirillo. Nonlinear control of infection spread based on a deterministic seir model. *Chaos, Solitons & Fractals*, 149:111051, 2021.

[94] Robert J Plemmons. M-matrix characterizations. i—nonsingular m-matrices. *Linear Algebra and its applications*, 18(2):175–188, 1977.

[95] Yiran Qian, Cheng Wang, and Shenggao Zhou. A positive and energy stable numerical scheme for the poisson–nernst–planck–cahn–hilliard equations with steric interactions. *Journal of Computational Physics*, 426:109908, 2021.

[96] YUZHE QIN, CHENG WANG, and ZHENGRU ZHANG. A positivity-preserving and convergent numerical scheme for the binary fluid-surfactant system. *International Journal of Numerical Analysis & Modeling*, 18(3), 2021.

[97] Muhammad Rafiq, J E Macias-Diaz, Ali Raza, and Nauman Ahmed. Design of a nonlinear model for the propagation of covid-19 and its efficient nonstandard computational implementation. *Applied Mathematical Modelling*, 89:1835–1846, 2021.

[98] Bastien Reyné, Nicolas Saby, and Mircea T Sofonea. Principles of mathematical epidemiology and compartmental modelling application to COVID-19. *Anaesthesia, Critical Care & Pain Medicine*, 41(1):101017, 2022.

[99] Shahram Rezapour, Hakimeh Mohammadi, and Mohammad Esmael Samei. SEIR epidemic model for COVID-19 transmission by Caputo derivative of fractional order. *Advances in difference equations*, 2020(1):1–19, 2020.

[100] MG Roberts and JAP Heesterbeek. *Mathematical models in epidemiology*, volume 215. EOLSS, 2003.

[101] José Luis Romo Lozano. Protocolo del semáforo epidemiológico covid-19 en méxico: una clasificación alternativa mediante el método flowsort. *Tesis de licenciatura, Universidad Nacional Autónoma de México, Facultad de Estudios Superiores Iztacala*, 2021.

[102] Eli S Rosenberg, Vajeera Dorabawila, Delia Easton, Ursula E Bauer, Jessica Kumar, Rebecca Hoen, Dina Hoefer, Meng Wu, Emily Lutterloh, Mary Beth Conroy, et al. Covid-19 vaccine effectiveness in new york state. *New England Journal of Medicine*, 386(2):116–127, 2022.

[103] Diego Rosselli. Epidemiología de las pandemias. *Medicina (Bogotá)*, 42(2), 2020.

[104] Luis B Ramos Sánchez, Héctor Sánchez Vargas, Pablo Ángel Galindo Llanes, Hilda Oquendo Ferrer, María C Julián Ricardo, Julio Madera Quintana, Yailé Caballero Mota, and Santiago Lajes Choy. Predicción temprana de la covid-19 en cuba con el modelo seir. *Anales de la Academia de Ciencias de Cuba*, 10(2):883, 2020.

[105] Konstantin S Sharov. Creating and applying SIR modified compartmental model for calculation of COVID-19 lockdown efficiency. *Chaos, Solitons & Fractals*, 141:110295, 2020.

[106] Hiwot S Taffese, Elizabeth Hemming-Schroeder, Cristian Koepfli, Gezahegn Tesfaye, Ming-chieh Lee, James Kazura, Gui-Yun Yan, and Guo-Fa Zhou. Malaria epidemiology and interventions in ethiopia from 2001 to 2016. *Infectious diseases of poverty*, 7(06):1–9, 2018.

[107] Marco Antonio Taneco-Hernández and Cruz Vargas-De-León. Stability and Lyapunov functions for systems with Atangana–Baleanu Caputo derivative: an HIV/AIDS epidemic model. *Chaos, Solitons & Fractals*, 132:109586, 2020.

[108] Juliana Tolles and ThaiBinh Luong. Modeling epidemics with compartmental models. *Jama*, 323(24):2515–2516, 2020.

[109] Pauline Van den Driessche and James Watmough. Reproduction numbers and sub-threshold endemic equilibria for compartmental models of disease transmission. *Mathematical biosciences*, 180(1-2):29–48, 2002.

[110] Vladimir M Veliov. On the effect of population heterogeneity on dynamics of epidemic diseases. *Journal of mathematical biology*, 51(2):123–143, 2005.

[111] María Vidal Ledo, Raúl Guinovart Díaz, Waldemar Baldoquín Rodríguez, Nely Cristina Valdivia Onega, and Wilfredo Morales Lezca. Modelos matemáticos para el control epidemiológico. *Educación Médica Superior*, 34(2), 2020.

[112] Alex Viguerie, Alessandro Veneziani, Guillermo Lorenzo, Davide Baroli, Nicole Aretz-Nellesen, Alessia Patton, Thomas E Yankeelov, Alessandro Reali, Thomas JR Hughes, and Ferdinando Auricchio. Diffusion–reaction compartmental models formulated in a continuum mechanics framework: application to covid-19, mathematical analysis, and numerical study. *Computational Mechanics*, 66(5):1131–1152, 2020.

[113] Jacco Wallinga and Peter Teunis. Different epidemic curves for severe acute respiratory syndrome reveal similar impacts of control measures. *American Journal of epidemiology*, 160(6):509–516, 2004.

[114] Yi Wang, Zhen Jin, Zimo Yang, Zi-Ke Zhang, Tao Zhou, and Gui-Quan Sun. Global analysis of an sis model with an infective vector on complex networks. *Nonlinear Analysis: Real World Applications*, 13(2):543–557, 2012.

[115] Howard Howie Weiss. The SIR model and the foundations of public health. *Materials matematics*, pages 1–17, 2013.

[116] Purnami Widyaningsih, Rifqi Choiril Affan, and Dewi Reno Sari Saputro. A mathematical model for the epidemiology of diabetes mellitus with lifestyle and genetic factors. In *Journal of physics: conference series*, volume 1028, page 012110. IOP Publishing, 2018.

[117] Chayu Yang and Jin Wang. Basic reproduction numbers for a class of reaction-diffusion epidemic models. *Bulletin of mathematical biology*, 82(8):1–25, 2020.

[118] Wuyue Yang, Dongyan Zhang, Liangrong Peng, Changjing Zhuge, and Liu Hong. Rational evaluation of various epidemic models based on the covid-19 data of china. *Epidemics*, 37:100501, 2021.

[119] Amin Yousefpour, Hadi Jahanshahi, and Stelios Bekiros. Optimal policies for control of the novel coronavirus disease (covid-19) outbreak. *Chaos, Solitons & Fractals*, 136:109883, 2020.

[120] Maoqin Yuan, Wenbin Chen, Cheng Wang, Steven M Wise, and Zhengru Zhang. An energy stable finite element scheme for the three-component cahn–hilliard-type model for macromolecular microsphere composite hydrogels. *Journal of Scientific Computing*, 87(3):1–30, 2021.

[121] Juan Zhang, Cheng Wang, Steven M Wise, and Zhengru Zhang. Structure-preserving, energy stable numerical schemes for a liquid thin film coarsening model. *SIAM Journal on Scientific Computing*, 43(2):A1248–A1272, 2021.

[122] Yuzhen Zhang, Bin Jiang, Jiamin Yuan, and Yanyun Tao. The impact of social distancing and epicenter lockdown on the covid-19 epidemic in mainland china: A data-driven seiqr model study. *MedRxiv*, 2020.